HOXD10 AND HOXD11 REGULATE MOTOR COLUMN PATTERNING IN THE LUMBOSACRAL SPINAL CORD

by

Mala Misra

BS, University of Virginia, 2003

Submitted to the Graduate Faculty of

University of Pittsburgh School of Medicine in partial fulfillment

of the requirements for the degree of

Doctor of Philosophy

University of Pittsburgh

2009

UNIVERSITY OF PITTSBURGH

SCHOOL OF MEDICINE

This dissertation was presented

by

Mala Misra

It was defended on

June 29, 2009

and approved by

Carl F. Lagenaur, PhD, Associate Professor, Department of Neurobiology, University of Pittsburgh

Laura E. Lillien, PhD, Associate Professor, Department of Neurobiology, University of Pittsburgh

Joseph W. Yip, PhD, Associate Professor, Department of Neurobiology, University of Pittsburgh

Deborah L. Chapman, PhD, Associate Professor, Department of Biological Sciences, University of Pittsburgh

Michael P. Matise, PhD, Associate Professor, Department of Neuroscience and Cell Biology, UMNDJ/RWJMS

Dissertation advisor: Cynthia Lance-Jones, PhD, Associate Professor, Department of Neurobiology

HOXD10 AND HOXD11 REGULATE MOTOR COLUMN PATTERNING IN THE LUMBOSACRAL SPINAL CORD

Mala Misra, PhD

University of Pittsburgh, 2009

Hox transcription factors have been implicated in many aspects of embryonic rostrocaudal (or anteroposterior) patterning. I have examined the roles of two members of this family, Hoxd10 and Hoxd11, in the development of the lumbosacral (LS) region of the embryonic chick spinal cord. Hoxd10 is expressed uniformly throughout the LS spinal cord at early stages of motoneuron development, but later restricted to subsets of motoneurons in rostral segments. In contrast, Hoxd11 is expressed exclusively in caudal LS segments. Data presented here from overexpression experiments provide evidence that Hoxd10 promotes the development of motoneurons of the lateral subdivision of the lateral motor column (LMCl). Motoneurons transfected with Hoxd10 were likely to acquire a molecular profile, position, and peripheral axonal trajectory consistent with an LMCl identity. In contrast, Hoxd11 suppresses LMCl formation, and imparts a caudal and medial identity upon motoneurons, most likely via repressive interactions with Hoxd10 and the retinoic acid synthetic enzyme RALDH2. To further elucidate the mechanisms governing these opposing actions, I have also created a hybrid protein in which the DNA-binding homeodomain of Hoxd10 is replaced with that of Hoxd11 (Hoxd10^{d11HD}). Hoxd10^{d11HD}, when expressed in LS segments, behaves in a manner similar to Hoxd11, and in direct opposition to Hoxd10, by suppressing the development of the LMCl. It is therefore likely that some of the functionally specific actions of Hoxd11 are governed by the properties of its homeodomain.

TABLE OF CONTENTS

LIST OF TABLES

LIST OF FIGURES

PREFACE

The completion of this thesis owes much to the hard work and dedication of others. Above all, I thank my mentor, Dr. Cynthia Lance-Jones, for her patience, concern, and kind (but firm) tutelage during my graduate career. I also thank my friend and lab manager, Emily Sours, for her technical wizardry, hilarious internet finds, and good company. Thanks, as well, to Veeral Shah, Jonathan Sager, Kathleen Salerno, Susan Harrison, and Emily Drill, for their patient instruction, encouragement, and good advice.

I am indebted of the laboratories of Drs. Thomas Jessell, Samuel Pfaff, Catherine Krull, Clifford Tabin, Peter McCaffery, Ellen Carpenter, Paula Monaghan-Nichols, Willi Halfter, and Gonzalo Torres for their generosity with reagents and equipment. Particular gratitude is owed to Dr. Monaghan-Nichols and the members of her laboratory for sharing their reagents, their technical expertise, and their birthday cake.

Many thanks to the members of my thesis committee, Drs. Carl Lagenaur, Laura Lillien, Joseph Yip, and Deborah Chapman, as well as Dr. Edwin Levitan, for their helpful suggestions and advice. I am also grateful to my outside examiner, Dr. Michael Matise, for participating in my thesis defense.

Thanks to the staff and administrators of the CNUP and the Department of Neurobiology for keeping things running smoothly, and for frequently offering a helping hand.

Finally, I thank my family, my friends, and Colin, for all they do.

This work was funded by NIH grants to Cynthia Lance-Jones (R01-HD025676) and myself (T32-NS007433-07).

1.0 INTRODUCTION

The experiments described in the following chapters were undertaken to investigate the fundamental mechanisms governing spinal motoneuron development, and to place these mechanisms within the broader contexts of embryonic rostrocaudal patterning and neural circuit formation. The spinal cord is a rigidly organized structure in which the rostrocaudal (or anteroposterior) position of a neuron directly correlates with its axonal target. This correlation raises an intriguing question: How do motoneurons at a given spinal level convert rostrocaudal positional information into instructions for axon targeting? The answer appears to reside in the spatially restricted expression of Hox transcription factors. Members of this family have been implicated in many aspects of embryonic development, from the rostrocaudal patterning of the hindbrain (see Jungbluth et al., 1999; Bell et al., 1999; Guidato et al., 2003) to the proximodistal and digital patterning of the limb (see Davis et al., 1995; Goff and Tabin, 1997; Carpenter et al., 1997; Zakany and Duboule, 1999; Boulet and Capecchi, 2004). In the spinal cord, expression of individual Hox genes is restricted to stereotyped rostrocaudal positions and therefore presents a unique molecular correlate for the rostrocaudal patterning of motoneurons within this structure.

Previous investigations of the role of Hox genes in spinal motoneuron development have focused primarily on rostral levels of the spinal cord (Dasen et al., 2003 and 2005). The work presented in this thesis fills a gap in previous literature by addressing two questions regarding the role of Hox genes in the caudal spinal cord: (1) How do Hox transcription factors contribute to

the patterning of the lumbosacral spinal cord as a whole, and (2) How do they affect rostrocaudal patterning within the boundaries of this region? To address these questions, I have utilized an experimental paradigm in which Hox genes are ectopically expressed in lumbosacral motoneurons of the developing chick embryo. By confining manipulations to neuronal populations, I was able to separate central, motoneuron-specific Hox effects from peripheral mesoderm-derived influences. The embryonic chick was used as a model system because of its amenability to both surgical manipulation and ectopic gene expression, and because of the wealth of literature describing its normal neural anatomy.

1.1 A PRELIMINARY NOTE REGARDING MODEL SYSTEMS

The following discussion of spinal cord development will reference and compare experiments utilizing chick, mouse, and zebrafish as model systems. The embryonic chick has long been a popular experimental system because fertilized eggs are readily available and inexpensive. Furthermore, chick embryos are particularly well suited to surgical manipulation and transplants because they can be cultured inside their natural environment, the egg. Mice, however, are better suited for complex genetic studies, and are often used in this capacity. Zebrafish embryos are ideal for studies of morphogenesis, due to their transparency, and are also adaptable to certain types of genetic manipulation. The general mechanisms governing the formation of the spinal cord have proven to be highly conserved among these organisms. Results from experiments involving one model system can therefore be extrapolated into general conclusions about vertebrate development, freeing investigators to select one model over another based on utility. For example, in the text below, I will discuss the role of the LIM homeodomain

transcription factors in the development of varied motoneuron subtypes. Members of this family exhibit a high degree of both structural and functional homology among species, and have been shown to play similar roles in motoneuron development in chick (Tsuchida et al., 1994), mouse (Kania et al., 2000), and zebrafish (Appel et al., 1995), as well as in *Drosophila* (Thor et al., 1999). Therefore, for the purposes of continuity in the remainder of this text, little explicit reference will be made to experimental model systems unless specifically relevant to the basic conclusions of the study.

1.2 DEFINING MOTONEURON IDENTITY

The somatic motoneurons of the spinal cord, which convey information to limb, axial, and body wall musculature, begin as a uniform neuronal population derived from a single progenitor domain (Leber et al., 1990; Jessell, 2000), but subsequently diversify in both molecular phenotype and axonal trajectory. What are the mechanisms governing their diversification? Current evidence suggests that individual neurons are guided to a particular fate by converting information from competing external morphogenetic cues into a cohesive intracellular transcriptional program.

1.2.1 Dorsoventral patterning of the spinal cord

In general terms, the dorsal spinal cord contains the interneurons and ascending tract neurons responsible for conveying peripheral sensory information to the central nervous system (CNS), while the ventral spinal cord contains predominantly motoneurons, through which the CNS

instructs appropriate motor responses to sensory stimuli. The patterning of the spinal cord along this axis occurs quite early in development as neural progenitors are exposed to morphogenetic signals from the roof and floor plates. Bone morphogenetic protein (BMP) and Wingless-related (Wnt) signals from the roof plate are responsible for restricting the fates of interneuron progenitors in the dorsal cord (reviewed in Chizhikov and Millen, 2005), while retinoic acid (RA) from the adjacent paraxial mesoderm (Diez del Corral et al., 2003; Novitch et al., 2003) and sonic hedgehog (Shh) emanating from the notochord and floor plate (Echelard et al., 1993; Roelink et al., 1995; Tanabe et al., 1995; Ericson et al., 1996) direct ventral progenitors to give rise to motoneurons and ventral interneuron subtypes. These ventral progenitors translate exposure to high levels of RA and graded levels of Shh into distinct instructions regarding the individual fates of their progeny via combinatorial expression of homeodomain-containing transcription factors (Ericson et al., 1997; Briscoe et al., 1999 and 2000; Vallstadt et al., 2001). The transcription factors are divided into two classes (I and II) based upon the nature of their response to Shh: Class I proteins Pax6, Pax7, Irx3, Dbx1, and Dbx2 are repressed by Shh, while Class II proteins Nkx2.2 and Nkx6.1 are induced (Briscoe et al., 2000). Combinatorial expression of and cross-repression between members of these classes result in the establishment of five molecularly and spatially discrete progenitor domains within the ventral half of the neural tube that ultimately give rise to four subclasses of ventral interneurons (V0-V3) and motoneurons.

1.2.2 General motoneuron differentiation

Shh-induced expression of one of the homeodomain-containing transcription factors mentioned above, Nkx6.1, in the absence of two others, Irx3 and Nkx2.2, initially defines the motoneuron

progenitor domain (pMN) (Briscoe et al., 2000; Sander et al., 2000; Vallstadt et al., 2001). Nkx6.1 and the closely related Nkx6.2 subsequently activate a signaling cascade leading directly to the differentiation of progenitors into post-mitotic motoneurons. The cascade begins with Nkx6-induced expression of the basic helix-loop-helix (bHLH) transcription factor Olig2 (Novitch et al., 2001). Olig2, in combination with RA emanating from the adjacent paraxial mesoderm, induces the activity of general promoters of neuronal differentiation, coordinates the expression of MNR2 and Lim3, two transcription factors predictive of motoneuron fate (Tanabe et al., 1998), and then directs the cell's eventual exit from the cell cycle (Novitch et al., 2001, 2003; Diez del Corral et al., 2003). MNR2 expression is initiated during the last division cycle of motoneuron progenitors and appears to be sufficient to direct motoneuron differentiation in concert with another homeodomain-containing transcription factor, Isl1 (Pfaff et al., 1996; Tanabe et al., 1998). Isl1, along with Lim3, then orchestrates the expression of a several downstream transcription factors characteristic of post-mitotic motoneurons, including Hb9 and Isl2 (Pfaff et al., 1996; Arber et al., 1999; Thaler et al., 1999 and 2002). Thus, early postmitotic expression of Hb9, Isl1, Isl2, and Lim3 defines a generic, homogeneous population of differentiated motoneurons. Many of these factors are utilized again, later in development, as determinants of motoneuron subtype identity.

1.2.3 Rostrocaudal patterning of the spinal cord

Most bilaterally symmetrical organisms are divided along their rostrocaudal (or anteroposterior) axes into repeating units, termed segments, of varying number. The spinal cord, along with the overlying vertebrae, maintains this ancient organizational framework. In most vertebrates, consecutive spinal segments are organized into alternating limb-innervating and non-

limb-innervating regions. Segments adjacent to the hindbrain in the rostral-most sector of the spinal cord are described as cervical. Those innervating the forelimb are brachial, while those projecting to hindlimb muscles are lumbar, or lumbosacral (L/LS). The intervening trunk segments are termed thoracic (T).

Within each region, the ventral cord is divided into a specific complement of "columns" (Landmesser, 1978; Hollyday, 1980) (Figure 1.1A). The medial motor column (MMC) spans the rostrocaudal length of the spinal cord and is divided into medial and lateral domains that contain the soma of motoneurons projecting to axial and body wall musculature, respectively (Gutman, 1993). The lateral motor column (LMC) exists only at limb levels and contains the soma of motoneurons that innervate fore- and hindlimb musculature. Like the MMC, the LMC is subdivided into lateral and medial domains. The lateral domain (LMCl) consists of the cell bodies of dorsal-projecting motoneurons, while the medial (LMCm) houses ventral-projecting motoneurons. Non-limb innervating thoracic segments also possess a unique columnar component, the Column of Terni (CT), which contains the cell bodies of preganglionic sympathetic neurons. These neurons project directly to sympathetic chain ganglia in the periphery (Levi-Montalcini, 1950; Prasad and Hollyday, 1991). Further, nested within the columnar subdivisions of the ventral cord are "motor pools", clusters of motoneurons that project to individual muscles in the limb (Landmesser, 1978; Hollyday, 1980) (Figure 1.1B).

The signals instructing motoneurons to adopt specific columnar and pool identities appear to originate primarily from extrinsic morphogenetic cues. The way in which motoneurons respond to these cues can depend on both rostrocaudal position within the cord and time of birth. Recent studies suggest that Wnt4/5 signals arising from the floor plate are responsible for specification of the MMC along the length of the neural tube (Aggaliu et al.,

2009). Mechanisms responsible for LMC induction, however, differ at rostral and caudal spinal cord levels. In brachial segments, significant evidence suggests secreted retinoic acid (RA) from adjacent paraxial mesoderm directs the formation of the LMC (Ensini et al., 1998; Liu et al., 2001; Sockanathan et al., 2003; Ji et al., 2006). Meanwhile, factors originating from the tailbud and Hensen's node are thought to dictate columnar organization at more caudal levels (Lance-Jones et al., 2001; Omelchenko and Lance-Jones, 2003; Sockanathan et al., 2003). Opposing rostral RA and caudal fibroblast growth factor (FGF) gradients induce the spatially restricted expression of a specific family of transcription factors, the Hox proteins, along the rostrocaudal axis. These are thought to direct the acquisition of segmental identity in both neural and non-neural tissues (see below; Liu et al., 2001; Bel-Vialar et al., 2002).

The LMC assembles in an inside-out manner, with early-born neurons settling medially, and later-born motoneurons migrating beyond their predecessors to occupy progressively more lateral positions in the cord (Hollyday and Hamburger, 1977) (Table 1.1). Thus, the LMCm is composed of early-born motoneurons, and the LMCl, of later-born. The establishment of these two distinct motoneuron subsets appears to be intimately connected to their time of birth. Early-born motoneurons secrete RA, an inducer of LMCl identity, but are largely refractory to its effects. In contrast, later-born motoneurons, upon encountering the RA produced by their predecessors, activate a transcriptional program leading to LMCl differentiation (Sockanathan and Jessell, 1998). Time of birth therefore dictates ultimate motoneuron subtype identity in the formation of LMC columnar divisions.

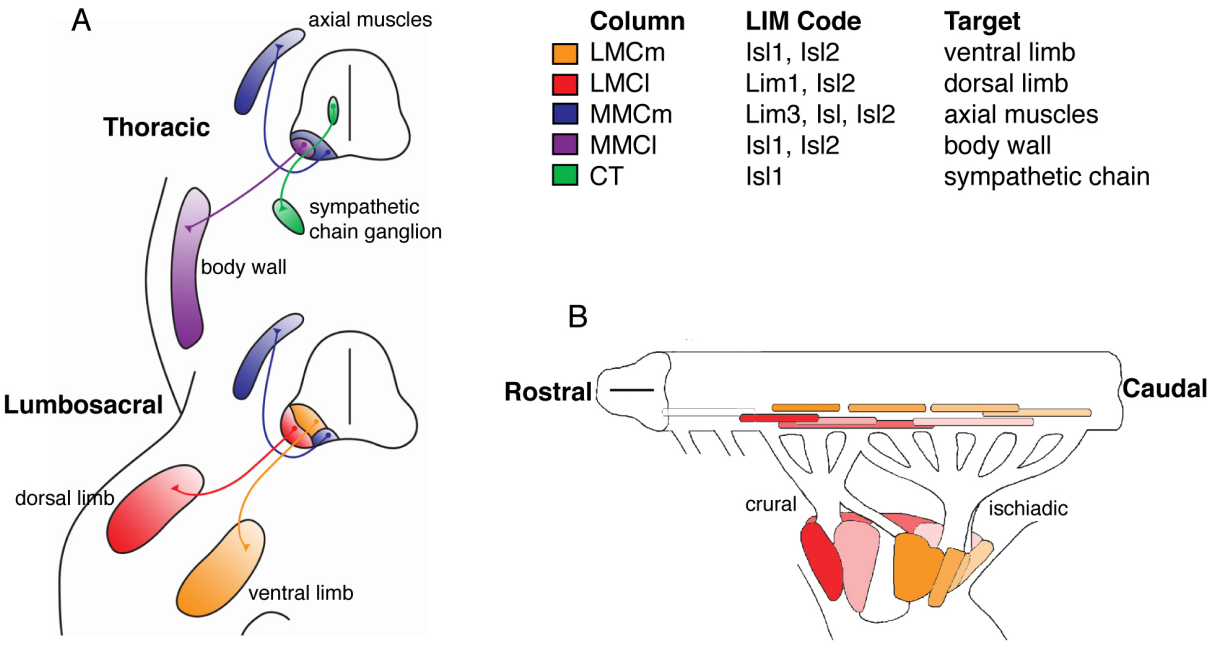

Figure 1.1 Schematic representation of motor column and pool organization.

A. The thoracic and LS regions of the spinal cord possess different complements of motor columns. Columns are identifiable by position, expression of LIM-HD proteins, and target. B. Within the columns of the LS, motoneurons projecting to individual hindlimb muscles cluster into motor pools.

1.2.4 Axonal trajectories of motoneurons

As described above, a motoneuron's position within a particular column or pool usually correlates with the targeting of its axon. Soon after their birth, lumbosacral motoneurons begin to extend axonal projections toward peripheral muscle targets (Table 1.1). These axons first exit the spinal cord through the closest ventral root to form individual spinal nerves. Initially, axons originating from motoneurons fated for different columns and pools commingle (Lance-Jones and Landmesser, 1981). From the time of their exit from the spinal cord to their eventual contact

Table 1.1 Timing of central and peripheral events in LS motoneuron development in the chick embryo.

Stages are based on Hamburger and Hamilton (1951).

HH Stage (embryonic day)	Peripheral events	Central events
St 17 (E2.5)		Initiation of motoneuron birthdate period (Hollyday and Hamburger, 1977)
St 18	First growth cones exit spinal cord (Tosney and Landmesser, 1985)	
St 19	Divergence of axons to axial muscle (Tosney, 1992)	
St 21 (E3.5)	First growth cones reach plexus (Tosney and Landmesser, 1985)	Motoneuron expression of the pool-specific cadherin MN-cad (Price et al., 2002); Earliest onset of LMCl marker Lim1 (Tsuchida et al., 1994)
St 22		Approximate end of motoneuron birthdate period (Hollyday and Hamburger, 1977)
St 23	Evidence of initial D-V axonal sorting (Lance-Jones and Landmesser, 1981)	
St 24 (E4)	First growth cones enter the limb. Anatomical evidence of dorsal and ventral nerve trunks (Tosney and Landmesser, 1985)	Motoneuron expression of the pool-specific ETS gene Er81 (Lin et al., 1998)
St 27 (E5)	Nerve trunks penetrate muscle masses (Tosney and Landmesser, 1985)	Motoneuron expression of pool-specific cadherins T-cad, cad-6b, cad-7 (Price et al., 2002)
St 29 (E6)		Motor pools are clustered Motoneuron expression of pool-specific ETS gene Pea3 (Lin et al., 1998)

with muscle targets, however, these axons encounter a series of "decision regions" (Tosney and Landmesser, 1985b) at which they segregate into branches corresponding to their columnar and pool identities (Lance-Jones and Landmesser, 1981). The most proximal region of axonal decision-making is that at which MMC axons destined for the dermomyotome (the precursor to axial muscles) turn sharply dorsally toward their target (Tosney and Landmesser, 1985a). Experimental evidence suggests that these axons are guided by FGF8 signals originating from the dermomyotome itself (Shirasaki et al., 2006).

The remaining lumbosacral motor axons of the spinal nerve continue on their distal trajectory, eventually penetrating the base of the limb mesenchyme and forming two distinct axon clusters, termed plexi. The more rostral plexus, the crural, is composed of axons from LS segments 1-3 that go on to innervate anterior dorsal and ventral muscles of the thigh. The more caudal plexus, or ischiadic, is composed of axons from LS segments 3-8, which innervate posterior thigh muscles, shank, and foot. Just proximal to the plexi, spinal nerves sort and fasciculate, forming dorsally projecting and ventrally projecting branches (Lance-Jones and Landmesser, 1981). The choice of ventral verses dorsal trajectory appears to be governed primarily by motoneuron expression of Eph receptors and limb mesenchymal expression of their repulsive ligands, ephrins (Helmbacher et al., 2000; Eberhart et al., 2002; Kania and Jessell, 2003; Luria et al., 2008), though recent studies have identified two other axon guidance factors, semaphorins and glial-derived growth factor (GDNF), that may also contribute (Huber et al., 2005; Kramer et al., 2006).

Within the plexus region at the base of the limb, axons sort according to their muscle targets (Lance-Jones and Landmesser, 1981). Axonal expression of varying levels of polysialic acid in association with the general neural adhesion molecule N-CAM appears to contribute to

the sorting and fasciculation of axons with common targets (Tang et al., 1994). These individual target-specific fascicles proceed along a common pathway into the distal limb, and then exit this pathway via muscle nerves as they encounter their target muscles (or the precursive muscle masses that will eventually mature into muscles) (Lance-Jones and Landmesser, 1981). Signals emanating from the limb itself appear to govern the process of individual muscle nerve fasciculation and pathfinding (Wang and Scott, 2000) but the exact nature of such signals is largely unknown. Likely candidates include GDNF (Haase et al., 2002), HGF (Helmbacher et al., 2003) and semaphorins (Taniguchi et al., 1997; Huber et al., 2005).

1.2.5 Molecular codes define motoneuron subtypes

Individual motoneurons comprising columns and pools can be defined not only by their position within the cord or their axonal trajectories, but also by their molecular complement (Table 1.2). The best characterized example of this is the so-called "LIM code" (Tsuchida et al., 1994). Each columnar subtype expresses a unique combination of LIM-HD transcription factors, which possess a LIM protein:protein interaction domain and a DNA binding homeodomain (reviewed in Hobart and Westphal, 2000). Several members of this family, including Isl1, Isl2, and Lim3, play an early role in the events leading to general motoneuron differentiation (see above; Pfaff et al., 1996; Thaler et al., 2000); as motoneurons mature, however, their expression is restricted to individual columns and/or columnar divisions (Figure 1.1A; Tables 1.1 and 1.2). For example, in the LS cord, LMCl motoneurons express LIM-HD proteins Lim1 and Isl2, while LMCm motoneurons express Isl1 and Isl2 (Tsuchida et al., 1994).

Several studies have also identified molecular markers for individual motor pools. Expression of members of the ETS family of transcription factors, specifically PEA3 and Er81,

can be used in conjunction with LIM proteins to define specific motor pools (Lin et al., 1998); for example, in LS2, motoneurons innervating the adductor co-express Er81 and Isl1, while those projecting to the Femorotibialis externus co-express Er81 and Lim1. Similarly, expression of the transcription factor Nkx6.1, mentioned above as a regulator of motoneuron progenitor fate, identifies motoneurons projecting to the adductor (De Marco Garcia and Jessell, 2007). Individual motor pools also differentially express type II cadherins (Price et al., 2002) and secreted semaphorins (Cohen et al., 2005), adhesive and repulsive guidance molecules (Table 1.1). In addition, combinatorial expression of members of the Hox family of transcription factors and their cofactors appears to delineate individual motor pools within the brachial and thoracic spinal cord (see below; Dasen et al., 2005).

The downstream effectors linking columnar and pool-specific transcription factor expression in individual motoneurons to projection patterns are largely unknown, but investigators have recently assembled one aspect of the puzzle: Lim1, a member of the LIM family of transcription factors and a marker of LMCl, regulates the expression of the repulsive guidance molecule receptor EphA4, which then directs axons away from ventral limb targets expressing its ligand ephrin A5 (Helmbacher et al., 2000; Eberhart et al., 2002; Kania and Jessell, 2003). In a symmetrical fashion, Isl1, a marker of LMCm, regulates the expression of another member of the Eph/ephrin family, EphB1, which then directs axons away from the ephrin B2-expressing dorsal limb (Luria et al., 2008). Thus, the choice to pursue a ventral or dorsal axonal trajectory is governed by the intrinsic expression of transcription factors, which subsequently regulate the expression of cell-surface receptors, thereby determining the sensitivities of individual motoneurons to external axon guidance cues.

Table 1.2. Molecular markers of LS motoneuron subtypes.

Markers highlighted in blue are used as subtype identifiers in subsequent chapters.

Subtype	Molecular Marker
MMCm	**Lim3**, Hb9, **Isl1**, Isl2, Scip
MMCl	Hb9, **Isl1**, Isl2, **Scip**
LMCm	Foxp1, Hb9, **Isl1**, Isl2, RALDH2
LMCl	Foxp1, Hb9, **Lim1**, Isl2, RALDH2

1.3 HOX GENES AND SEGMENTAL IDENTITY

As discussed above, several studies have provided evidence that extrinsic morphogenetic factors from the paraxial mesoderm (Ensini et al., 1998, Liu et al., 2001; Sockanathan et al., 2003; Ji et al., 2006), the floor plate (Aggaliu et al., 2008), and Hensen's node (Lance-Jones et al., 2001; Omelchenko and Lance-Jones, 2003) work in concert to direct gross regional variations in motor column profile. Superimposed upon motor columns, however, are individual motor pools spanning only a subset of segments. How, then, is the specific motoneuron complement of a given segment determined?

Evidence from spinal reversal experiments suggests that the future targeting of spinal motor axons is determined soon after neural tube closure (Lance-Jones and Landmesser, 1980; Matise and Lance-Jones, 1996), before axonal contact with potential limb signals, and even before motoneuron birthdates. In these experiments, reversal of 3-4 segments along the rostrocaudal axis of the lumbosacral cord at developmental stage 15 (Hamburger and Hamilton, 1951), a few hours after neural tube closure and before motoneuron differentiation, did not

disrupt the normal correlation between segmentally restricted motor pools and their original axonal targets. This requires that the forces controlling individual segmental identity are activated quite early in spinal development and can subdivide, molecularly, broader spinal regions into segments or groups of segments with unique motoneuron complements and peripheral targets. The Hox family of transcription factors meets such criteria.

1.3.1 General properties of Hox transcription factors

Hox/Hom genes were first identified in Drosophila melanogaster. Mutations in the Drosophila HOM-C complex resulted in "homeotic" transformations, or gross morphological transformations in segmental identity, along the anteroposterior axis of the body (Lewis, 1978). For example, a mutation in the Drosophila homeotic gene Antennapedia causes legs to develop in an anterior segment normally possessing antennae. Soon after the discovery of the HOM-C complex, similar Hox genes were identified in nearly every examined bilateral organism, including vertebrates (reviewed in Pearson et al., 2005). Interestingly, while Drosophila possess just eight Hox/Hom genes, the vertebrate genome contains thirty-nine Hox transcription factors, most likely a result of multiple evolutionary duplication events (reviewed in McGinnis and Krumlauf, 1992).

Hox genes are characterized as such by the nature of their DNA-binding motif, a sixty amino acid "homeodomain" that includes a signature helix-turn-helix (reviewed in McGinnis and Krumlauf, 1992). In vertebrates, members of this family are segregated into four paralogous chromosomal clusters (Figure 1.2A). Each of the four clusters, labeled A-D, contains all Hox genes in a particular family, numbered 1-13. Individual Hox genes are expressed by both neural and non-neural tissues in restricted overlapping domains along the rostrocaudal axis of the body

and the proximodistal axis of the limb (Figure 1.2B). This property allows these transcription factors to activate or repress the expression of unique sets of downstream targets in defined spatial units (e.g. spinal segments). Interestingly, the members of each cluster share a unique property, termed "colinearity": their order of expression along the axis of the body, both spatially and temporally, parallels the 3' to 5' order in which they exist on the chromosome (reviewed in Kmita and Duboule, 2003). Paralogous Hox genes, or numerically equivalent Hox genes from different clusters (Figure 1.2A), tend to share similar DNA sequences, domains of expression, and function (Krumlauf, 1994).

1.3.2 Neural Hox induction

The caudal parts of the CNS (including hindbrain and spinal cord) initially develop in a rostral to caudal gradient, and the specification of progressively more caudal segments coincides with a massive caudal extension of the embryonic axis. The expression of Hox genes parallels this pattern, with 3' members of the family restricted to the earliest structures (hindbrain and cervical spinal cord), and 5' members appearing slightly later in more caudal regions of the spinal cord (reviewed in Kmita and Duboule, 2003). Onset of Hox expression within the lumbosacral spinal cord occurs fairly soon after neural tube closure, at stages 14-16 (Lance-Jones et al., 2001; Liu et al., 2001), but evidence from transplant experiments at both hindbrain and spinal cord levels suggest that Hox expression may be "pre-patterned" well before this stage (Grapin-Botton et al., 1997; Lance-Jones et al., 2001).

Colinear induction of Hox expression along the body axis appears to occur in response to two competing morphogenetic signals: RA from rostral paraxial mesoderm and FGF8 arising from Hensen's node and the tailbud. A detailed study by Liu et al. (2003) utilized cultured

neural explants from future rostral cervical levels of the spinal cord to determine that young neural tissue, when exposed to increasing concentrations of FGF8 from the node, could be made to express progressively more 5' members of the HoxC family (see also Bel-Vialar et al., 2002). These studies confirmed suggestions from other investigators (Lance-Jones et al., 2001, Omelchenko and Lance-Jones, 2003) that signals arising from Hensen's node and the tailbud were responsible for the patterning Hox genes at caudal levels. The failure of FGF8 to induce more rostral spinal HoxC genes (namely, Hoxc5), however, implied that alternative mechanisms contributed to Hox induction in rostral segments.

Several studies have implicated paraxial mesoderm as an inducer of neural Hox expression (Itasaki et al., 1996; Grapin-Botton et al., 1997; Ensini et al., 1998). In the hindbrain, transplanted rhombomeres (r; hindbrain segments) alter their Hox profile based on their ultimate proximity to the paraxial mesoderm flanking the cervical spinal cord (Itasaki et al., 1996). The primary inductive signal supplied by this rostral paraxial mesoderm was later shown to be retinoic acid (Studer et al., 1994; Gould et al., 1998; Neiderreither et al., 2000; Liu et al., 2003; see also Simeone et al., 1990 and Bel-Vialar et al., 2002). To examine the effect of RA on spinal Hox expression, Liu et al. (2003) extended the studies with neural explants described above to demonstrate that RA alone or its local source, cervical paraxial mesoderm tissue, is sufficient to induce expression of rostral spinal Hoxc genes (Hoxc5 and Hoxc6). Conversely, exposure to RA and cervical paraxial mesoderm prevented the expression of caudal Hoxc genes (Hoxc8-10), even in explants from more caudal spinal levels. These experiments suggest that RA and FGF8 exist in opposing gradients along the rostrocaudal axis of the spinal cord, and work in concert to define the restricted domains of Hox genes.

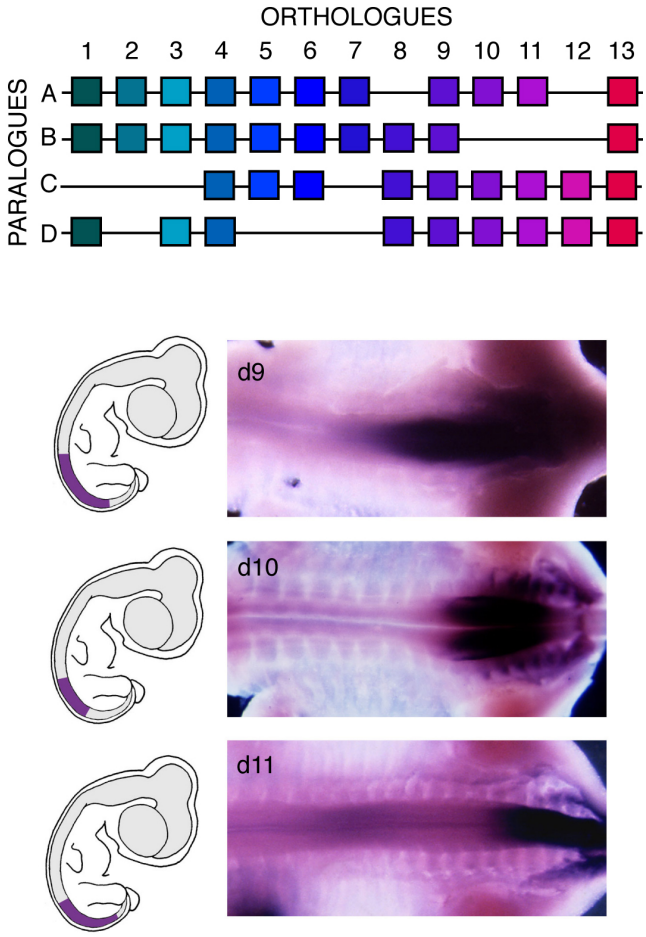

Figure 1.2 Schematic representation of Hox clusters and overlapping expression of caudal Hox genes.

A. Hox genes exist in numerical order (1-13) on four paralogous chromosomal clusters (A-D) (after Krumlauf, 1994). B. Expression of three caudal HoxD orthologues demonstrates overlapping expression patterns with varied rostral and caudal boundaries. Whole mount in situ hybridization, HH stage 29.

1.3.3 Hox genes and segmental patterning in the hindbrain

Soon after neural tube closure, the region of the neural tube comprising the hindbrain contracts at progressive points along its rostrocaudal axis, thereby delineating the borders of eight distinct rhombomeres. A notable feature of these rhombomeres is their restricted expression of specific 3' Hox genes; for example, r4 expresses Hoxb1 and Hoxb2, while r5 expresses Hoxb2, and Hoxb3 (reviewed in Hunt and Krumlauf, 1991). The existence of this so-called "Hox code" suggests the possibility that Hox expression actively determines individual rhombomeric identity. Indeed, gain- and loss-of-function studies have repeatedly demonstrated the importance of Hox genes in the establishment of rhombomeres and the properties of the motoneurons contained therein. For example, loss of Hoxb1, which is uniquely expressed by r4, results in inappropriate motoneuron migration within r4 and r5 and the partial phenotypic conversion of r4 to an r2-like identity (Studer et al., 1996). Conversely, ectopic misexpression of Hoxb1 in r2 reroutes motoneuron projections originating therein to ectopic caudal targets that are normally innervated by r4 (Bell et al., 1999). Hox expression therefore appears to be a powerful determinant in segmental identity.

1.3.4 Hox genes and segmental patterning in the spinal cord

As in the hindbrain, the spatial limits of expression of individual Hox genes in the spinal cord often correspond to shifts in motoneuron complement and axonal targets along the rostrocaudal axis. For example, the rostral limit of the expression of Hoxc9 corresponds to the transition between brachial and thoracic spinal cord (Dasen et al., 2003). Similarly, the rostral limit of the expression of Hoxd10 aligns with the thoraco-lumbosacral border (Carpenter et al., 1997) (see

Figure 1.2B). In light of such expression patterns, several investigators have utilized gain-and loss-of-function paradigms to show decisively that Hox genes, individually or in combination, are capable of conferring specific molecular and axon targeting identities in spinal motoneurons. For example, Hoxc6 and Hoxc9 appear to be essential for the columnar specification of motoneurons at the brachial and thoracic levels, respectively (Dasen et al., 2003). The columnar composition of the brachial spinal cord consists of an LMC and an MMC. An alternate composition is found at thoracic levels – here, motoneurons occupy the MMC or the Column of Terni (CT), which sends projections to autonomic targets. Ectopic expression of Hoxc9 at brachial levels causes some motoneurons to erroneously adopt a CT fate, while expression of Hoxc6 at thoracic levels induces LMC-like motoneurons.

Studies of individual motor pool formation also point to Hox genes as the possible directors of motoneuron subtype specification (Dasen et al., 2005). Within the Hoxc6-expressing brachial region of the spinal cord, Hoxc5 and Hoxc8 are expressed by different populations of motoneurons: Hoxc5 is expressed by the motor pool that projects to the scapulohumeraris anterior (Sca), while Hoxc8 is expressed by the pectoralis (Pec) pool. Blocking the expression of Hoxc8 caused an expansion of the domain of Hoxc5 and a corresponding expansion of the Sca motor pool. Likewise, misexpression of Hoxc8 increased the size of the Pec pool at the expense of the Sca. Furthermore, the target muscle connectivity of these neurons corresponds to their ectopic identities. Such findings are intriguing because they support previous observations that mechanisms governing motoneuron identity, including columnar, pool, and target identity, are entirely programmed by cell intrinsic factors very early in the development of the LMC (Lance-Jones and Landmesser, 1980; Matise and Lance-Jones, 1994).

1.3.5 Downstream targets of Hox genes

In their ability to specify neural and non-neural segmental identity, Hox proteins demonstrate a striking degree of influence on a variety of cellular processes, including adhesion, migration, proliferation, and apoptosis. Surprisingly, investigators have thus far identified but a few direct targets of Hox control (reviewed in Akin and Nazarali, 2005; Svingen and Tonissen, 2006). Among these are several cell adhesion and axon guidance molecules such as N-CAM (Jones et al., 1993; reviewed in Edelman and Jones, 1998), osteopontin (Shi et al., 1999 and 2001), Eph/ephrins (Bruhl et al., 2004; Salsi and Zappavigna, 2006), Slit/Robos (Geisen et al., 2008) and basic FGF (Caré et al., 1996). Cadherins are another likely target (Inoue et al., 1997; Shen et al., 2000), though direct binding of Hox proteins and cadherin promoters have not been confirmed. Alterations in the expression of any of these factors might contribute to the changes in axonal trajectory observed in both hindbrain and spinal cord following Hox misexpression. Furthermore, Hox proteins have been found to regulate the expression of a number of critical transcription factors associated with neuronal subtype specification, including members of the Pax (Pruitt et al., 2004), and Irx (Theokli et al., 2003) families. The stark effects of Hox misexpression and/or loss of function, coupled with the wide range of known or potential downstream targets, suggest that Hox proteins occupy a position at or near the top of the signaling hierarchies responsible for hindbrain and spinal cord patterning.

1.4 FUNCTIONAL SPECIFICITY OF HOX TRANSCRIPTION FACTORS

Hox genes have long been known to play diverse roles in segmental patterning; yet, a striking characteristic of this family is the high degree of sequence similarity among DNA-binding regions of paralogous and even orthologous Hox genes. Homeodomains from even the most divergent Hox proteins still resemble each other; for example, Hoxa11 and Hoxa4 are descendents of different ancestral homeotic genes (Hoxa11 is most similar to Drosophila AbdB, while Hoxa4 parallels Drosophila Deformed), but they maintain 48% amino acid sequence identity (Zhao and Potter, 2002). As a result of this homology, all Hox proteins appear to recognize and bind to similar DNA recognition sites in vitro, notably 5'-TTAT-3', 5'-TTAC-3', and 5'-TAAT-3' sequences (Desplan et al., 1988; Chang et al., 1996; Shen et al., 1997). The relative ubiquity of such short sequences complicates any explanation of individual Hox functional specificity.

1.4.1 Hox cofactors

Though the complete reconciliation of diverse function with structural homogeneity has proven difficult to accomplish, convincing data have emerged in support of the importance of heterodimerization of Hox proteins with cofactors in fine-tuning binding specificity. The two best characterized of these cofactors are Pbx1 and Meis, both members of the large TALE class of homeodomain-containing transcription factors. Pbx1 (and the related factors Pbx2, 3, and 4) interacts directly with Hox paralogues 1-8 via the Hox hexapeptide motif, a conserved six amino acid sequence situated just N-terminal to the homeodomain (Chang et al., 1995; Knoepfler and Kamps, 1998). Paralogues 9 and 10 are also capable of interacting with Pbx1 through a

conserved tryptophan residue (Shen et al., 1997b). Because Pbx is a transcription factor with its own unique DNA recognition sites, Hox:Pbx heterodimers bind only to DNA targets meeting the sequence requirements of both proteins (reviewed in Mann and Affolter, 1998), thus limiting the total number of possible binding sites. The inclusion of Meis to form a heterotrimer further increases the selectivity of Hox-DNA interactions.

A number of studies have suggested that Hox:Pbx heterodimerization not only increases target specificity, but also is a requirement for appropriate Hox function. Patterning defects observed in Pbx loss-of-function mutations in mice in some ways mimic the effects of Hox loss-of-function mutations (Selleri et al., 2001; Manley et al., 2004). Interruption of Pbx:Hox dimerization has also been reported to disrupt patterning (Remacle et al., 2004). In the hindbrain, mutation of the hexapeptide motif in Hoxa1 results in a loss of r4 and r5, cranial nerve defects, and abnormal skeletal development, phenotypic characteristics that mirror those seen in Hoxa1 knockout mice (Remacle et al., 2004). In general, however, Hox:cofactor interactions appear to be far more important for the function of rostrally expressed Hox proteins than caudally expressed (LaRonde-LeBlanc and Wolberger, 2003). In fact, Hox paralogues 11-13 do not associate with Pbx1 at all (Shen et al., 1997b). In vitro studies have suggested that caudal Hox proteins heterodimerize with Meis, but the in vivo relevance of such associations has not been established (Shen et al., 1997a). Further confounding the notion that Hox functional specificity can be explained by Hox:cofactor interactions is the observation that highly homologous Hox proteins, when bound by PBX1, all bind with highest affinity to the same recognition sites (Neuteboom and Murre, 1997). Therefore, while PBX and other cofactors can under certain circumstances limit the number of appropriate binding sites for Hox proteins, the

exact mechanisms by which they activate unique downstream targets remains somewhat mysterious.

1.4.2 Homeodomain binding

As mentioned above, all Hox family members recognize and bind to similar short DNA sequences and share a high level of homology among their homeodomains. As a result, most investigators largely discounted the possibility that subtle variations among homeodomains could mediate individual Hox functional specificity. Those few existing studies into the role of the homeodomain have focused primarily on the development of non-neural tissues, including the appendicular skeleton, axial skeleton, kidney, and male and female reproductive tracts. The importance, or lack thereof, of the homeodomain in Hox-guided specification of neuronal fate has not yet been characterized.

Thus far, most examinations of homeodomain functional specificity in vertebrates have utilized an experimental paradigm in which the homeodomain-coding regions of two Hox genes of known function are reciprocally swapped (Sreenath et al., 1996; Zhao and Potter, 2000, 2001). Results from these swap experiments have varied greatly from study to study. An early examination of the role of the Hox genes in vertebral patterning determined that the functional specificity of Hoxa4, which actively suppresses the development of ribs at the cervical level of the spine, was unaffected by replacement of its homeodomain with that of Hoxc8, a potent inducer of rib growth (Sreenath et al., 1996). Thus, the two homeodomains are functionally redundant in this context, and the specificity of the actions of Hoxa4 and Hoxc8 is likely tuned by protein:protein interactions. Zhao and Potter (2001, 2002) performed a similar series of homeodomain swapping experiments with Hoxa13, Hoxa11, Hoxa10, and Hoxa4. In the first,

the homeodomain of Hoxa11 was replaced by that of Hoxa13 in a transgenic mouse line. In these mice, the developing kidneys, male reproductive organs, and axial skeleton seemed largely unaffected, again suggesting functional redundancy among homeodomains. Mutant phenotypes, however, were observed in the limbs and female reproductive tract - the fibula and tibia were separated distally, and the vagina and cervix were shortened at the expense of the uterus. The latter finding strongly implied that the mutant Hoxa11 actually adopted properties of Hoxa13 and caused a segmental "posteriorization" in the uterus. In a second set of experiments, the homeodomain of Hoxa11 was replaced by that of Hoxa10 or Hoxa4. Mice expressing a mutant Hoxa11 containing the relatively divergent homeodomain of Hoxa4 (48.3% amino acid sequence identity) appeared indistinguishable in most respects from Hoxa11 knockouts, suggesting that the Hoxa4 homeodomain could in no way substitute for the native Hoxa11 homeodomain. However, mice expressing Hoxa11 with the Hoxa10 homeodomain (68% identity), exhibited a much milder, intermediate phenotype. Thus, the Hoxa10 homeodomain was partially but not entirely redundant with that of Hoxa11. These results support the notion that the functional specificity of Hox genes does in fact rely, to some extent, on the specific attributes of the homeodomain itself, but also requires alternative mechanisms, such as independent interactions with cofactors or other transcription factors, to confer all aspects of segmental identity.

1.4.3 Non-transcriptional activities of Hox proteins

The presence of a signature homeodomain in Hox proteins has focused most examinations of their functional specificity on the control of Hox-directed transcriptional activation or repression. Several recent studies, however, have introduced the possibility of non-transcriptional roles for Hox proteins in segmental patterning. For example, misexpression of a mutated, non DNA-

binding form of Hoxd13 in the limb (Caronia et al., 2003, Williams et al., 2006) partially mimicked the effects of misexpression of wild-type Hoxd13 (Goff and Tabin, 1997) by causing a shortening of the proximal long bones. In addition, microarray studies have identified a number of factors that are upregulated by both Hoxd13 and the non-DNA-binding form thereof, though the latter appears to be unable to mimic the repressive effects of the wild-type (Williams et al., 2006).

An intriguing example of the non-transcriptional effects of Hox genes on segmental identity arose from the discovery of an interaction between Hoxd12 proteins and Gli3, a transcriptional mediator of Shh signaling (Chen et al., 2004). In the limb, the presence of Shh prevents the cleavage of Gli3 into a transcriptional repressor, thereby allowing it to maintain and activate expression of those downstream targets in the Shh hierarchy responsible for the establishment of patterned digits. Chen et al. noted that physical interaction between Hoxd12 and the cleaved repressor form of Gli3 converts the latter into a transcriptional activator. The total ratio of Gli3:Hoxd proteins guides the differential activation of Gli3 target genes, thereby controlling the patterning of digits. This interaction does not require homeodomain-DNA binding. Thus, the contributions of Hox genes to regional tissue (in this case, digital) identity may depend on their non-transcriptional activities to a greater extent than previously thought.

2.0 MATERIALS AND METHODS

2.1 EXPERIMENTAL ANIMALS

The experiments detailed in this manuscript utilized the developing chick embryo as a model system to investigate the mechanisms governing Hox function and lumbosacral motoneuron development. As described in Chapter 1, the embryonic chick is an ideal system in which to study the neurons of the spinal cord and their projections because of the wealth of information available regarding their development and anatomy. Furthermore, the organism is easily accessible within the egg for experimental manipulations. For the studies discussed here, fertilized chick eggs (CBT Farms) were incubated in a forced-draft incubator at 37°C. Eggs to be used for *in ovo* electroporation were opened at embryonic day (E) 2.5 (stages 14-16 of Hamburger and Hamilton, 1951) and stained with a 0.5% neutral red in physiological saline to increase visibility and facilitate stage assessment. Following electroporation, eggs were incubated until E4-7 (stages 22-31). At sacrifice, embryos were placed in cold avian saline, staged, and dissected to a trunk/limb preparation. E4-7 non-electroporated embryos were used for assessment of normal developmental features.

2.2 IN OVO ELECTROPORATION

For the experiments described in Chapters 3-5, misexpression of Hox genes in spinal motoneurons was accomplished via *in ovo* electroporation. This technique is used to deliver foreign plasmid DNA directly to the neuronal progenitors lining the central canal. DNA is first injected into the neural tube of the developing embryo. A low voltage is then briefly applied across the neural tube by placing electrodes on either side. Electrical pulses introduce nanometer size pores into the walls of cells, allowing the plasmid DNA to move into them. Because DNA is negatively charged, it moves toward the positive electrode, and consequently enters only the cells on the "positive" side of the neural tube. Once the current is removed, the pores close, and the progenitors divide normally, passing the foreign DNA on to their immediate progeny (see Muramatsu et al., 1997; Itasaki et al., 1999; Krull, 2004). In the studies presented here, neural tubes from stage 14-16 chick embryos were microinjected at future T and LS levels with 1.25 μg/μl DNA plasmid constructs encoding wild-type or mutant Hoxd10, Hoxd11, and/or EGFP (see below for construct design). DNA was diluted in Tris-EDTA, pH 8.0, with 0.05% Fast green for visibility during injection. Following injection, embryos were bathed in sterile saline and electroporated using gold 0.5 mm electrodes. Current was delivered in 3 pulses (50 millisecond duration, charging voltage of 17V) by a square pulse electroporator (BTX).

2.3 DNA CONTRUCTS

Experimental embryos discussed in the studies present here were electroporated with a number of different constructs (Figure 2.1).

2.3.1 β-actin::Hox

One set of constructs was made by insertion of a full-length chicken *hoxd10* or *hoxd11* (provided by C. Tabin) into the multiple cloning site of the pMES vector (provided by C. Krull) (Figure 2.1A). The pMES vector consists of pCAX (M. Kobayashi) with the addition of the *ires-egfp* fragment from pIRES2-EGFP (Clontech). Gene expression is driven ubiquitously at high levels in progenitor and postmitotic neural cells by a β-actin promoter and CMV enhancer. The presence of the *ires-egfp* (IRES, internal ribosomal entry site; EGFP, enhanced green fluorescent protein) sequence allows the translation of both the gene of interest and EGFP from a single mRNA transcript. Thus, EGFP acts a marker of all transfected cells. Throughout the text, embryos electroporated with constructs expressing the gene of interest under the β-actin promoter are labeled "β-actin::Hox"; embryos expressing EGFP alone under this promoter are labeled "β–actin::control". Transfection efficiency (the percent of motoneurons expressing EGFP at stage 29) with this vector was 25% for Hoxd10, 34% for Hoxd11, and 37% for control embryos (n=3).

2.3.2 Hb9::Hox

A second group of constructs was generated by inserting full-length *hoxd10*, *hoxd11*, or $hoxd10^{d11HD}$ (see below), and the *ires-egfp* fragment from pIRES2-EGFP, in frame, into a pBluescript-based vector containing the 9kb Hb9 promoter (provided by S. Pfaff), which drives gene expression specifically in postmitotic motoneurons (Arber et al., 1999, Thaler et al., 1999) (Figure 2.1B). To accomplish this, the genes of interest were first inserted into the pIRES-EGFP vector. The fragment encoding *hox+ires-egfp* was then amplified using a polymerase chain

reaction (PCR). Forward primer 5'- GGC GCG CCT TAT GAC CGA GTT TGA CGA TTG CAG T-3' and 5'-GGC GCG CCT TAT GTC CTT TCC CAA CAG CTC TCC T-3' added an AscI restriction site to the 5' ends of *hoxd11* and *hoxd10/hoxd10*^{d11HD}, respectively. Reverse primer 5'- CTG ATT ATG ATC TAG AGT CGC GGC CGC T-3' hybridized near the 3' end of the EGFP sequence and contained a BsaBI (blunt cutter) restriction site. The PCR product was digested with AscI and BsaBI and inserted into the Hb9 vector between its AscI and PmeI (blunt cutter) sites. Correct insertion was confirmed by sequencing. Genes of interest were similarly cloned into an alternate Hb9 vector containing an abbreviated Hb9 promoter sequence and a minimal CMV enhancer (also provided by S. Pfaff) (Figure 2.1C). Results derived from experiments in which Hox overexpression was driven by the full-length Hb9 promoter did not differ from those of equivalent experiments with the abbreviated Hb9 promoter. Data from the two types of Hb9 constructs were therefore pooled. Throughout the text, embryos electroporated with Hb9 promoter-driven Hox constructs are labeled "Hb9::Hox"; those electroporated with Hb9-driven EGFP alone are labeled "Hb9::control". Transfection efficiency (the percent of motoneurons expressing EGFP at stage 29) with this vector was 15% for Hoxd10, 26% for Hoxd11, and 26% for control embryos. The low transfection efficiency for Hb9::d10 reflects its rapid downregulation before stage 29 (see Figure 3.2; n=3).

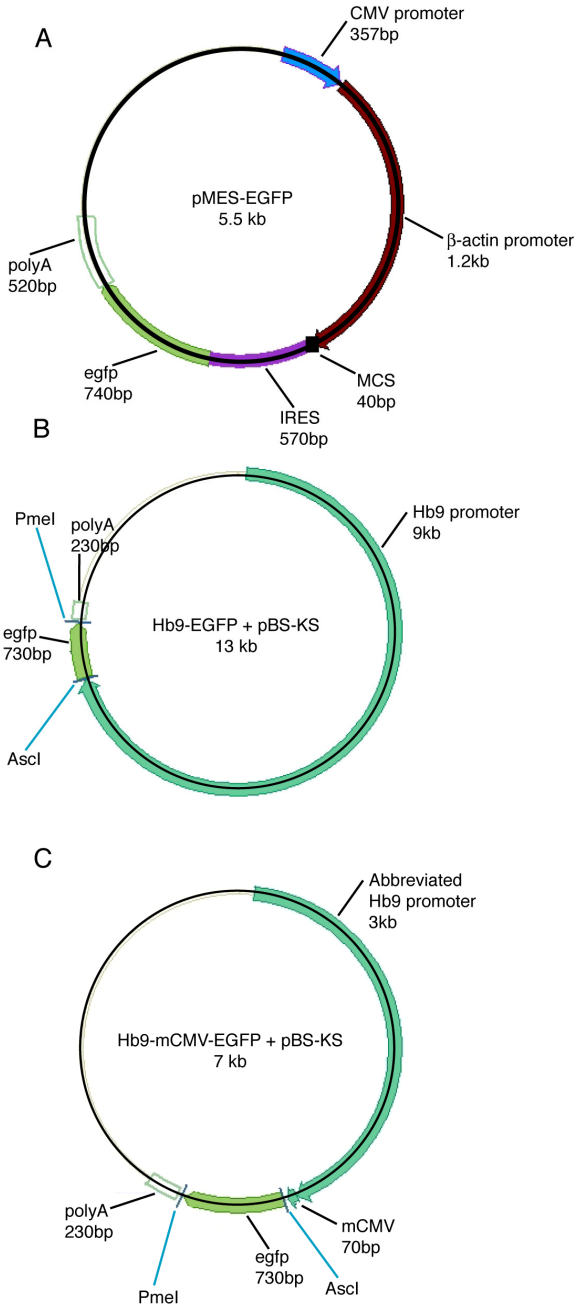

Figure 2.1 Schematic representation of primary vectors.

2.3.3 Hoxd10^{d11HD}

Experiments described in Chapter 5 utilized a mutated form of *hoxd10* in which the sequence encoding the homeodomain of the protein has been replaced with that encoding the homeodomain of Hoxd11. Domain replacement was accomplished via the "megaprimer" method of PCR (Barik, 2002), a large-scale site-directed mutagenesis technique. This method involves serial PCR reactions to first produce an oligonucleotide containing the desired mutations and then use this "megaprimer" to introduce those mutations into the gene of interest (Figure 2.2). To make Hoxd10^{d11HD}, the 180bp homeodomain-encoding region of *hoxd11* was amplified via traditional PCR (PCR-I) using the following primers: forward (A), 5'-AAC CAG CAA TTG GCT AAC TGC AAA GAG TTC GAG GAA AAA GAG GTG-3', and reverse (B), 5'-CGG ATT CGG TTC TCC CTT CAT CCT TCG ATT CTG GA-3'. These primers added a sequence identical to the flanking sequences of the homeodomain-encoding region of *hoxd10* (underlined) to each end of the amplified *hoxd11* homeodomain sequence. The forward primer included an XcmI restriction site for subsequent cloning. The product of PCR-I was then used as a forward megaprimer (AB) for a second PCR reaction (PCR-II). The reverse primer (C), 5'-CTG AAC GAC TAC TAT TCC ACA TAT GC-3', shared homology with a sequence 3' of the *hoxd10* homeodomain and contained an NdeI restriction site. The product of PCR-II was digested with XcmI and NdeI and inserted into the *hoxd10* cDNA, replacing its endogenous homeodomain. Correct mutation and insertion were confirmed via sequencing.

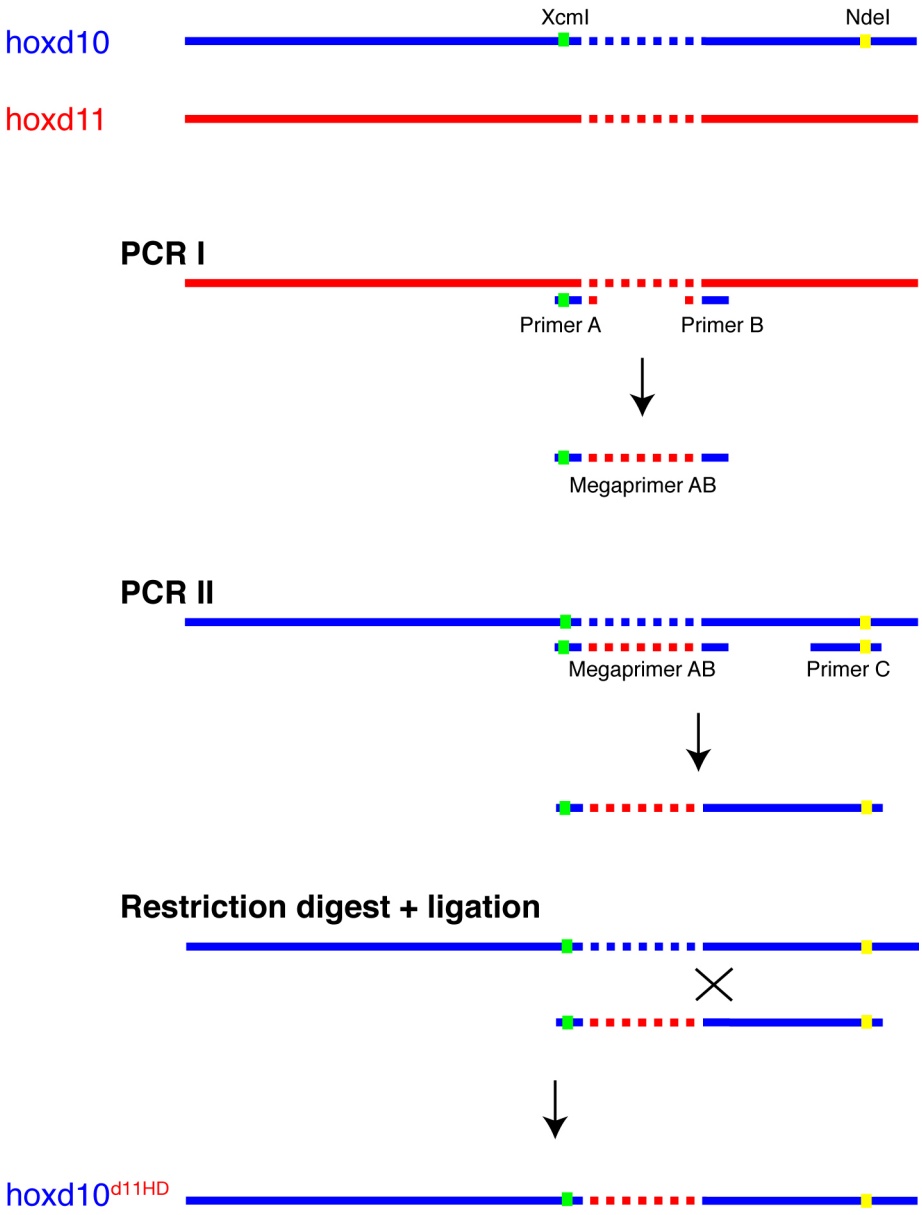

Figure 2.2 Schematic representation of the construction of Hoxd10^{d11HD}.

Homeodomain-encoding sequences are represented by dotted lines.

2.4 IN SITU HYBRIDIZATION AND IMMUNOHISTOCHEMISTRY

Several types of histological processing were used in these studies to visualize the expression of protein and mRNA in electroporated embryos. In preparation for processing, dissected chick embryos were first fixed in 4% paraformaldehyde for a minimum of 1.5 hours, maximum overnight, washed, cryoprotected in 30% sucrose, embedded in 50:50 30% sucrose:OCT, frozen, and sectioned at 14 um. Serial transverse sections were placed on three sets of slides in an alternating pattern to permit processing of adjacent sections with different techniques. For in situ hybridization, digoxygenin-labeled RNA probes were synthesized according to the supplier's protocol (Roche Applied Sciences). Hybridization was performed using modified protocols of Nieto et al. (1996) and Schaeren-Wiemers and Gerfin-Moser (1993). A construct encoding the Isl1 RNA probe was provided by T. Jessell. Immunohistochemistry was performed according to standard protocols. The antibodies used are listed in Table 2.1. Cy2-, Cy3-, and Cy5-conjugated secondary antibodies raised in both donkey and goat (Jackson Immunoresearch) were used for fluorescent imaging. For bright field imaging, 3,3-diaminobenzidine (DAB) immunoprocessing with an ABC kit (Vector Laboratories) was used.

2.5 RETROGRADE LABELING

In order to examine motor pools and motoneuron projections in experimental embryos, individual muscles or muscle groups in the hindlimb of stage 29-30 chicks were injected with 10% rhodamine-conjugated dextran in 0.5% Triton-X/saline solution. (Yip et al., 1998). Dissected embryos were incubated in oxygenated Tyrode's saline for 4-8 hours at 32°C. During

this time, the dye was retrogradely transported to the cell bodies of the motoneurons projecting to the injected muscle. Embryos were then fixed and sectioned horizontally at 14μm. Rhodamine-labeled cells were easily identifiable using fluorescence microscopy. Retrograde labeling was often combined with EGFP immunofluorescence staining.

2.6 GENERAL CELL QUANTIFICATION TECHNIQUES

To quantify differences between transfected and non-transfected sides of the spinal cord following electroporation, or to compare Hox-transfected and EGFP-transfected embryos, counts of neuronal subtypes were made on transverse sections through LS segments at various developmental stages. Segment number and boundaries were identified by reference to dorsal root ganglia and spinal nerves on the non-transfected side. Three sections per segment were chosen for counting based on their position in that segment (i.e. three sections equidistant from one another in the middle of a segment). Somatic motoneuron status was assigned to cells positive for Isl1(2) antibody staining (a pan-motoneuron marker) and located within three cell-widths of the dorsal edge of the visible somatic motor column cluster. Chx10 was used as a marker of V2 interneurons. Cells exhibiting a molecular profile of interest were identified in micrographs of LS spinal cord sections, dotted in Adobe Photoshop, and imported into a counting program (designed by N. Roy, Massachusetts Institute of Technology). Expression of a diffuse non-nuclear protein, RALDH2, was quantified by utilizing the imaging software NIH ImageJ (1.37v) to measure mean pixel intensity in circumscribed regions of micrographs. Finally, to quantify positions of transfected motoneurons, a grid was superimposed on the ventral spinal cord (see Figure 3.5). The medial edge and dorsal edges of the grid were aligned with the

Table 2.1 List of antibodies.

Antibody	Species	Source	Dilution	Identifies	Reference
Lim3	rabbit	S. Pfaff	1:2500	MMC	Sharma et al., 1998
Hoxd10	guinea pig	T. Jessel	1:8000	LS spinal cord	Dasen et al., 2005
Hoxd11	rabbit	T. Jessel	1:16000	Caudal LS spinal cord	Dasen et al., 2005
Lim1	rabbit	T. Jessel	1:40000	LMCl	Tsuchida et al., 1994
Scip	guinea pig	T. Jessel	1:8000	MMCl	Dasen et al., 2008
Foxp1	rabbit	T. Jessel	1:32000	LMC	Dasen et al., 2008
Chx10	rabbit	T. Jessel	1:4000	V2 interneurons	Thaler et al., 1999
EGFP	rabbit	Invitrogen	1:1500	transfected motoneurons	
EGFP	mouse	Invitrogen	1:500	transfected motoneurons	
EGFP	goat	Rockland Immunochemicals	1:500	transfected motoneurons	
Isl1(2)	mouse	DSHB	1:100	all motoneurons	Tsuchida et al., 1994
Lim3	mouse	DSHB	1:100	MMC	Ericson et al., 1997
RALDH2	rabbit	P. McCaffery	1:2500	LMC	Berggren et al., 1999
activated caspase 3	rabbit	Promega	1:250	apoptotic nuclei	

ventricular zone and the dorsal edge of the LMC cluster, respectively. The lateral edge of the grid was aligned with the lateral edge of the LMC cluster such that the dorsoventral midpoint of the grid coincided with the widest point in the spinal cord. Significance of effects was determined by comparing data sets using the Student's t-test. For comparisons of transfected and non-transfected sides of spinal cord sections, the data were paired; an unpaired test was used for comparisons of Hox-transfected and control EGFP-transfected sections.

2.7 MICROSCOPY AND PHOTOGRAPHY

The images appearing in this thesis were taken using a Nikon Eclipse E600 compound microscope and a QImaging Retiga 2000R camera. Tissue sections labeled with three antibodies

were examined and photographed using an Olympus Fluoview FV1000 confocal unit fitted to an Olympus BX61 microscope.

3.0 HOXD10 MEDIATES DEVELOPMENT OF THE LATERAL LMC IN THE LUMBOSACRAL SPINAL CORD OF THE DEVELOPING CHICK

3.1 INTRODUCTION

As described in Chapter 1, individual spinal segments possess unique complements of motoneuron subtypes. These subtypes sort within the spinal cord, forming discrete motor columns and motor pools with well-defined rostrocaudal and mediolateral spatial coordinates. A distinguishing feature of the lumbosacral (LS) and brachial spinal regions is the presence of a lateral motor column (LMC), which is composed of somatic motoneurons that project to muscles of the adjacent limb. Within the LMC, motoneurons sort into lateral and medial divisions (LMCl and LMCm) that contain the soma of dorsal-projecting and ventral-projecting motoneurons, respectively (see Figure 1.1A). Further, within these divisions, motoneurons cluster by muscle target, forming multisegment-spanning motor pools. For example, motoneurons projecting to the sartorius, a dorsal hindlimb muscle, exist in a pool within the LMCl of lumbosacral segments 1-2. Thus, the position of a motoneuron along the mediolateral and rostrocaudal axes of the spinal cord is tightly coupled to the identity of its peripheral target (see Figure 1.1B).

Although individual motoneurons ultimately adopt highly specialized fates, they all arise from an apparently homogeneous progenitor population (Leber et al., 1990; Jessell, 2000). As such, they provide an ideal experimental system for defining the molecular mechanisms

responsible for postmitotic neuronal diversification. Investigators have identified and characterized many components of the transcriptional hierarchy active in the specification of postmitotic motoneurons, including members of the LIM and ETS transcription factor families (reviewed in Jessell, 2000; Shirasaki and Pfaff, 2002). Recent studies suggest that members of the Hox family of transcription factors, markers of segmental identity in a variety of developing systems, occupy a high-ranking position within this hierarchy. Hox genes are expressed within restricted domains along the rostrocaudal axis of the spinal cord. These domains partially overlap, but have different rostral and caudal limits, such that individual segments at varying axial levels express a unique complement of Hox genes, just as they possess a unique complement of motoneuron subtypes. Limits of Hox expression often correspond with limits of unique regional anatomical features; for example, the caudal limit of Hoxc6 expression coincides with the caudal boundary of the brachial spinal cord, and therefore demarcates a transition in motoneuron columnar organization from brachial (medial motor columns and LMC) to thoracic (medial motor columns (MMC) and sympathetic preganglionic Columns of Terni (CT)) (Dasen et al., 2003).

In light of such expression patterns, recent investigations have sought to establish a functional link between Hox expression and motoneuron subtype complement. Gain- and loss-of-function studies in brachial segments have shown that Hox genes are sufficient to pattern motoneuron columnar and pool subtypes in the spinal cord. For example, misexpression of Hoxc9 in brachial segments results in columnar shift, as evidenced by the appearance of motoneurons bearing molecular and positional characteristics of the thoracic CT (Dasen et al., 2005). Hox5, Hoxc6, and Hoxc8 have been examined in similar fashion and, in each case, were

shown to dictate the position and size of specific motoneuron populations (Dasen et al., 2003, 2005). Thus, Hox expression is not so much a marker of regional identity as a determinant of it.

The Hox studies described above focused primarily on the diversification of motoneurons in the brachial spinal cord, which innervates forelimb musculature. Less is known about the role of Hox genes in lumbosacral segments and hindlimb innervating motoneurons. It was previously shown that the anterior boundary of Hoxd10 expression demarcates the transition between the thoracic and lumbar/lumbosacral regions of the spinal cord (Burke et al., 1995; Carpenter et al., 1997; Lance-Jones et al., 2001) (Figures 3.1A and 1.2), raising the intriguing possibility that it contributes to patterning the segmental limits of the lumbosacral spinal cord. Hoxd10 loss-of-function mouse mutants seem to confirm this hypothesis; they exhibit posterior shifts in the thoraco-lumbar boundary, and consequently in the position of the lumbar LMC (Carpenter et al., 1997; Lin and Carpenter, 2003). Conversely, misexpression of Hoxd10 in chick thoracic segments leads to the appearance of ectopic LMC-like cells with positional, molecular, and projectional characteristics of anterior lumbosacral motoneurons (Shah et al., 2004).

Wu and colleagues (2008) recently examined the effects of loss of both Hoxc10 and Hoxd10 function in LS spinal motoneurons. They noted a caudal shift in the thoraco-lumbar boundary, consistent with previous loss-of-function studies (Carpenter et al., 1997; Lin et al., 2003). In addition, however, they observed that Hoxc10/Hoxd10 double mutant animals exhibited a complete or near-complete loss of the LMCl. No change was detected in the LMCm or medial motor columns (MMC). They concluded that Hoxc10 and Hoxd10 coordinately regulate both the rostrocaudal placement of the LMC and the development of the LMCl. They were unable, however, to make conclusions regarding the individual contributions of each Hox gene to this process. Studies presented in this chapter address the specific role of Hoxd10 in the process of

lumbosacral motoneuron subtype specification in the embryonic chick. Spatial and temporal variations in its expression within the developing LS cord suggest that it may serve multiple functions during motoneuron development. This hypothesis was tested by evaluating the effects of Hoxd10 overexpression on lumbosacral motoneuron subtype development. The results of these experiments suggest that Hoxd10 is critical to the development of LMCl motoneurons in rostral LS segments.

3.2 HOXD10 EXPRESSION IN THE LUMBOSACRAL SPINAL CORD OF THE DEVELOPING CHICK

While prior studies detailed the distribution of *hoxd10* transcript (Lance-Jones et al., 2001), limited information on protein expression was available (Dasen et al., 2005). I therefore began my analysis of Hoxd10 function by assessing protein distribution at Hamburger-Hamilton stages 24 and 29 and comparing it to that of the LIM HD transcription factors, markers of motoneuron subtype identity. In Figure 3.1C-E and I-K, LMC divisions are indicated by immunofluorescence staining with antibodies against Lim1 (green), which marks LMCl, and Isl1(2), which marks all motoneurons (Tsuchida et al., 2004). At stage 24, as motor columns are forming and motoneurons are diversifying (see Table 1.1), Hoxd10 is expressed throughout the rostrocaudal axis of the LS cord (Figure 3.1F-H; see also Lance-Jones et al., 2001). Its expression is widespread among all but the most recently born motoneurons, as indicated by co-labeling with the pan-motoneuron marker Isl1(2) (Figure 3.1B). However, by stage 29, once motor columns and their divisions have formed, expression of Hoxd10 is restricted to subsets of motoneurons (Figure 3.1L-N). Comparison of Hoxd10 expression with motoneuron columnar divisions

indicates that at stage 29 in rostral LS segments, Hoxd10 is confined to LMCl motoneurons (Figure 3.1I,L), while in middle LS segments, it overlaps with medial motoneurons (Figure 3.1J,M). Interestingly, Hoxd10 appears to have been largely downregulated in caudal LS segments between stages 24 and 29. Its absence in these segments parallels the near absence of LMCl cells, as shown in Figure 3.1K and N. The transition from uniform expression to segment- and subtype-specific expression strongly suggests a shift in the role of Hoxd10 between stages 24 and 29, perhaps from that of a general promoter of LS identity, as suggested by previous studies (Carpenter et al., 1997; Shah et al., 2004), to that of a specific promoter of individual motoneuron subtypes.

3.3 HOXD10 EXPRESSION UNER THE HB9 PROMOTER IS RAPIDLY DOWNREGULATED

To more closely examine the function of Hoxd10 in LS motoneuron development, I chose to utilize an experimental paradigm based on overexpression. This was accomplished via *in ovo* electroporation (see Chapter 2). The full-length sequence of hoxd10, along with the ires-egfp sequence from pIRES2-EGFP (Clontech), was cloned into vectors that drive gene expression under the postmitotic motoneuron-specific Hb9 promoter. A construct expressing EGFP alone under the same promoter was used as a control. Vector plasmids were transfected into the neural tube via *in ovo* electroporation at stages before motoneurons are born (stages 14-16, Hollyday and Hamburger, 1977) and most embryos were sacrificed at stages during (stages 22- 25) or after motor column formation (stages 29-30).

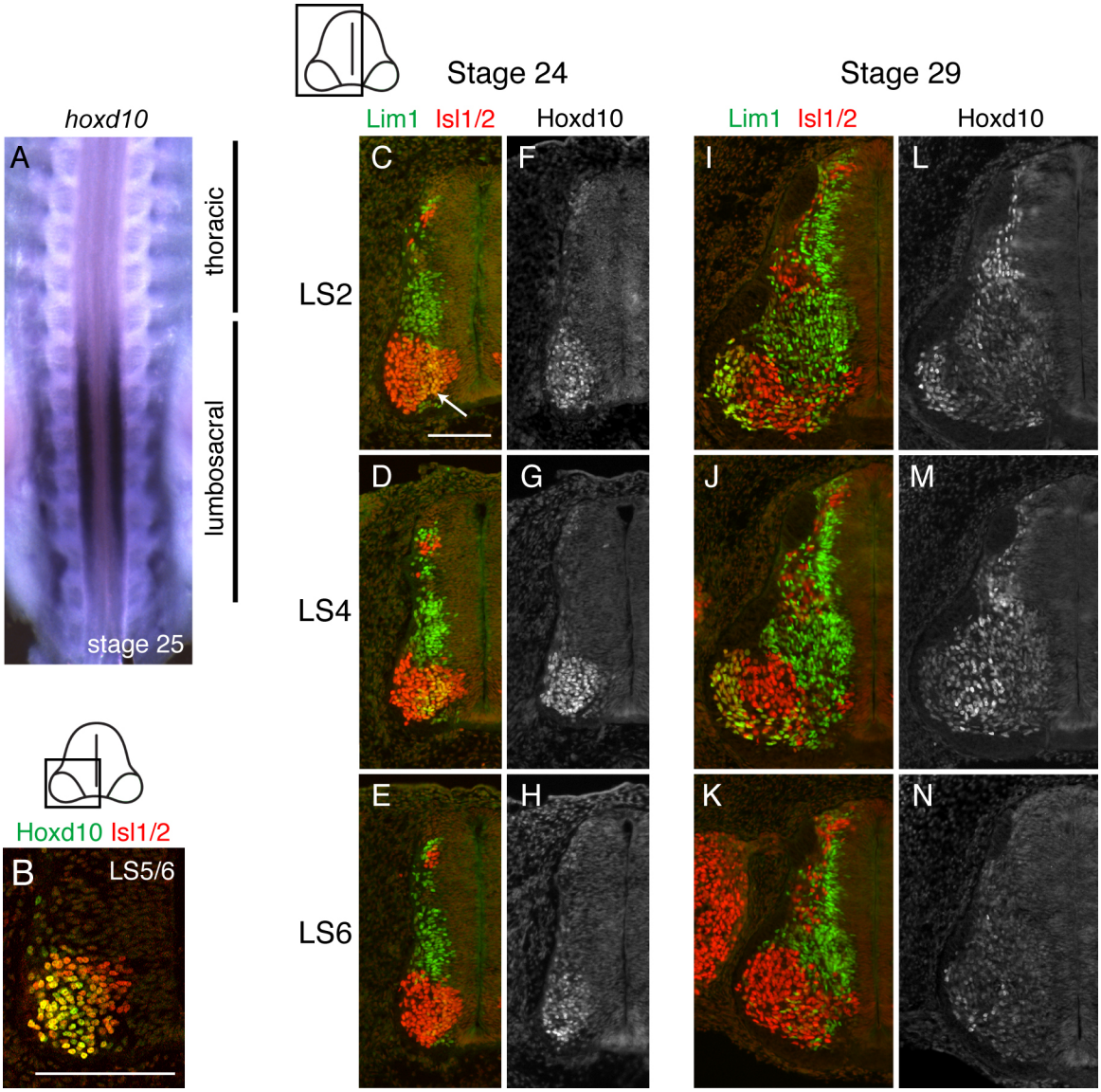

Figure 3.1 Normal expression of Hoxd10 in the LS segments of stage 24-29 chick embryos.

A. Whole mount in situ hybridization at stage 25 demonstrating that the rostral limit of Hoxd10 expression coincides with the thoraco-lumbosacral boundary. B-N. Transverse sections through the LS cord at various stages and levels. B. Hoxd10 is expressed by most Isl1(2)+ motoneurons at stage 24. C-H. Expression of Hoxd10 along the length of the LS cord during stages of motor column formation and motoneuron diversification. Note the onset Lim1 expression in a subset of motoneurons (arrow). I-N. Restricted expression of Hoxd10 at stages after motor column formation. Scale bar = 100μm.

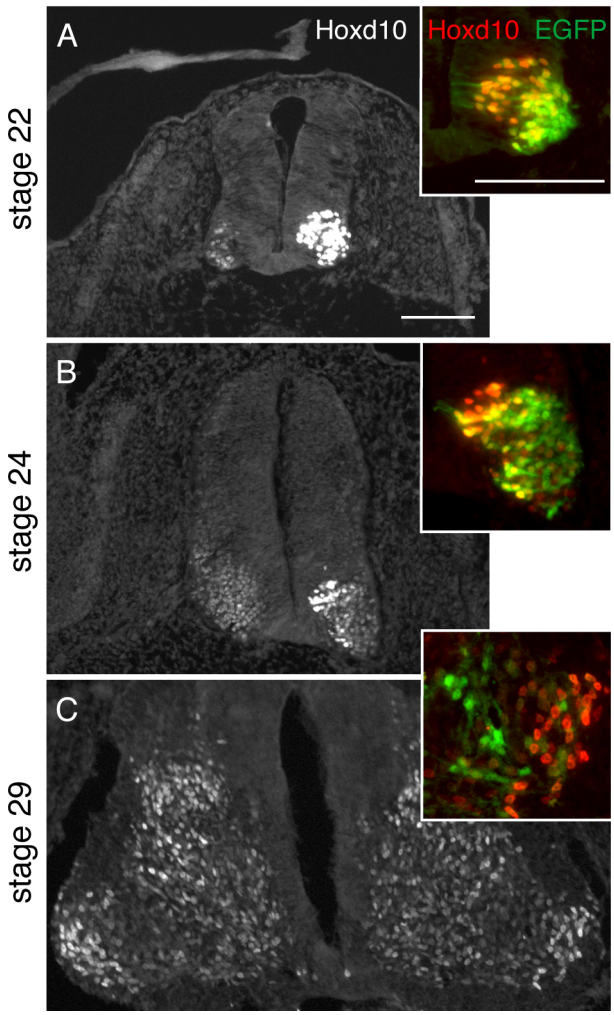

Figure 3.2 Ectopic expression of Hb9::Hoxd10 in rostral LS segments.

A-C. Transverse sections through rostral LS segments at stages 22-29. A-B. Ectopic Hoxd10 and EGFP expression levels are high on transfected sides of the spinal cord in young embryos. Insets indicate levels of EGFP/Hoxd10 colocalization. C. Expression of ectopic Hoxd10 and EGFP is extinguished by stage 29. Scale bars = 100μm.

Following electroporation with Hb9::d10, evidence of Hoxd10 overexpression was readily detectable in lumbosacral segments at stages 22-24 (Figure 3.2A-B, n=10). Transfected sides of spinal cords expressed visibly higher levels of Hoxd10 than their non-transfected counterparts. At stage 22, Hox expression colocalized precisely with EGFP (Figure 3.1A, inset). Overall expression levels and EGFP colocalization decreased, however, with increasing embryonic age. At stage 24, Hoxd10 overexpression was detectable only in newborn cells just leaving the ventricular zone (Figure 3.2B), suggesting that earlier born motoneurons had already ceased to produce ectopic Hoxd10. Moreover, by stage 29, visible Hoxd10 overexpression was either completely extinguished (Figure 3.2C, n=3/4) or present in only a few lateral motoneurons (n=1/4; data not shown). Overall EGFP levels at this stage were quite low compared to both early time points and EGFP levels in stage 29 Hb9::control embryos (see Figure 4.6A). Ectopic Hoxd10 under the Hb9 promoter is therefore only transiently expressed in developing motoneurons, and may directly or indirectly regulate its own expression.

3.4 BRIEF HOXD10 OVEREXPRESSION TRANSIENTLY UPREGULATES EXPRESSION OF LMCL MARKERS

As noted above, caudal LS segments possess a much smaller complement of LMCl motoneurons than rostral segments at stage 29. This pattern parallels that of Hoxd10 – its expression is diminished in caudal LS segments and highest in rostral segments, where the LMCl is prominent (see Figure 3.1H-M). These observations suggest a direct correlation between Hoxd10

expression levels and LMCl size. I therefore began my assessment of electroporated Hb9::d10 embryos by examining the distribution of motoneuron columnar subtypes.

To determine the effects of the early and transient increase in Hoxd10 resulting from electroporation with Hb9::d10, LS2 sections from stage 23-25 experimental embryos were immunolabeled with antibodies against Isl1(2) and Lim1. As described above, Isl1(2) is expressed by all motoneurons (LMC and MMC), while Lim1 marks only LMCl. An antibody against EGFP was used to identify all transfected cells. Counts of motoneuron subtypes within transverse sections revealed that while the total number of motoneurons ($Isl1(2)^+$ cells) on the transfected side of the cord did not differ from that on the non-transfected control side, the number of $Lim1^+$ motoneurons was increased by about 26% (Figure 3.3A-B, E; Table 3.1). Further, while $Lim1^+$ motoneurons made up only 29% of the total motoneuron population on the transfected side, they made up 42% of the $EGFP^+$ population (Table 3.1). It should be noted that in this and all subsequent experiments, counts of motoneurons were made on three non-adjacent sections per embryo with 4-6 embryos making up each experimental group (see Chapter 2).

The observed increase in $Lim1^+$ motoneurons suggested that Hoxd10 overexpression initiated an early fate switch in motoneurons from medial (LMCm or MMC) to lateral (LMCl) differentiation pathways. In order to determine whether the increase came at the expense of the LMCm or the MMC, transfected LS2 sections were immunolabeled with Foxp1, a Forkhead domain transcription factor that is normally expressed by both LMCl and LMCm motoneurons, but not by MMC motoneurons (Rousso et al., 2008; Dasen et al., 2008). Total numbers of $Foxp1^+$ motoneurons cells were similar on transfected and non-transfected sides, implying that increases in LMCl likely came at the expense of LMCm (Figure 3.3C-D,E; Table 3.1), and that MMC numbers were unaffected by Hoxd10 overexpression.

Table 3.1 Quantification of motoneuron transcription factor expression in control and Hoxd10-electroporated chick LS segments.

Experimental subsets	# of motoneurons				% of motoneurons			% of transfected motoneurons			
	n[1]	nt[2]	t		nt	t		n	control[4]	Hox	
Hb9::Hoxd10 - Stage 23-25											
LS2											
Isl1(2)+	4	149±9	149±9								
Lim1+	4	34±5	43±1	**[3]	22±2	29±2	**			42±3	
Foxp1+	6	123±6	117±6								
Hb9::Hoxd10 - Stage 29											
LS2											
Isl1(2)+	4	191±7	187±10								
Lim1+	4	62±4	59±3		32±1	32±2					
Isl1(2)^{high}+	4	72±3	72±5		38±1	39±2					
β-actin::Hoxd10 - Stage 29											
LS2											
Isl1(2)+	5	162±5	119±5	***							
Lim1+	5	58±3	51±3	**	35±1	43±2	***	4	39±3	48±2	*
Isl1+	4	72±6	37±4	***	51±3	40±3	***	4	36±4	19±2	***
LS5											
Isl1(2)+	4	181±5	119±7	***							
Lim1+	4	43±3	40±2		24±1	34±2	***				
Hb9::control - Stage 29											
LS2											
Isl1(2)+	6	204±8	186±8								
Lim1+	6	79±5	71±3		38±1	38±1					
Isl1(2)^{high}+	6	76±4	73±4		37±1	39±1					
β-actin::control - Stage 29											
LS2											
Isl1(2)+	5	158±6	160±3								
Lim1+	5	63±3	61±3		40±1	38±2					

1. n=number of embryos analyzed. In each embryo, three non-adjacent sections within the same segment were counted.
2. nt, non-transfected side of the spinal cord; t, transfected side of the spinal cord.
3. Asterisks represent significance, based on paired or un-paired t-tests. *$p<0.05$; **$p<0.01$; ***$p<0.001$.
4. The term "control" describes embryos electroporated with a control construct expressing EGFP alone. "Hox" describes embryos electroporated with a construct encoding EGFP and either Hoxd10 or Hoxd11.

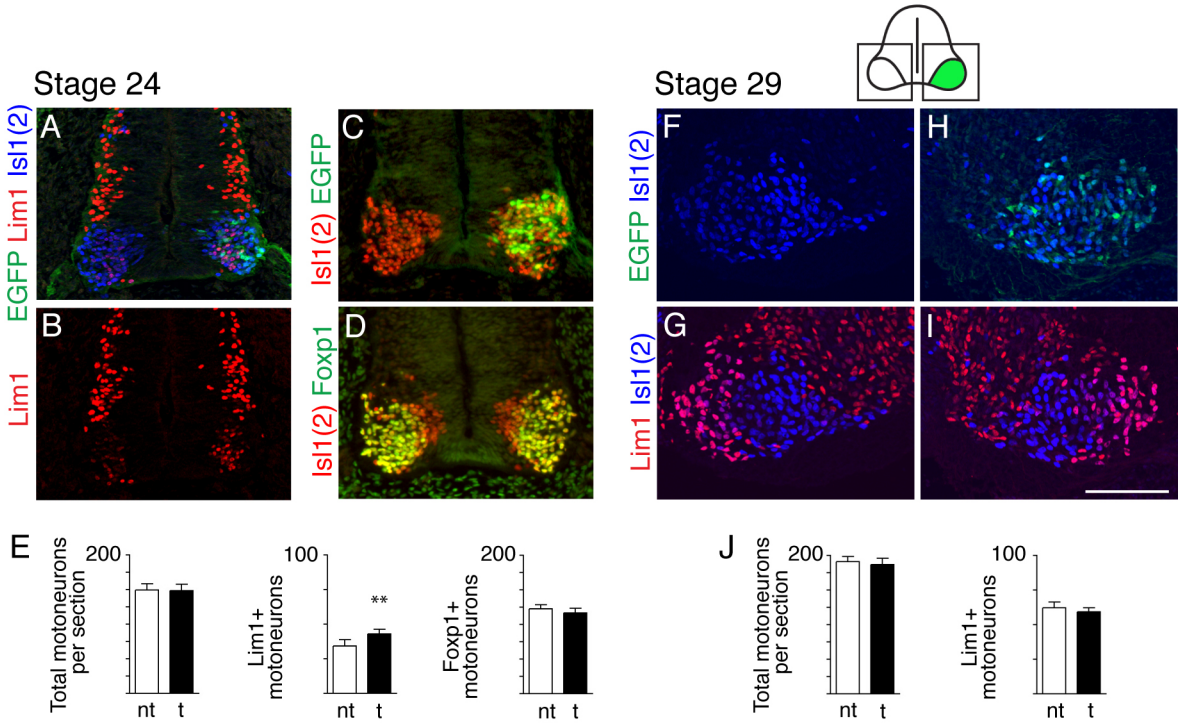

Figure 3.3 Hb9::d10 transiently induces increases in the expression of the LMCl marker Lim1.

A-D. Transverse sections from stage 24 experimental embryos. Transfected sides of the cord show an increase in Lim1+ motoneurons but no change in total motoneuron or LMC (Foxp1+) numbers. Isl1(2) was used as a pan-motoneuron marker. E. Histograms depicting quantification of effects in A-D. F-J. Increases in Lim1+ motoneurons are not maintained through stage 29. Scale bar = 100μm.

Transfected LS2 sections were also examined in stage 29 Hb9::d10 embryos, by which time evidence of Hoxd10 overexpression was lost. In contrast to embryos sacrificed at earlier stages, counts of both total motoneuron numbers and Lim1^{+} populations were similar on transfected and non-transfected sides (Figure 3.3F-J; Table 3.1). Taken together, these data demonstrate that transient Hoxd10 overexpression is sufficient to induce but not maintain the expression of the LMCl marker Lim1. In normal embryos, LMCl motoneurons in LS2 retain high levels of

Hoxd10 through stage 29 (Figure 3.1L) suggesting that these cells may require sustained Hoxd10 expression to maintain their Lim1$^+$ phenotype.

3.5 SUSTAINED HOXD10 OVEREXPRESSION SHIFTS MOTONEURON PROPORTIONS IN FAVOR OF LMCL

Given that short-term increases in Hoxd10 expression led to short-term increases in presumptive LMCl numbers, I next sought to test the hypothesis that sustained overexpression of Hoxd10 effects long-term changes in subtype complement. To do so, Hoxd10 was cloned into the pMES vector for use in *in ovo* electroporations of the LS neural tube. This vector utilizes a β-actin promoter to drive ectopic gene expression in all neural cells and includes an *ires-egfp* to report protein expression (see Figure 2.1A). A construct expressing EGFP alone under the β-actin promoter was used as a control. Figure 3.4A demonstrates that transfected cells in LS2 sections from β-actin::d10 embryos co-express high levels of Hoxd10 through stage 29.

LS2 sections from stage 29 β-actin::d10 embryos were initially stained with antibodies against Isl1(2) and Lim1 to identify total motoneurons and LMCl motoneurons, respectively, on transfected and non-transfected sides of the cord. At stage 29, however, rostral segments contain a unique population of LMCl motoneurons (those innervating the Femorotibialis internus (iF), a thigh muscle) that express neither Lim1, nor the LMCm and MMC marker Isl1 (Tsuchida et al., 1994; Lin et al., 1998). Adjacent sections were therefore stained with a digoxigenin-tagged in situ probe against Isl1 mRNA transcript in combination with the pan-motoneuron Isl1(2) antibody in order to specifically distinguish the Isl1-expressing LMCm and MMC populations. This technique causes Isl1$^+$ motoneurons to appear as dark brown in Figure 3.4E and F. The size

of the iF pool was ultimately estimated by subtracting the $Lim1^+$ and $Isl1^+$ numbers from the total number of motoneurons.

Counts revealed two noteworthy effects of Hoxd10 overexpression with the β-actin::d10 construct. The first was an unanticipated reduction in total motoneuron numbers on transfected sides of the cord, with no comparable loss in β-actin::control embryos (Figure 3.4G; Table 3.1). This reduction amounted to about 26%, and was observed in both rostral (LS2) and caudal (LS5) lumbosacral segments (Table 3.1). To determine if the diminished numbers resulted from early motoneurons and progenitors initiating apoptotic cell death, sections from stage 23-24 transfected embryos were immunostained with antibodies targeting activated caspase, a component of apoptotic signaling pathways. A slight increase in apoptotic nuclei was observed, from an average of a single apoptotic cell on non-transfected sides to 5 on transfected sides (Figure 3.4B; $n=5$; $p<0.0001$). Prior studies conducted in the lab (Shah, 2006) similarly reported an increase in apoptotic cells on the transfected sides of embryos sacrificed at stage 18. The severity of the reduction observed at stage 29 therefore likely reflects the cumulative effects of Hoxd10-initated apoptosis over time. Interestingly, electroporations with another HoxD family member, Hoxd11, under the β-actin promoter also caused a reduction in total motoneuron numbers (see Chapter 4; Figure 4.7F, Table 4.1), suggesting that Hox genes may have a generic effect on motoneuron survival when expressed at high levels.

The second effect of β-actin::d10 electroporation was to disproportionately reduce the size of the $Isl1^+$ LMCm+MMC population (darkly stained cells in Figure 3.4E and F) in comparison to the $Lim1^+$ LMCl population (yellow cells in Figure 3.4C and D). Though both LMCm+MMC and LMCl numbers were reduced in LS2 (Figure 3.4G; Table 3.1), the percentage of motoneurons expressing $Isl1^+$ decreased from 51% to 40% on non-transfected versus

transfected sides of the spinal cord, while Lim1$^+$ LMCl percentages increased from 35% to 43% (Figure 3.4H; Table 3.1). Lim1$^+$ proportions in LS5 of β-actin::d10 embryos showed a similar effect, increasing from 24% to 34% (Table 3.1). The direction of these proportional shifts therefore mirrored the observed absolute increases in Lim1$^+$ cells observed in Hb9::d10 embryos, despite motoneuron loss.

While overall shifts in motoneuron subtype proportions hint at a possible role for Hoxd10 in LMCl specification, establishing a direct link between Hoxd10 expression and Lim1 expression required analysis of subtype proportions specifically within the transfected population of motoneurons. To accomplish this, LS2 sections from β-actin::control and β-actin::d10 embryos were triple labeled with anti-Lim1, -Isl1(2), and -EGFP antibodies (Figure 3.5A,E). This type of processing precluded the inclusion of Isl1 mRNA staining; therefore, to roughly identify and isolate LMCm+MMC motoneurons from the Lim1- LMCl population, I capitalized on the bimodal distribution of fluorescence intensity seen among the Isl1(2)$^+$ population. This antibody was originally generated against rat Isl1 (Tsuchida et al., 1994), and appears to show a marked preference for Isl1-expressing motoneurons in both mice and chicks. "Brightly" stained Isl1(2)$^+$ cells (Isl1(2)^{high}) normally appear in medial portions of the motor columns and correspond spatially to the position of Isl1$^+$ motoneurons (indicated by the long arrow in Figure 3.5C). "Lightly" stained populations (Isl1(2) $^{low)}$) are located laterally, corresponding to the positions of the Lim1$^+$/Isl2$^+$ and Lim1$^-$/Isl2$^+$ LMCl populations (the short arrow in Figure 3.5C). I utilized a fluorescence intensity threshold function in Adobe Photoshop to isolate and count transfected Isl1(2)^{high} motoneurons (Figure 3.5D,H). The threshold was set such that all Lim1$^+$ motoneurons, and therefore all cells with the same Isl1(2) staining intensity as the Lim1$^+$

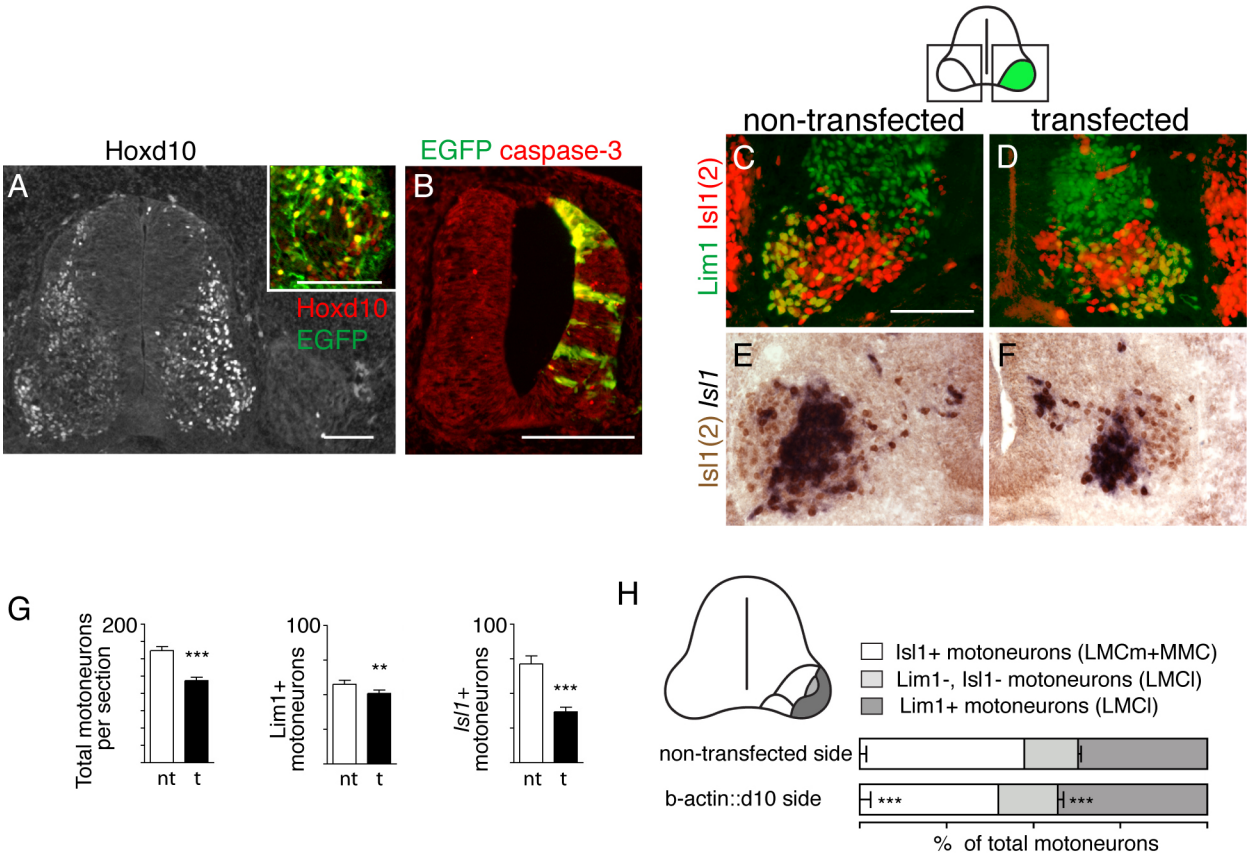

Figure 3.4 β-actin::d10 induces sustained changes in motoneuron subtype proportions.

A. Transverse section through rostral LS demonstrating ectopic Hoxd10 at stage 29 in β-actin::d10 experimental embryos. Inset shows colocalization of EGFP and Hoxd10. B. Section stained with antibody against activated caspase-3 demonstrates increased apoptotic cell death on transfected side of spinal cord. C-H Transfected sides of the cord demonstrate shifts in expression of LIM HD transcription factors Lim1 and Isl1, as indicated by Lim1 antibody staining and Isl1 in situ hybridization. Isl1(2) was used as a pan motoneuron marker. H. The proportion of Lim1+ LMCl motoneurons is increased, while the proportion of Isl1+ LMCm+MMC motoneurons is decreased. Schematic shows motor columns and divisions corresponding to graph. Scale bars = 100 μm.

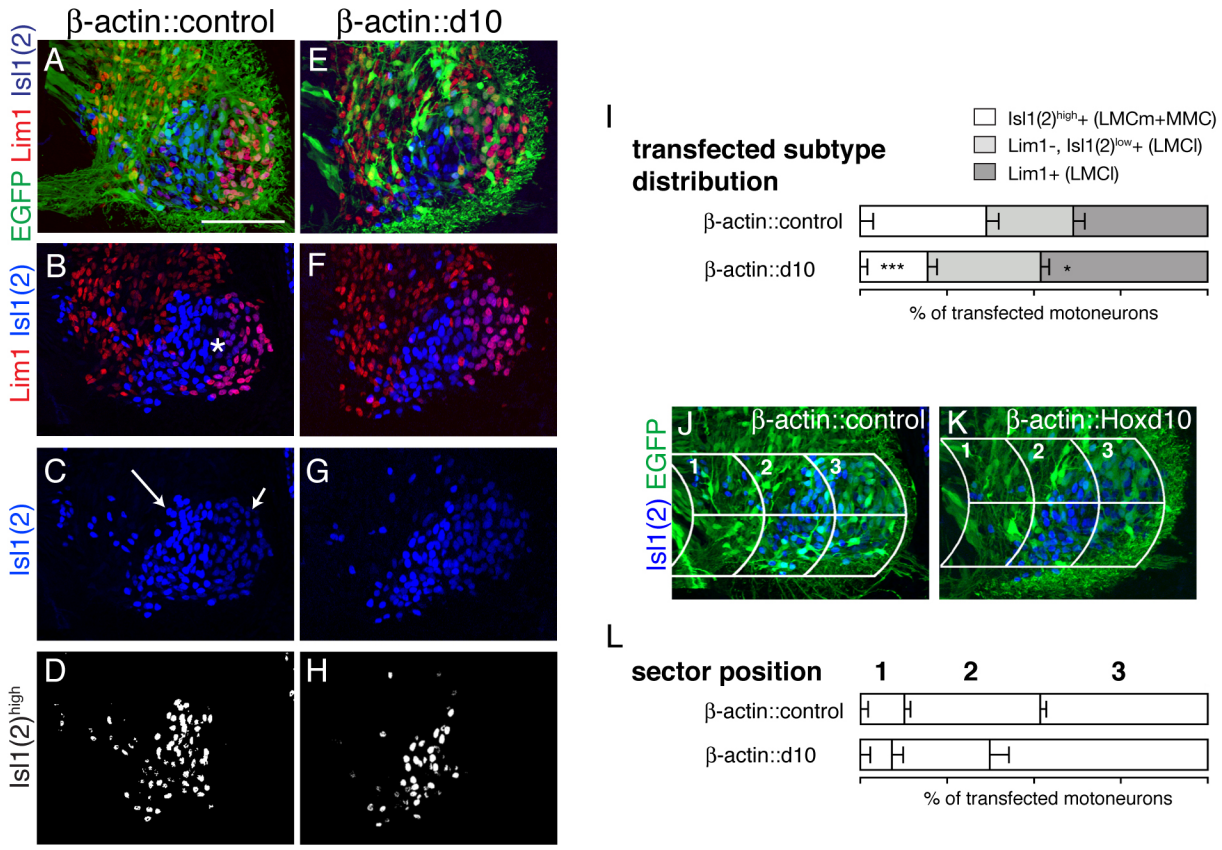

Figure 3.5 Hoxd10-transfected motoneurons adopt molecular and positional properties of LMCl.

A. Control transfected motoneurons are evenly distributed among motoneuron subtypes, as indicated by LIM staining. B-D. Isolation of Isl1(2)high motoneurons, presumptive LMCm+MMC. Asterisk in B indicates iF Isl1-, Lim- iF motoneurons. Short arrow in C indicates Isl1(2)^{low}, long arrow indicates Isl1(2)^{high}. D. Threshold function isolates Isl1(2)high motoneurons. E. Hoxd10-transfected motoneurons frequently express Lim1. F-H. Isolation of Isl1(2)^{high} motoneurons in a section from a β-action::d10 embryo. Total number of Isl1(2)^{high} cells appears smaller than control (D). I. Quantification of molecular distribution of transfected motoneurons in control and Hoxd10 embryos. J-K. In control embryos, transfected motoneurons are evenly distributed among the sectors of the grid. In experimental embryos, most transfected motoneurons are in sector 3. Isl1(2) is used as a pan-motoneuron marker. L. Quantification of positional distribution of transfected motoneurons in control and Hoxd10 embryos. Scale bar = 100μm.

population, were excluded. Among $EGFP^+$ transfected motoneurons in β-actin::d10 embryos, 48% coexpressed Lim1, compared to 39% in β-actin::controls (Figure 3.5I; Table 3.1). Conversely, 19% of $EGFP^+$ cells in experimental embryos coexpressed $Isl1(2)^{high}$, compared 36% in controls. Thus, shifts in motoneuron subtype marker expression within the population of Hoxd10-transfected motoneurons paralleled shifts in the motor columns as a whole, and directly linked Hoxd10 expression with the LMCl marker Lim1.

3.6 HOXD10-TRANSFECTED MOTONEURONS PREFERENTIALLY ADOPT A LATERAL POSITION AND A DORSAL AXON TRAJECTORY

Expression of the LIM transcription factor Lim1 is just one distinguishing feature of the motoneurons comprising the LMCl. These motoneurons are also defined by their lateral position and dorsal axonal trajectory. In order to quantify the positions of Hoxd10-transfected motoneurons in β-actin::d10 embryos, a tripartite grid was superimposed over micrographs of individual LS2 sections. This grid divided the ventral cord into three sectors: a sector adjacent to the ventricular zone (1), a medial motor sector (2), and lateral motor sector (3) (Figure 3.5J-K). In β-actin::control embryos, transfected motoneurons ($EGFP^+$, $Isl1(2)^+$ cells) were primarily located in sectors 2 and 3, with slightly more in the lateral sector (Figure 3.5J,L; $n=4$, $p< 0.006$, paired t-test). In contrast, in β-actin::d10 embryos, the mean percent of transfected motoneurons in sector 3, the most lateral position, was significantly increased when compared to that of β-actin::control embryos (Figure 3.5K-L; $n=4$, $p<0.02$, unpaired t-test). In fact, Hoxd10-

transfected motoneurons were more than twice as likely to be located in sector 3 than in sector 2 (Figure 3.5L; $p<0.0001$). These findings indicate that overexpression of Hoxd10 not only induced the expression of Lim1 of motoneurons, but also directed them toward a lateral settling position.

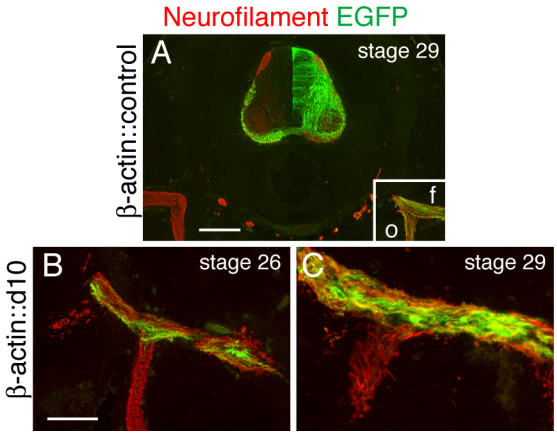

Figure 3.6 Axons for Hoxd10-transfected motoneurons preferentially adopt a dorsal trajectory in crural (anterior) limb regions.

A-C. Transverse sections, stained with anti-EGFP and anti-neurofilament, a general axon marker. A. Control transfected axons choose dorsal vs. ventral pathways indiscriminately. f, femoral nerve; o, obturator. B-C. Hoxd10-transfected motor axons preferentially project to limb via the femoral nerve. Scale bar in A = 200μm, in B = 100μm.

To determine the trajectories of transfected motor axons in β-actin::d10 embryos, the positions of axons expressing EGFP and/or the general axonal marker neurofilament axons in the anterior (crural) plexus region at stage 29 and at an early stage of muscle nerve formation (stage 26-27) were examined. In β-actin::control embryos (n=3, stage 27, n=3, stage 29), $EGFP^+$ axons contributed substantially to both the femoral and obturator nerve trunks, which project to dorsal and ventral thigh regions, respectively (Figure 3.6A). These observations suggest that the electroporation protocol generally resulted in the transfection of both dorsally and ventrally projecting neurons. In contrast, in half of the stage 26-27 embryos (n=3/6) and in all stage 29 embryos (n=6), most EGFP+ axons appeared to diverge at the crural plexus to project along dorsal pathways (Figure 3.6B-C). Thus, Hoxd10-transfected motoneurons not only express the LMCl marker Lim1, but also adopt a position and an axon trajectory consistent with LMCl identity.

3.7 HOXD10 OVEREXPRESSION DOES NOT ALTER MOTONEURON RETINOIC ACID SYNTHESIS BY RALDH2

In normal embryos, early born (future LMCm) motoneurons express RALDH2, the major synthetic enzyme of retinoic acid (RA) (Berggren et al., 1999). Experimental data suggests that motoneuron-derived RA induces Lim1 expression and the development of an LMCl phenotype in migrating late-born motoneurons, and that overexpression of RALDH2 increases total $Lim1^+$ motoneuron numbers (Sockanathan and Jessell, 1998). These effects parallel those observed following Hoxd10 overexpression, suggesting a possible mechanistic link between the two factors. Furthermore, misexpression of Hoxd10 in the thoracic spinal cord has been shown to

induce ectopic RALDH2 expression in transfected motoneurons (Shah et al., 2004). To approach the question of whether Hoxd10 increases Lim1 expression by upregulating RA levels, RALDH2 expression was examined in both Hb9::d10 and β-actin::d10 embryos, as well as corresponding controls, at stages 23-24 and 29, during and after motor column formation.

Because prior studies focused primarily on brachial levels, I first assessed normal RALDH2 patterns in the LS cord. At stage 24, RALDH2 is expressed at all LS levels, but only by Isl1(2)$^{+}$ motoneurons that have migrated into the definitive motor column regions. These are likely to be early born, future LMCm motoneurons (Figure 3.7A-C). By stage 29, RALDH2 expression in LS segments is more limited. In LS2, RALDH2 expression is restricted to a lateral crescent-shaped cluster, corresponding in position to the Lim1^{+} LMCl (Figure 3.7D). In mid-LS segments (LS4), the domain of RALDH2 expression has shifted to medial regions and overlaps with the area of bright Isl1(2)$^{+}$ cells (LMCm) (Figure 3.7E). Expression levels gradually taper in more caudal segments – by LS6 motoneuron RALDH2 is barely detectable (Figure 3.7F). These patterns present an interesting parallel to Hoxd10 expression patterns (see Figure 3.1), and suggest that, like Hoxd10, motoneuron-derived RALDH2 may play multiple and varied roles in motoneuron development over time.

To examine the effects of Hoxd10 overexpression on RALDH2, sections from mid-LS (LS3-4) segments of stage 23-24 Hb9::d10 and β-actin::d10 embryos and stage 29 β-actin::d10 embryos were stained with antibodies targeting RALDH2 and Isl1(2). Due to the diffuse staining of the RALDH2 antibody, pixel intensity in micrographs was used to quantify RALDH2 levels in place of traditional cell counts. Regions containing high Isl1(2) expression (i.e. regions normally expressing RALDH2) were manually circumscribed and mean pixel intensity of RALDH2 staining determined for that region using NIH ImageJ software. The circumscribed

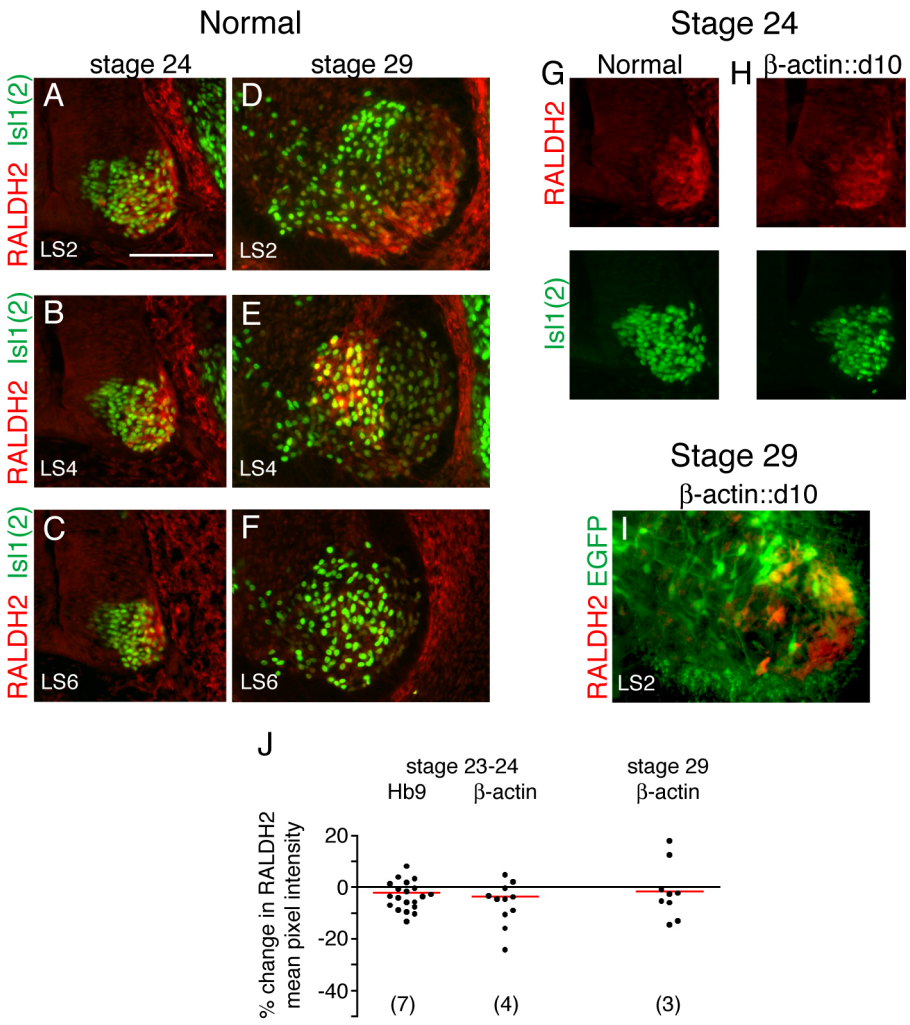

Figure 3.7 RALDH2 is unaffected by Hoxd10 overexpression in mid-LS segments.

A-F Normal expression patterns of RALDH2 in the LS cord. Initially widespread among motoneurons (as indicated by Isl1(2) staining), by stage 29 it is restricted to subpopulations in LS1-5, and downregulated in LS6. G-H Effects of β-actin::control and β-actin::d10 expression on RALDH2 levels. They appear largely unaffected. I. Hoxd10-transfected cells in LS2 are competent to expression RALDH2. J. Quantification of mean pixel intensity in micrographs of Hoxd10-transfected sections shows no change between transfected and non-transfected sides of the cord. Scale bar = 100μm.

area comprised the entire motor column at stage 23-24, whereas in stage 29 sections, it corresponded to medial motor column regions. Surprisingly, overexpression of Hoxd10 did not appear to affect RALDH2 expression levels – mean pixel intensity on transfected sides was similar to normal (Figure 3.7G-H,J; n=5, stage 23-25; n=8, stage 29). The area of the RALDH2 domain was often smaller than normal, but the reduction was generally proportionate to overall reductions in motor column size. Some transfected cells co-expressed RALDH2, demonstrating that they were in fact competent to do so (Figure 3.7I). Thus, Hoxd10 has no detectable effect on motoneuron expression of RALDH2 at LS levels during stages of motor column formation and consolidation, and may act through a novel mechanism to induce Lim1 expression.

3.8 DISCUSSION

3.8.1 Hoxd10, the lateral LMC, and the establishment of rostral LS identity

Evidence of involvement of Hoxd10 in the promotion of LMCl motoneuron subtype development in lumbar segments comes from both gain- and loss-of-function studies. As demonstrated in this chapter, temporally restricted overexpression of Hoxd10 in early postmitotic motoneurons results in a transient increase in motoneurons with molecular characteristics of LMCl subtypes ($Lim1^+$, $Isl1^-$). Prolonged overexpression initiated at progenitor stages with β-actin-driven constructs and maintained through stages of motor column formation increases the proportion of motoneurons with the molecular phenotype, position, and axon trajectory characteristic of LMCl motoneurons despite decreases in the overall size of the motoneuron population. Furthermore, complementary analyses of Hoxd10 loss-of-function mouse mutants

(C. L.-J.) revealed a marked decrease in LMCl motoneurons in rostral lumbar segments at stages just after motor column formation. These findings parallel those of Wu and colleagues (2008), who describe a severe reduction in LMCl numbers in Hoxc10/Hoxd10 double knockout mice. Surprisingly, these investigators report no obvious change in subtype complement in single Hoxd10 knockout mice. This inconsistency in outcome could reflect differences in the methods used to delete Hoxd10 function – our loss-of-function mice were created via insertion of a *neo* cassette into the coding region *hoxd10*, whereas those of Wu et al. lacked *hoxd10* entirely (see Wu et al., 2008). Regardless, our findings strongly suggest a role for Hoxd10 in LMCl specification.

At early stages of motoneuron differentiation, Hoxd10 is expressed throughout the LS region of the spinal cord, suggesting an early, uniform role in LS development. Based on evidence from previous studies, one aspect of this early function may be the establishment of the LS as a whole, as defined by the presence of a hindlimb-innervating LMC. Hoxd10 loss-of-function mice exhibit a half-segment caudal shift in the rostral boundary of the lumbar spinal cord (Carpenter et al., 1997; C. L.-J.), and combined mutations in Hoxd10 and Hoxa10 (Lin and Carpenter, 2003), or Hoxd10 and Hoxc10 (Wu et al., 2008), result in even more severe multisegment shifts. Conversely, ectopic expression of Hoxd10 in chick thoracic segments results in the induction of features characteristic of LS motoneurons, effectively instituting a rostral shift in the thoraco-lumbar boundary (Shah et al., 2004; Dasen et al., 2008). As such, Hoxd10 shares features in common with Hoxc6, a Hox protein critical for the specification of the brachial LMC and its boundaries (Dasen et al., 2003).

At later stages of motoneuron differentiation, the widespread initial expression of Hoxd10 within motoneuron populations narrows, such that by stage 29, expression is largely

limited to subsets of motoneurons in LS1-5. In the most rostral of these segments (LS1-2), expression is restricted to LMCl motoneurons that occupy a position corresponding to the motor pools of two prominent dorsal thigh muscles, the sartorius and anterior iliotibialis (Landmesser, 1978). Conversely, in caudal segments, where the LMCl is quite diminished in size, and most motoneurons adopt an LMCm identity, Hoxd10 is largely absent by stage 29. These correlations support the above observation that sustained overexpression of Hoxd10 is required to maintain the altered LMCl:LMCm proportions seen in experimental embryos. However, there is not a universal link between the maintenance of Hoxd10 expression and the maintenance of an LMCl phenotype in all LS segments at these later stages. In middle LS segments (LS3-4) in the stage 29 chick embryo, Hoxd10 is expressed not by LMCl motoneurons, but by LMCm motoneurons that likely project to ventral muscles. The normal function of Hoxd10, therefore, varies by segment within of the LS cord, suggesting that different hierarchies of transcription factors mold motoneuron subtype specification in rostral and middle LS segments. Interestingly, overexpression of Hoxd10 in caudal segments (LS5, see Table 3.1) also leads to increases in $Lim1^+$ motoneurons, implying that segmental variations in Hoxd10 function may have more to do with Hoxd10 concentration than with a specific cellular or positional context.

3.8.2 Hoxd10-Hb9 interactions

The use of an Hb9 promoter to drive expression of Hoxd10 presented an unforeseen experimental complication – ectopic Hoxd10 was rapidly extinguished from motoneurons, while EGFP in Hb9::control embryos was not. A suppression of Isl1 could be one explanation for this phenomenon, as Isl1 binds directly to the Hb9 promoter (Lee and Pfaff, 2003) and is required for endogenous Hb9 expression in motoneurons (Pfaff et al., 1996). While overexpression of

Hoxd10 has been shown here to increase the number or proportion of cells expressing the LMCl marker Lim1, prior studies have demonstrated cross-repressive interactions between Lim1 and Isl1 (Kania and Jessell, 2003). It is feasible, then, that Hb9::Hoxd10 operates by limiting $Isl1^+$ LMCm formation, and thereby feeds back to repress its own expression.

Though Hb9 is expressed throughout the spinal cord and Hoxd10 is restricted to LS segments, the two seem to parallel each other in several interesting ways. First, both Hb9 and Hoxd10 are initially expressed by all motoneurons, and later restricted to lateral motoneuron subsets (Figure 3.1; William et al., 2003). Second, the loss of either results in a significant loss of $Lim1^+$ motoneurons, RALDH2 expression, and total motoneuron numbers (Arber et al, 1999; Thaler et al., 1999; Wu et al., 2008). It therefore seems possible that the two participate in, and interact as part of, a larger program directing the specification of LMCl motoneurons. The possibility of a direct interaction provides an alternative explanation for the rapid downregulation of Hoxd10 when expressed under the Hb9 promoter, given that Hb9 has been hypothesized to negatively regulate its own expression (Arber et al., 1999). A detailed analysis of Hb9 expression in Hoxd10-electroporated embryos would be required to begin to understand the dynamics of such an interaction.

3.8.3 Hoxd10-Retinoid interactions

Given the apparent link between Hoxd10 and LMCl specification discussed above, it was surprising to find that Hoxd10 overexpression did not affect motoneuron expression of the retinoic acid synthesizing enzyme RALDH2. Motoneuron-derived RA sequentially directs several aspects of spinal cord development, including regulation of total motoneuron number, brachial LMC formation, and brachial and lumbosacral LMCl specification (Sockanathan and

Jessell, 1998; Sockanathan et al., 2003; Vermot et al., 2005). Hox10 genes and RALDH2 have been linked in both loss- and gain-of-function studies – RALDH2 expression is noticeably downregulated in Hoxc10/Hoxd10 double mutant mice (Wu et al., 2008), and induced at thoracic levels following ectopic expression of Hoxd10 (Shah et al., 2004). Furthermore, at stages during and after LS motor column formation, Hoxd10 and RALDH2 are maintained in overlapping motoneuron populations. Despite these correlations, Hoxd10 overexpression did not appear to alter RALDH2 expression. Hoxd10 may therefore direct LMCl specification through a RALDH2-independent mechanism. A possible candidate is the direct modulation of RA receptor expression, rendering motoneurons hypersensitive to normal ambient RA levels. A similar conclusion was derived from studies of a Hoxc8 loss-of-function mouse. In these animals, the absence of Hoxc8 caused minimal alterations in RALDH2 at forelimb levels but noticeably downregulated expression of the retinoid receptor RARβ (Vermot et al., 2005). Like Hoxd10 loss-of-function mutants, these mice exhibit a specific loss of $Lim1^{+}$ LMCl motoneurons. The possible effects of Hoxd10 on RA receptor expression therefore warrant further investigation.

4.0 HOXD11 SPECIFIES MEDIAL MOTONEURON SUBTYPES IN THE CAUDAL LUMBOSACRAL SPINAL CORD OF THE DEVELOPING CHICK

4.1 INTRODUCTION

As described in the preceding chapters, the spinal cord of the embryonic chick is subdivided into regions identifiable by the presence or absence of specialized motor columns; for example, the presence of a lateral motor column (LMC) separates the brachial and lumbosacral (LS) regions from the thoracic. Investigators have devoted much effort toward determining the mechanisms responsible for the gross regionalization of the spinal cord, and in the process have identified a number of key molecular players. The initial signals controlling this process are thought to be morphogens arising from nearby non-neural tissues. At brachial levels, secreted retinoic acid (RA) from the adjacent paraxial mesoderm governs the regional acquisition of LMC characteristics (Ensini et al., 1998; Liu et al., 2001; Sockanathan et al., 2003; Ji et al., 2006). Meanwhile, factors originating from the tailbud have been hypothesized to initiate LMC induction at lumbosacral levels (Lance-Jones et al., 2001; Liu et al., 2001; Omelchenko and Lance-Jones, 2003; Sockanathan et al., 2003). Gradients of RA from the paraxial mesoderm and fibroblast growth factor from the tailbud act in opposition to induce the spatially restricted expression of Hox transcription factors along the rostrocaudal axis of the spinal cord (Liu et al.,

2001; Bel-Vialar et al., 2002; Dasen et al., 2003). In this manner, morphogenetic gradients are translated into region-specific transcriptional programs.

Both gain- and loss-of-function studies have demonstrated the importance of Hox genes in the establishment of regional spinal cord character. For example, Hoxc6 and Hoxc9 appear to be essential for the columnar specification of motoneurons at the brachial and thoracic levels, respectively. The caudal limit of Hoxc6 expression and the rostral limit of Hoxc9 correspond to the brachio-thoracic boundary (Dasen et al., 2003). Ectopic expression of Hoxc9 at brachial levels causes some motoneurons to erroneously adopt characteristics of the Column of Terni, a unique feature of the thoracic cord. In doing so, it effectively shifts the brachio-thoracic boundary rostrally. Conversely, expression of Hoxc6 at thoracic levels induces the appearance of LMC-like motoneurons, thereby extending the brachial region caudally. Thus, restricted expression of Hox genes is essential in defining regional boundaries.

Like Hoxc6 at brachial levels and Hoxc9 at thoracic levels, Hoxd10 directs the development of a single region of the spinal cord, the LS, and its characteristic feature, the hindlimb-innervating LMC. In the developing chick, the rostral limit of Hoxd10 expression aligns with the thoraco-lumbosacral border (Figure 5A; Lance-Jones et al., 2001). Gain- and loss-of-function studies have demonstrated that the position of this border is malleable and dependent upon the presence and rostrocaudal extent of Hoxd10 expression (Carpenter et al., 1997; Shah et al., 2004). Thus, Hoxd10 functions as a determinant of LS identity. As discussed in Chapter 3, however, it may also play an additional, segment-specific role in LS patterning. Its expression is eventually extinguished from caudal LS segments and maintained in specific subsets of motoneurons in rostral LS (Figure 3.1K-M). This shift in expression suggests that perhaps Hoxd10 transforms from a generic promoter of LS regional identity to a specific

promoter of "subregional" identity in the rostral LS during the period of motoneuron diversification.

The suggestion that Hox genes govern the acquisition of subregional identity is not without precedent. Recent work by Dasen and colleagues (2005) revealed that combinatorial expression of Hox transcription factors within the brachial spinal cord governs two aspects of subregionalization, the rostrocaudal placement and intrasegmental diversification of motor pools. Motor pools, as discussed in previous chapters, are multi-segment-spanning clusters of motoneurons that innervate individual limb muscles and occupy stereotyped positions within the cord. As such, they provide a well-defined model for analyzing subregional variations within the LMC. Dasen et al. discovered that overexpression of certain Hox genes resulted in shifts in the rostrocaudal placement and extent of motor pools, while changes in others altered the complement of pools present at a given segmental level.

The factors involved in the establishment of subregional identity within the lumbosacral spinal cord have not yet been investigated. As discussed above and in Chapter 3, Hoxd10 appears to play a late role in the specification of rostral LS motoneuron subtypes. In contrast to Hoxd10, the orthologous gene Hoxd11 is expressed exclusively in caudal LS segments throughout the stages of motoneuron diversification (Figure 4.1; see also Figure 1.2). It was previously known that Hoxd11 manipulations in non-neural systems led to rostrocaudal conversions of the axial skeleton (Davis and Capecchi, 1994; Zakany et al, 1996; Boulet and Capecchi, 2002). Its role in the spinal cord, however, has not been addressed prior to this study. In the experiments detailed below, I utilized an overexpression paradigm to characterize the role of Hoxd11 in rostrocaudal segmental diversification within the LS. Data derived from these

studies suggests that Hoxd11 is involved in the specification of motoneuron subtypes characteristic of caudal LS segments.

4.2 ROSTROCAUDAL VARIATIONS IN HOX AND LIM EXPRESSION WITHIN THE LS SPINAL CORD

To begin to understand the function of Hoxd11 in the spinal cord, I first characterized its normal expression patterns. Previous studies in mice suggested that the rostral limit of Hoxd11 within the spinal cord occurred in middle LS segments (Burke et al., 1995). In chick, both transcript (Figure 4.1A) and protein expression (Figure 4.1F,L) extended rostrally to LS4. A caudal boundary was not specifically identified, but appears to exist somewhere within the embryonic tail. Within individual segments, the expression of Hoxd11 appeared to be widespread among the ventral cell populations at stages both during (stage 24; Figure 4.1E-G) and after (stage 29; Figure 4.1K-M) motor column formation. At early stages, all but the most recently born (most medial) Isl1(2)$^{+}$ motoneurons coexpressed Hoxd11 (Figure 4.2A).

The spatial distribution of Hoxd11 proved to be especially informative when compared to that of Hoxd10. In caudal LS segments at early stages of motor column formation, Hoxd11 and Hoxd10 are coexpressed in most, but not all, motoneurons (Figure 4.2C). By stage 29, however, both Hoxd10 and the lateral LMC (LMCl) marker Lim1 are virtually undetectable in LS6, where Hoxd11 expression peaks (see Figure 3.1, 4.1G). The dearth of LMCl cells at these levels leads to a shift in motoneuron projections; that is, while dorsal-projecting LMCl motor pools dominate in the rostral LS, ventral-projecting medial LMC (LMCm) motor pools represent the greatest percentage of the motoneuron population at caudal LS levels (Figure 4.3A-B; histogram derived

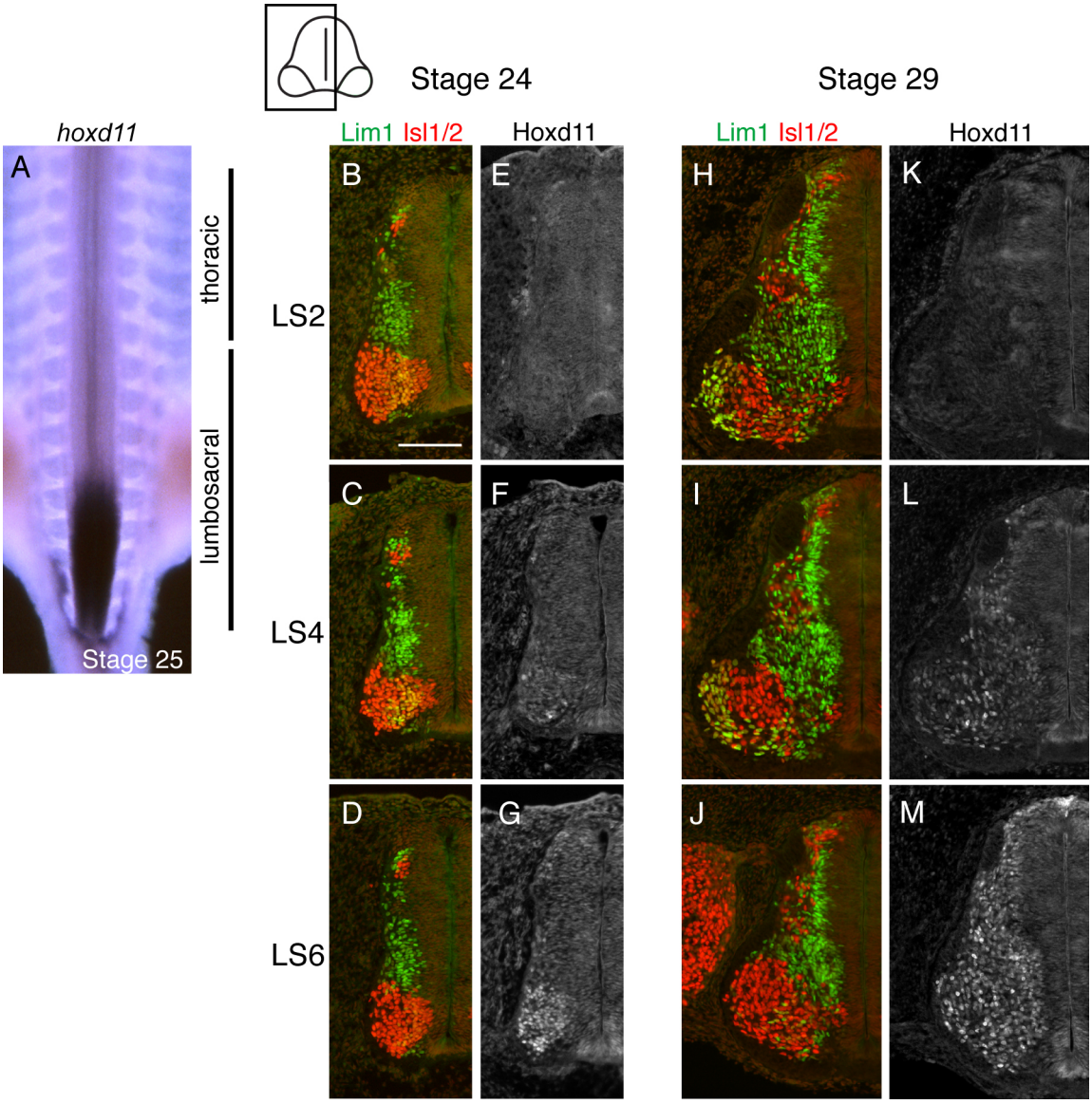

Figure 4.1 Normal expression of Hoxd11 and LIM HD transcription factors in the LS spinal cord.

A. Whole mount in situ hybridization at stage 25 showing the rostral limit of Hoxd11 at LS4. B-G. Hoxd11 is widespread in the ventral spinal cord at stage 24, when motor columns are forming. H-M. Hoxd11 remains widespread in the ventral half of the caudal spinal cord at stage 29, after motor columns and motor pools have formed. Scale bar = 100μm.

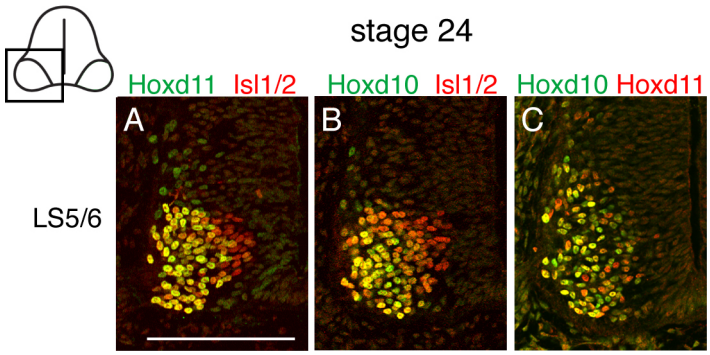

Figure 4.2 Expression of Hoxd10 and Hoxd11 overlaps in caudal LS segments of stage 24 embryos.

Sections stained with combinations of the pan-motoneuron marker Isl1(2), Hoxd10, and Hoxd11. A-B. All motoneurons but the most recently born express Hoxd10 and Hoxd11. C. Coexpression of Hoxd10 and Hoxd11 at caudal LS levels. Scale bar = 100μm.

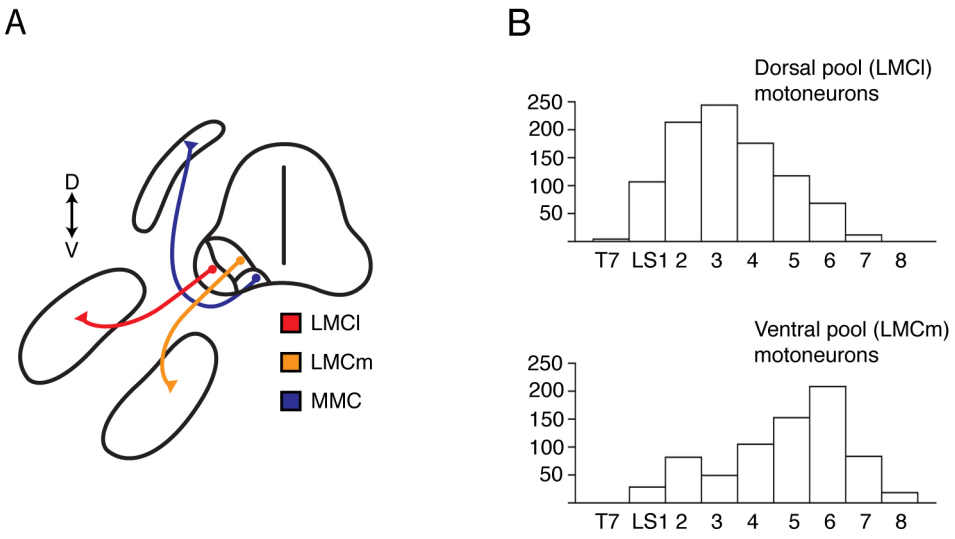

Figure 4.3 Rostrocaudal distribution of dorsal and ventral pool motoneurons.

A. Schematic representation of the axon trajectories of motoneurons residing in specific motor columns. B. Dorsal-projecting motor pools dominate rostral LS segments, but taper off in caudal segments. Conversely, ventral-projecting pools are abundant in caudal LS segments. Histograms represent a summation of individual motor pool numbers at stage 36 (Landmesser, 1978).

from Landmesser, 1978, and used with permission of the author). The spatial correlation among Hoxd10 and LMCl diminution, LMCm expansion, and peak Hoxd11 expression, when examined in the context of previous studies linking Hox expression to motor column subregionalization (see Dasen et al., 2005), pointed to a possible role for Hoxd11 in motoneuron subtype specification within the caudal half of the LS cord.

4.3 ECTOPIC HOXD11 SUPPRESSES MARKERS OF LATERAL LMC AND PROMOTES EXPRESSION OF MEDIAL MOTONEURON MARKERS

To address the relationship between Hoxd11 and motoneuron subtype proportions, I examined the effects of ectopic expression of Hoxd11 in rostral LS segments, hypothesizing that such a manipulation might lead to the development of caudal LS-like features (low LMCl, high LMCm). Electroporations were carried out as for Hoxd10 overexpression studies using both Hb9 and β-actin promoter driven expression vectors (see detailed description of methods in Chapter 2). In contrast to studies conducted with Hb9::d10, spinal cords transfected with Hb9::d11 maintained expression of ectopic Hoxd11 until at least stage 29 (Figure 4.4A-B). Subtype complement was therefore assessed only at stage 29, after motor columns had fully assembled.

Sections from LS2 of stage 29 Hb9::d11 embryos were first labeled with Isl1(2), the pan-motoneuron marker, and Lim1, the LMCl marker. Counts of $Lim1^+$ motoneurons revealed a 40% decrease on transfected sides of the cord (Figure 4.5D-F, Table 4.1). The magnitude of this decrease exceeded a small overall reduction in the total motoneuron population (Figure 4.5C; Table 4.1), suggesting that the absent $Lim1^+$ LMCl motoneurons may have been converted to

one of several possible alternative fates: Lim1$^-$, Isl1$^-$ LMCl (the Femorotibialis internus pool), Isl1$^+$ LMCm, or Isl1$^+$ medial motor column (MMC; see Figure 1.1).

To determine if any of these populations increased in size at the expense of Lim1$^+$ motoneurons, I again capitalized on the bimodal staining intensity of the Isl1(2) antibody. Brightly stained (Isl1(2)^{high}) and lightly stained (Isl1(2)^{low}) motoneurons were used to approximate the Isl1$^+$ LMCm+MMC populations and the Isl1$^-$ LMCl population, respectively, as described in Chapter 3. A standard threshold function in Adobe Photoshop allowed the isolation of Isl1(2)^{high} motoneurons and the exclusion of Isl1(2)^{low} motoneurons (Figure 4.5G-H). Concomitant with a decrease in Lim1$^+$ motoneurons, LS2 sections from Hb9::d11 embryos showed significant increases averaging about 22% in the number of Isl1(2)^{high} cells on transfected vs. non-transfected sides (Figure 4.5I; Table 4.1). In accord with these results, sections specifically probed for the LMCm+MMC marker *Isl1* also showed visible increases in *Isl1* expression on transfected sides (Figure 4.5J-K). Thus, the overall effect of ectopic Hoxd11 expression in LS2 was to shift motoneuron proportions away from the LMCl and toward medial phenotypes (Figure 4.5L).

To establish a direct link between ectopic Hox expression and motoneuron identity, I also analyzed subtype proportions within the transfected population alone. While transfected cells in Hb9::control embryos appeared equally likely to express either Lim1 or Isl1(2)^{high}, Hoxd11-transfected cells demonstrated an obvious preference for a medial molecular phenotype (Lim1$^-$ and Isl1(2)^{high}) (Figure 4.6A-B; Table 4.1). Among the transfected population in these embryos, changes in Lim1$^+$ and Isl1(2)^{high} motoneuron proportions paralleled those seen in the motor columns as a whole (Figure 4.6C), but were more extreme (Table 4.1). For example, the proportion of transfected motoneurons expressing Lim1 in Hb9::d11 embryos vs. Hb9::control

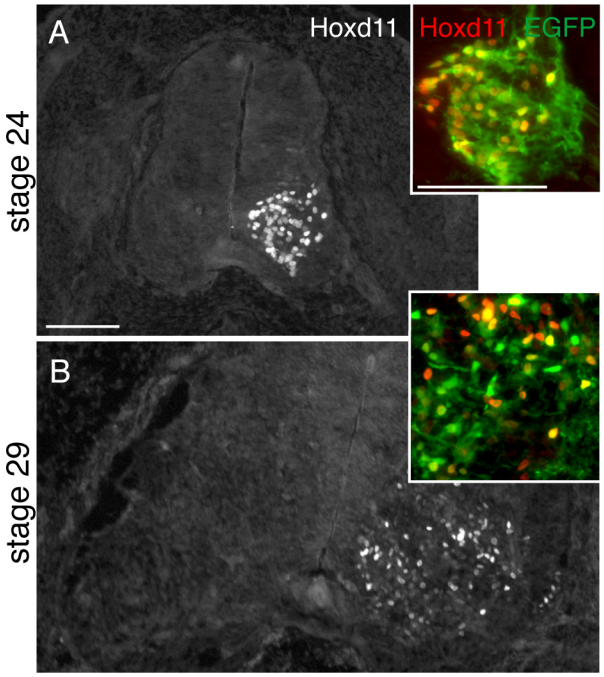

Figure 4.4 Hb9::d11 expression is maintained through stages of motor column formation.

A. Transverse section through rostral LS segment at stage 24. Inset: Ectopic EGFP colocalizes with Hoxd11. B. At stage 29. Most EGFP+ cells, but not all, are still expressing ectopic Hoxd11. Scale bar = 100μm.

embryos was 12%:34%, whereas the proportion of total Lim1^{+} motoneurons on transfected vs. non-transfected sides of Hb9:d11 embryos was 25%:37%. It therefore seems quite likely that the changes initiated by ectopic Hoxd11 expression arose in part by cell-autonomous mechanisms.

Experimental embryos electroporated with β-actin::d11 were analyzed in order to determine if higher levels of ectopic Hoxd11, beginning in progenitors rather than postmitotic motoneurons, would direct cells to adopt an alternate phenotypic fate. Electroporation with β-actin::d11, as with β-actin::d10, resulted in a substantial decrease in the size of the transfected motor columns (Figure 4.7F; Table 4.1). Nevertheless, β-actin::d11 generally mimicked the effects of Hb9:d11

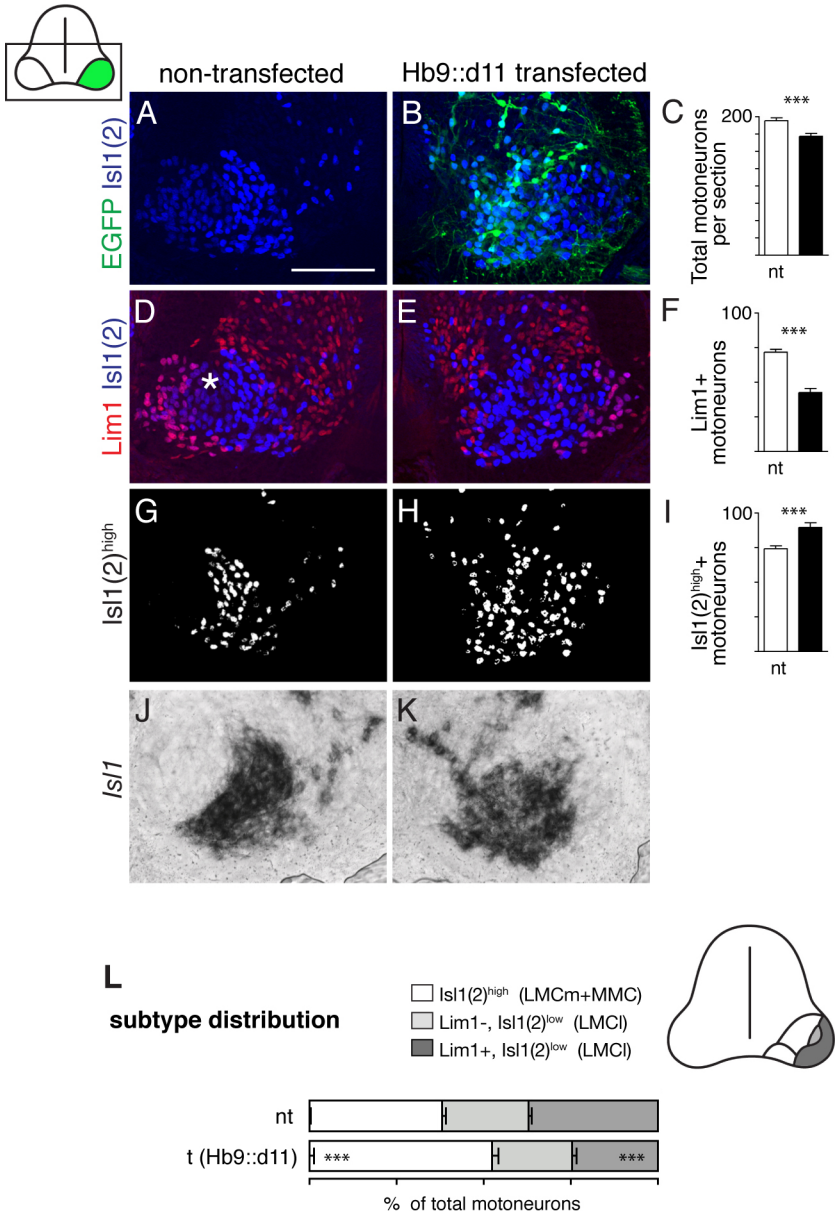

Figure 4.5 Hb9::d11 shifts motoneuron proportions in favor of medial subtypes.

A-C. Transverse sections through LS2 of Hb9::d11 embryos. Total motoneuron numbers, as indicated by Isl1(2) staining, were slightly reduced on transfected sides of the cord. D-F. Lim1^{+} (LMCl) motoneuron numbers were more severely reduced than total motoneuron numbers. Asterisk indicates Lim1-, Isl1(2)^{low} LMCl neurons. G-I. Isl1(2)^{high} (LMCm+MMC) numbers are higher on transfected sides. J-K. In situ hybridization for *Isl1* also suggests an increase in LMCm+MMC numbers. L. Motoneuron proportions on transfected sides are shifted toward medial subtypes. Scale bar = 100 μm.

Table 4.1 Quantification of motoneuron transcription factor expression in control and Hoxd11-electroporated chick LS segments.

Experimental subsets	# of motoneurons				% of motoneurons			% of transfected motoneurons			
	n[1]	nt[2]	t		nt	t		n	control[4]	Hox	
Hb9::Hoxd11 - Stage 29											
LS2											
Isl1(2)+	6	194±5	172±5	***							
Lim1+	6	72±2	43±3	***	37±1	25±1	***	4	34±3	12±2	***
Isl1(2)^{high}+	6	74±2	90±3	***	38±1	52±1	***	4	44±3	69±3	***
Foxp1+	5	158± 5	106± 6	***							
Lim3+	6	27± 4	35± 2	**							
Scip+	4	21± 1	27± 2	**							
Scip+/Foxp1+	5	16± 1	15± 1								
Scip+/Isl1(2)^{high}+	4	9± 1	17± 2	***							
β-actin::Hoxd11 - Stage 29											
LS2											
Isl1(2)+	5	146±7	111±5	***							
Lim1+	5	57±4	40±2	***	39±1	36±1	***	4	39±3	16±3	***
Isl1+	4	61±3	62±5		44±2	54±3	*	4	36±4	67±5	***
LS5											
Isl1(2)+	3	167±10	141±12	**							
Lim1+	3	45±4	25±2	**	27±3	19±2	**				
Hb9::control - Stage 29											
LS2											
Isl1(2)+	6	204±8	186±8								
Lim1+	6	79±5	71±3		38±1	38±1					
Isl1(2)^{high}+	6	76±4	73±4		37±1	39±1					
β-actin::control - Stage 29											
LS2											
Isl1(2)+	5	158±6	160±3								
Lim1+	5	63±3	61±3		40±1	38±2					

1. n, number of embryos analyzed. In each embryo, three non-adjacent sections within the same segment were counted.

2. nt, non-transfected side of the spinal cord; t, transfected side of the spinal cord.

3. Asterisks represent significance, based on paired or un-paired t-tests. *$p<0.05$, **$p<0.01$, ***$p<0.001$.

4. The term "control" describes embryos electroporated with a control construct expressing EGFP alone. "Hox" describes embryos electroporated with a construct encoding EGFP and either Hoxd10 or Hoxd11.

on subtype proportions. It caused a disproportionate reduction in the LMCl population in both LS2 and LS5 (Figure 4.7B-C,F; Table 4.1), shifting overall proportions in favor of LMCm and MMC. Conversely, LS2 sections from β-actin::d11 embryos probed for the LMCm+MMC marker *Isl1* showed significant increases in the proportion of medial subtypes on transfected vs. non-transfected sides (Figure 4.7D-E, F; Table 4.1). Subtype distribution within the transfected populations in experimental embryos magnified these effects and established a cell-specific link between Hoxd11 expression and medial subtype markers (Figure 4.8). These results confirm the general hypothesis stated above – Hoxd11, when ectopically expressed in rostral LS segments, has the overall effect of shifting motoneuron proportions toward the medial phenotypes that dominate the caudal LS segments in which it is normally expressed.

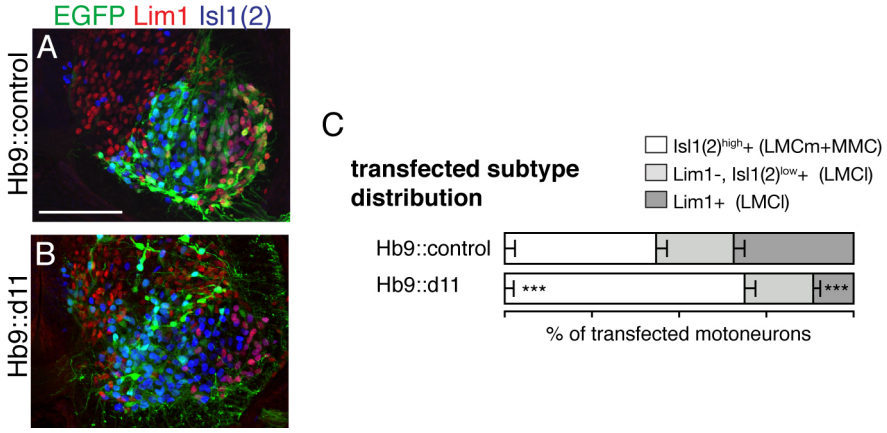

Figure 4.6 Hb9::d11-transfected motoneurons preferentially express medial subtype markers.

Transfected motoneurons in Hb9::control embryos show no preference for LMCm+MMC (Isl1(2)^{high}) or LMCl (Lim1^{+} or Isl1(2)^{low}) fates. B. Most Hb9::d11-transfected motoneurons are Isl1(2)^{high}. C. The medial shift in subtype proportions among the transfected population is more extreme than among the motoneuron population as a whole (see Figure 4.5). Scale bar = 100um.

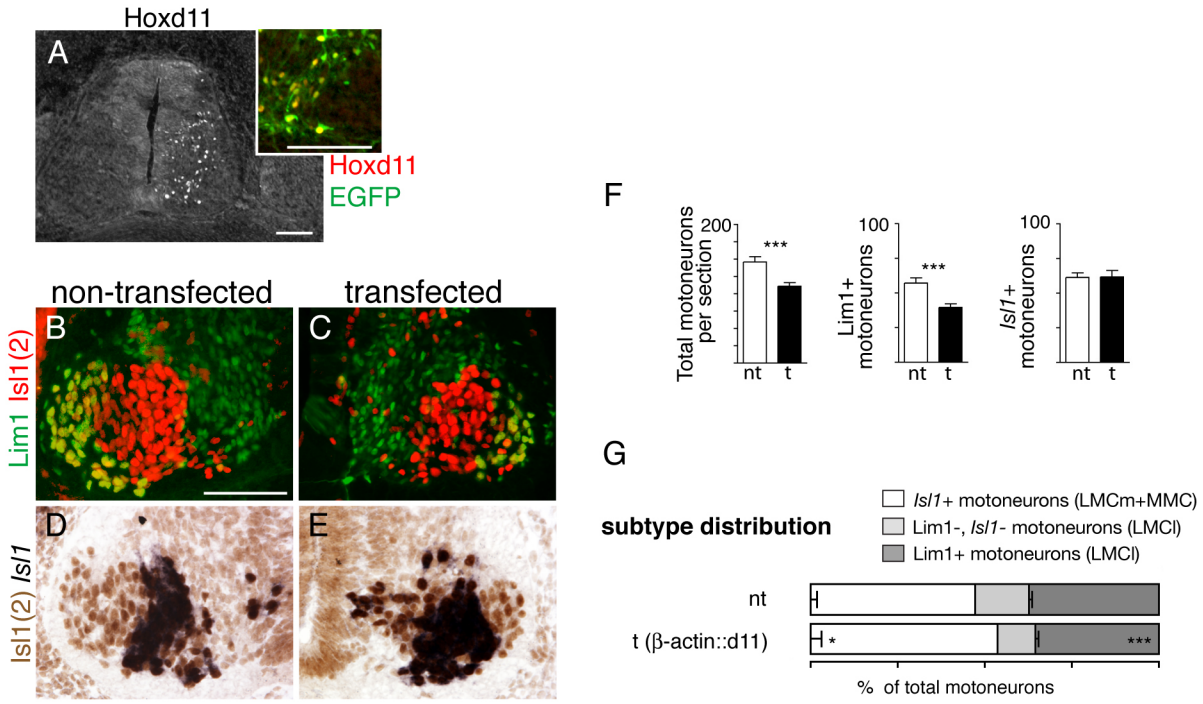

Figure 4.7 β-actin::d11 also shifts motoneuron proportions in favor of medial subtypes.

A. Transverse section from LS2 of a stage 29 β-actin::d11 embryo. The transfected side of the cord expresses ectopic Hoxd11. Inset shows colocalization of EGFP and Hox. B-C. Total motoneuron numbers, as determined by Isl1(2) staining, were significantly reduced on transfected sides of the cord. This reduction disproportionately affected the Lim1^{+} (LMCl) population (yellow). D-E. Combination of *Isl1* in situ hybridization and Isl1(2) immunostaining. Transfected sides of the cord have a normal or slightly enlarged population of Isl1^{+} LMCm+MMC motoneurons. F. Histograms depicting motoneuron subtype numbers. G. Motoneuron proportions are shifted in favor of Isl1^{+} phenotypes on transfected sides of the cord. Scale bars = 100μm.

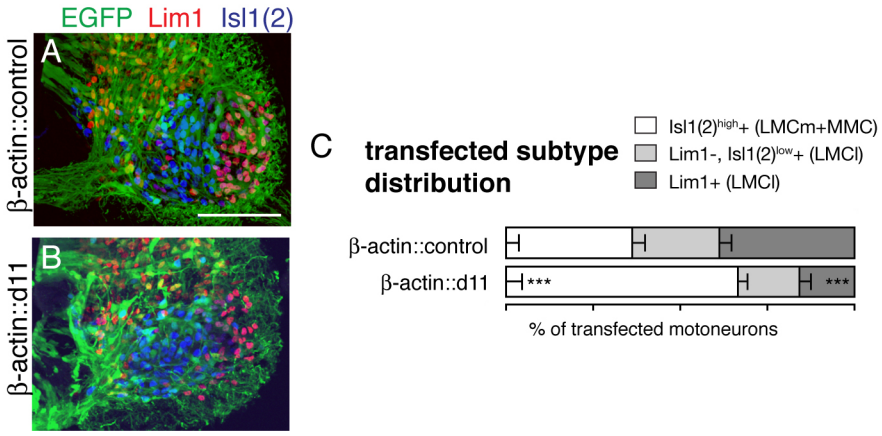

Figure 4.8 β-actin::d11-transfected motoneurons also preferentially express medial subtype markers.

A. Transfected motoneurons in β-actin::control embryos show no preference for LMCm+MMC (Isl1(2)^{high}) or LMCl (Lim1^{+} or Isl1(2)^{low}) fates. B. Most Hb9::d11-transfected motoneurons are Isl1(2)^{high}. C. The medial shift in subtype proportions among the transfected population is more extreme than among the motoneuron population as a whole (see Figure 4.5). Scale bar = 100um.

4.4 HOXD11-TRANSFECTED MOTONEURONS ADOPT A MEDIAL POSITION WITHIN THE SPINAL CORD, BUT NOT A VENTRAL TRAJECTORY

The findings described above demonstrate that ectopic Hoxd11 is capable of specifying, or respecifying, the molecular fate of developing motoneurons. As previously discussed, however, molecular complement is only one aspect of motoneuron identity. The ultimate fate of a motoneuron is also linked to its position within the spinal cord and the trajectory of its axon. To assess changes in neuronal position in LS2 of both Hb9::d11 and β-actin::d11 embryos, I used the tripartite grid described in Chapters 2 and 3. The grid divided the ventral cord into three sectors of equivalent size along the mediolateral axis: an extreme medial sector abutting the

ventricular zone (1), a medial motor sector (2), a lateral motor sector (3). Hoxd11-transfected motoneurons were twice as likely to be found in sector 2 than in sector 3 (Figure 4.9A-C; for Hb9, n=5; for β-actin, n=4; $p<0.0001$). To address the possibility that this positional preference was due to a general slowing of motoneuron migration, the same analysis was performed on β-actin::d11 embryos sacrificed one day later than normal, at stage 31. As in younger embryos, Hoxd11-transfected motoneurons in stage 31 embryos appeared to predominantly occupy sector 2 (Figure 4.9D; n=3).

Because later-born motoneurons normally adopt an LMCl phenotype, cells born after a "late"-stage electroporation should be more likely to settle in a lateral position within the ventral spinal cord. To determine definitively that Hoxd11 expression directs motoneurons to adopt a medial fate, the spatial distribution of Hoxd11-transfected motoneurons was assessed in embryos electroporated at stages 17-18, after an initial cohort of motoneurons has been born (Hollyday and Hamburger, 1977). β-actin::control embryos were used to examine the normal distribution of transfected motoneurons following late stage electroporations. As predicted, in control embryos, far more transfected cells were located in sector 3 than in sectors 1 and 2 (Figure 4.10A,C; n=8, $p<0.0001$), confirming that the transfected population consisted primarily of late-born presumptive LMCl motoneurons. In contrast, in β-actin::d11 embryos, most transfected motoneurons were still located medially, despite the late stage of the electroporation (Figure 4.10B-C; n=8, $p<0.0001$). Of interest is the significant increase in the mean number of Hoxd11-transfected cells in sector 2 when compared to β-actin::control embryos (Figure 4.10D; n=8, $p=0.006$) despite an overall loss of motoneurons in β-actin::d11 embryos (Table 4.1). This increase would not be expected if Hoxd11 transfection selectively impaired the ability of late -

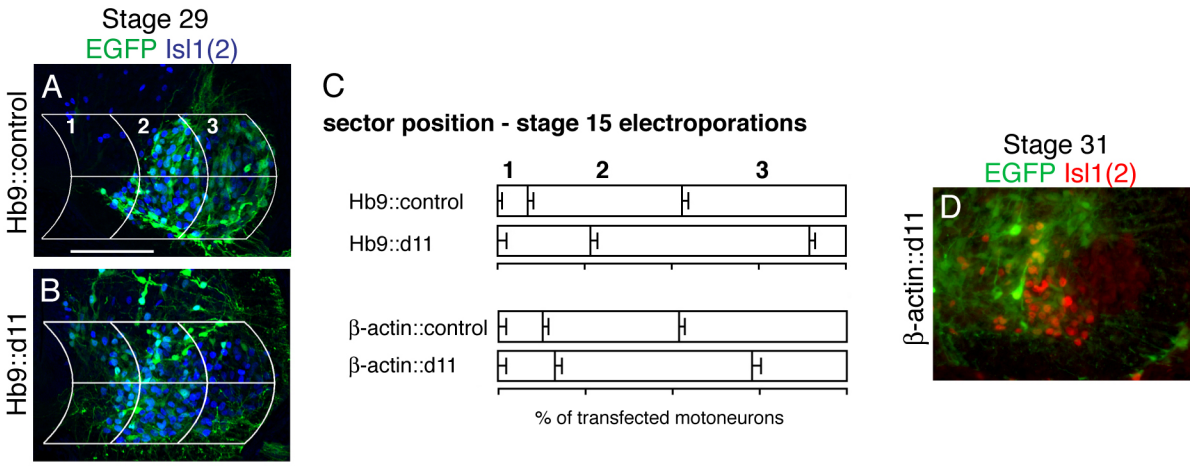

Figure 4.9 Hoxd11-transfected motoneurons adopt a medial position within the motor column region. A-B. Transverse sections of stage 29 Hb9::control and Hb9::d11 embryos overlayed with a tripartite grid. In control embryos, transfected motoneurons are evenly distributed between sectors 2 and 3 of the grid. In experimental embryos, most transfected motoneurons occupy sector 2. C. Quantification of spatial distribution of motoneurons in Hb9 and β-actin embryos. In both sets of experimental embryos, most motoneurons are found in medial sectors (1 and 2). D. Section from a stage 31 β-actin::d11 embryo. Hoxd11-transfected motoneurons maintain their medial position at later stages. Scale bar = 100μm.

born motoneurons to survive. Rather, these observations suggest that Hoxd11 is capable of inducing late-born motoneurons to adopt a medial positional fate.

Given that most Hoxd11-transfected motoneurons in rostral LS segments showed a preference for medial positions and expressed molecular markers indicating an LMCm identity, it was assumed that they would also preferentially project to ventral targets (see Figure 4.3A-B). In Hoxd11-transfected embryos, however, no qualitative difference was evident in the

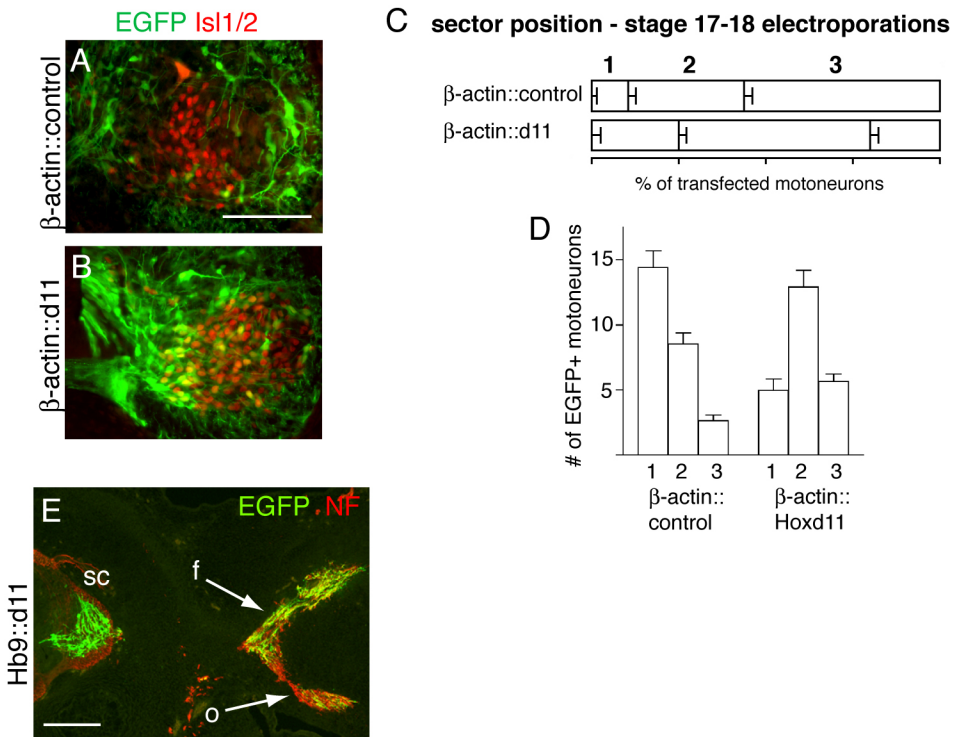

Figure 4.10 Ectopic Hoxd11 specifies position but not D-V axon trajectory.

A-B. Transverse sections from stage 29 β-actin::control and β-actin::d11 embryos electroporated at stage 17-18, after the birthdates of most early-born motoneurons. Control transfected motoneurons occupy a lateral position in the cord, consistent with a later-born LMCl identity. Hoxd11-transfected motoneurons settle medially despite their time of birth. C-D. Quantification of spatial distribution of late-electroporated motoneurons. E. Hoxd11-transfected motor axons show no qualitative preference for dorsal (femoral, f) or ventral (obturator, o) trajectory. Scale bar in A-B = 100μm, in C = 200μm.

distribution of the axons of transfected motoneurons to dorsal vs. ventral nerve trunks (Figure 4.10E, n=6). This surprising finding reveals that in some Hoxd11-misexpressing motoneurons, axon trajectory is uncoupled from molecular phenotype and somal position.

4.5 ECTOPIC HOXD11 REROUTES MOTOR AXONS FROM ROSTRAL LS SEGMENTS TO THE CAUDILIOFLEXORIUS, BUT NOT THE ILIOFIBULARIS OR VENTRAL SHANK

Data described above suggests that Hoxd11-transfected motoneurons acquire both molecular and positional characteristics of the LMCm, and that at least a percentage of these cells project to ventral targets. The observed dominance of LMCm subtypes over LMCl in the Hoxd11-expressing segments of normal embryos suggest that the actions of ectopic Hoxd11 in rostral segments represent not only a "medialization" of motoneuron identity, but also a "caudalization". Such an effect would fit nicely into the broader definition of Hox genes as determinants of rostrocaudal identity.

An aspect of a motoneuron's identity that directly reflects its rostrocaudal position is the targeting of its axon to a peripheral target. I therefore endeavored to examine the axonal projections of Hoxd11-transfected motoneurons, hypothesizing that if Hoxd11 were a caudalizing factor in motoneuron development, ectopic expression in rostral LS segments would respecify motoneurons therein to project to muscles normally innervated by caudal motoneurons. To test this hypothesis, the ventral shank, iliofibularis, and caudilioflexorius motor pools were retrogradely labeled and mapped via injection of hindlimb muscles with rhodamine-conjugated dextran at stages 29-30. Injections of the iliofibularis were preformed in part by me. All other

injections and analyses were performed by C.L.-J., but are included here in support of the major conclusions of this chapter.

The ventral shank muscle complex is normally innervated by medial motoneurons from LS3-7 (Landmesser, 1978). As such, its motor pool was initially chosen for retrograde labeling because it overlaps to a large extent with segments that normally express Hoxd11 (LS4+; see Figure 4.1A). In β-actin::d11 and Hb9::d11 embryos (n=8), the ventral shank pool was medially positioned and included numerous transfected motoneurons (Figure 4.11B), though most transfected motoneurons occupied a more medial position than the pool (Figure 4.11C-D). Ventral shank pools were located in a normal position on the rostrocaudal axis (Figure 4.11A; LS3-7), and no ectopic projections from transfected motoneurons in LS1-2 were observed. Thus, Hoxd11-transfected cells are competent to project to the ventral shank, but only within the normal rostrocaudal domain of its motor pool.

The iliofibularis is a large dorsal thigh muscle also innervated by motoneurons from LS3-7 (Landmesser, 1978). In β-actin::d11 embryos (n=5), the iliofibularis pool was normally positioned on both the mediolateral and rostrocaudal axes. This result was unsurprising, given that Hoxd11 appears to induce LMC motoneurons to adopt characteristics of medial subtypes, and the iliofibularis is normally innervated by lateral, dorsal-projecting cells. The retrogradely labeled pool did occasionally include a small number of laterally-positioned Hoxd11-transfected cells; however, most transfected cells were located medially and were not retrogradely labeled (Figure 4.11E).

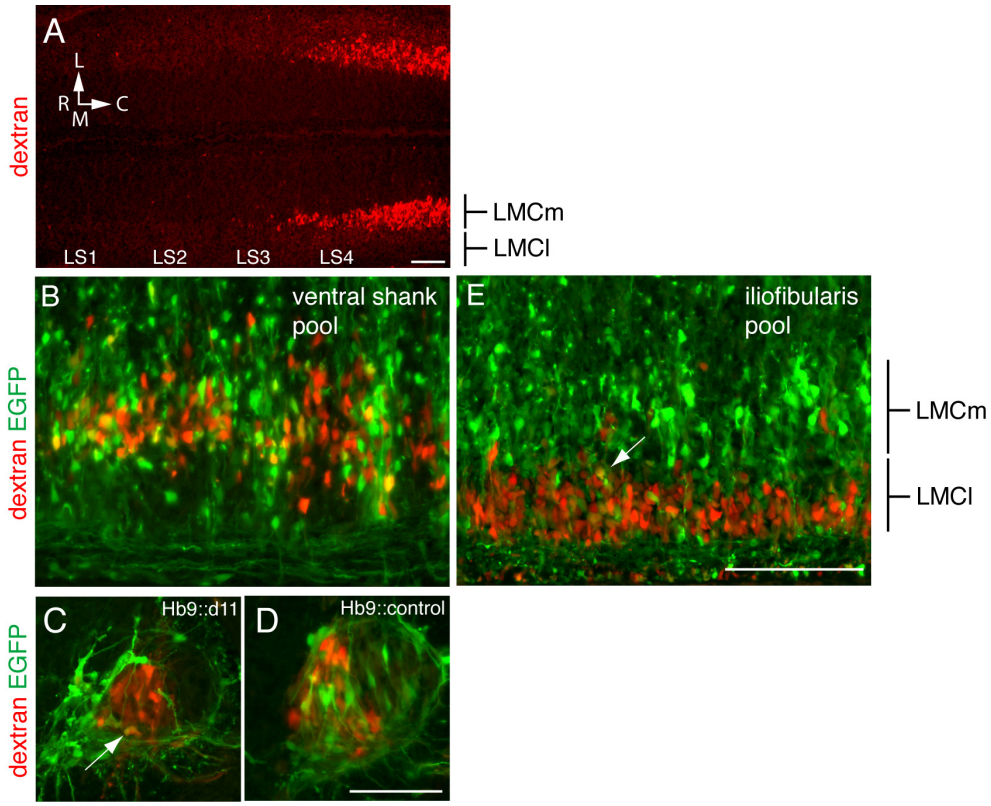

Figure 4.11 Rostrocaudal position of ventral shank and iliofibularis motor pools are unaffected by Hoxd11 misexpression.

A-B. Horizontal sections from a stage 29 Hoxd11-transfected embryo. Red cells are labeled by dextran injection of the ventral shank muscle of the dorsal thigh. Rostral limits of motor pools are equivalent on transfected (bottom) and non-transfected sides (top) B. Higher magnification of A. Numerous transfected motoneurons project to the ventral shank. C. Transverse sections from experimental embryos show that though some ventral shank motoneurons are transfected (arrow), most Hoxd11-transfected motoneurons are positioned medial to the ventral shank motor pool. Control transfected motoneurons show no such preference. E. Horizontal sections from stage 29 experimental embryo following iliofibularis injection. Hoxd11-transfected motoneurons rarely project to the iliofibularis (arrow). Scale bars = 100μm.

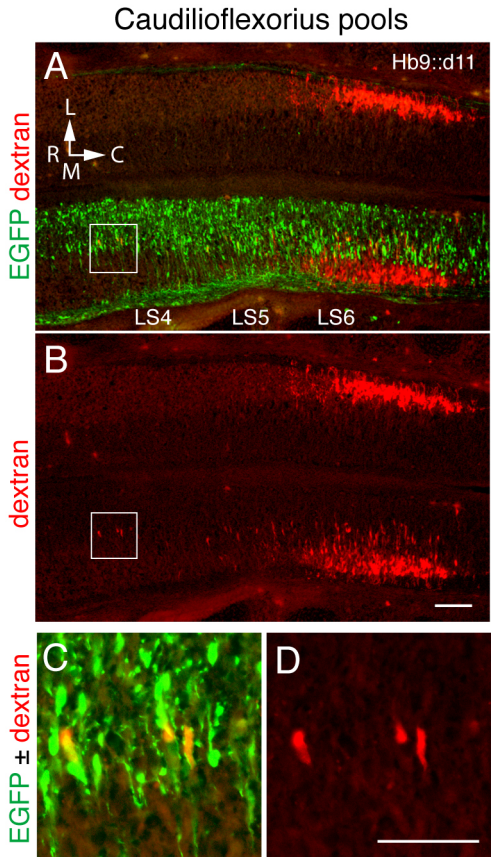

Figure 4.12 Ectopic expression of Hoxd11 alters the rostrocaudal extent of the caudilioflexorius motor pool.

A-B. Horizontal sections through an Hb9::d11 embryos. Red motoneurons have been retrogradely labeled following injection of the caudilioflexorius (Cf) muscle of the thigh. B. On the non-transfected side, the Cf pool is positioned caudal to LS6. On the transfected side, it extends into LS4. C-D. Higher magnification image confirms that ectopic Cf pool motoneurons are Hoxd11-transfected. Scale bars = 100μm.

The caudilioflexorius (Cf) is a thigh muscle normally innervated by LMCm motoneurons located exclusively within segments expressing high levels of Hoxd11 (LS6-8, Landmesser, 1978; Hollyday, 1980). In Hb9::d11 embryos, Cf pools on transfected and non-transfected sides were similar in size (n=7, mean pool size on transfected side=210 ± 36 cells, mean pool size on non-transfected side=197 ± 51 cells), and the vast majority of dextran$^+$ motoneurons were located in a normal rostrocaudal position (Figure 4.12A-B). However, the number of dextran$^+$ cells located in segments rostral to LS6 was increased on transfected sides. When expressed as mean percentage of total, dextran$^+$ cells in LS3-5 made up 2±1% of the caudilioflexorius pool on non-transfected sides, but 15.4±6% on transfected sides (p= 0.051). While, as with the ventral shank, most transfected motoneurons were located medial to the Cf pool, ectopic rostrally positioned Cf-innervating cells did express EGFP (Figure 4.12C-D). These observations suggest that a small number of transfected motoneurons in rostral segments may have acquired a novel caudal LS identity instructing them to project to the Cf, and thus lend considerable weight to the hypothesis that Hoxd11 is a promoter of caudal identity in developing motoneurons.

The relatively small number of transfected motoneurons projecting to the ventral shank and Cf and the apparent disorganization within these pools (compare transfected and non-transfected sides of Figure 4.12B) were somewhat disconcerting. Dextran injections at other sites also yielded low numbers or a complete absence of EGFP$^+$, dextran$^+$ cells in the cord (n=4 injections of full dorsal and ventral thigh and shank musculature; n=3 injections of the adductors of the ventral thigh; n=4 injections of the ischioflexorius of the ventral thigh). To address this issue, the peripheral course of EGFP$^+$ axons in Hb9::d11 embryos at stages 26-27 (n=6) and stage 29 (n=6) was examined. EGFP$^+$ axons made substantial contributions to major limb nerve trunks and to axial nerves (Figure 4.13A). However, the distal extent of EGFP$^+$ axons was often

less than that of non-transfected axons (as visualized with a neurofilament antibody; Figure 4.13B), suggesting that axon outgrowth from transfected motoneurons was delayed, or that these axons were unable to detect and respond appropriately to peripheral guidance cues. Such a conclusion is supported by the failure of most transfected cells to express the Cf marker Pea3. Pea3, a member of the ETS transcription factor family, is normally induced in Cf motoneurons in response to peripheral signals (Lin et al., 1998). While $Pea3^{+}$, $EGFP^{+}$ motoneurons were occasionally found in Hb9::d11 embryos, they were very rare (Table 4.13C; approximately 1-3 cells per embryo, n=6 embryos).

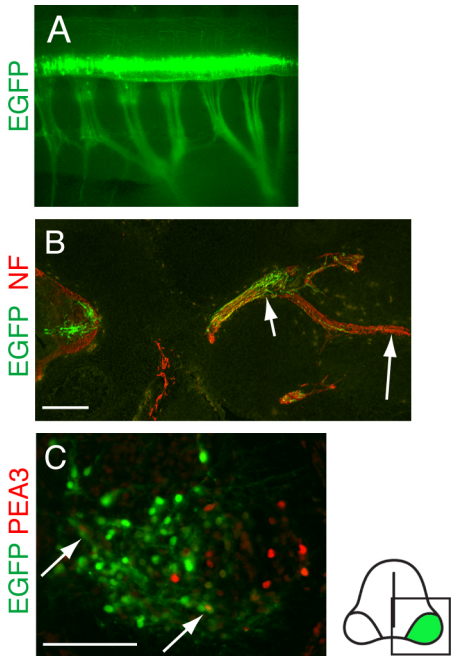

Figure 4.13 Hoxd11-transfected motoneurons do not penetrate far into the limb.

A. Whole mount of a stage 27 Hb9::d11. Transfected motor axons contribute significantly to cord and limb nerves. B. Transverse sections showing distal branching in an Hb9::d11 embryo. Short arrow indicates the presence of EGFP+ axons at proximal levels. Long arrow indicates a relative absence at more distal levels. C. Caudal LS motor column showing extensive Hoxd11 transfection but few EGFP+, Pea3+ cells (arrows). Scale bar in B = 200µm, in C = 100µm.

4.6 ECTOPIC HOXD11 SUPPRESSES LMC DIFFERENTIATION

The above data reveal that misexpression of Hoxd11 in rostral LS segments increases the proportion of Isl1$^+$ motoneurons. This marker is normally expressed by all newly generated motoneurons but maintained only in mature LMCm and MMC motoneurons (Tsuchida et al., 1994; Pfaff et al., 1996). To differentiate between effects on LMC and MMC, I next examined expression of the forkhead transcription factor Foxp1 and the LIM transcription factor Lim3, which have recently been shown to act in opposition to one another to direct motoneurons towards an LMC or medial MMC (MMCm) fate, respectively (Rousso et al., 2008; Dasen et al., 2008). In stage 29 embryos, electroporation with Hb9::d11 resulted in a 33% reduction in the number of Foxp1$^+$ motoneurons on the transfected side of the spinal cord, from a mean of 158 to 106 (Figure 4.14A-C; Table 4.1), though a few transfected cells did coexpress Foxp1 (arrows in Figure 4.14D). In contrast, Lim3$^+$ motoneuron numbers increased by ~30%, from 27 to 35 cells (Figure 4.14E-G), and numerous Lim3$^+$ cells were evident among the transfected population (Figure 4.14H). Thus, ectopic Hoxd11 appears to promote the development of MMCm motoneurons at the expense of the LMC. The absolute increase in Lim3$^+$ numbers, however, was considerably smaller than the decrease in Foxp1$^+$ numbers, suggesting that at least some would-be LMC motoneurons had adopted an alternative fate (Figure 4.14C,G; Table 4.1).

Several investigators have recently discussed the existence of lateral MMC (MMCl) cells at limb-innervating levels (Luria and Laufer, 2007; Rousso et al., 2008; Dasen et al., 2008) (see Figure 1.1). These motoneurons express neither Foxp1 nor Lim3, but do express high levels of the POU transcription factor Scip as well as high levels of Isl1 (Rousso et al., 2008). In order to include this population in analyses of Hoxd11 effects on motoneuron subtypes, I examined expression of Scip in a subset of stage 29 Hb9::d11 embryos. It is important to note that, in

chick, Scip was also expressed by some MMCm motoneurons, by a small, dispersed population of Foxp1^{+} LMCm motoneurons at all levels, and by a discrete dorsolateral pool of Foxp1^{+} LMCm motoneurons at caudal LS levels (see asterisk in Figure 4.14N; Luria and Laufer, 2007; Rousso et al, 2008). The MMCl can be distinguished from the latter two LMC groups because it expresses high levels of Isl1 (Isl1(2)^{high}), but not Foxp1 (Rousso et al., 2008). Following electroporation with Hb9::d11, the total number of Scip^{+} motoneurons in LS2 was increased by 29% (Figure 4.14I-K). There was no change in Scip$^{+/}$Foxp1^{+} motoneurons (Table 4.1), implying that Hoxd11 misexpression affected the MMC exclusively. It was difficult to differentiate between effects on MMCl vs. MMCm, given that some MMC motoneurons also expressed Scip; however, I did note that while most medially positioned Scip^{+} transfected motoneurons coexpressed Lim3, some did not (arrows in Figure 4.9L).

Taken together, these observations suggest an increase in the MMC motoneurons. It is noteworthy that this increase was smaller than the total increase in Isl1(2)^{high} cells (see Figure 4.6; Table 4.1), implying that both the LMCm and MMC populations were expanded in Hoxd11-electroporated embryos. Furthermore, the magnitude of the increase in MMC size did not compensate entirely for the decrease in LMC cells (as determined by Foxp1 counts), suggesting that some motoneurons may have failed to differentiate into a recognized, mature phenotype. Interestingly, in examining the normal expression patterns of these MMC markers, it was apparent that far caudal segments (LS7-8) possess an expanded population of MMC motoneurons (Figure 4.14M-N). Therefore, by increasing the proportion of MMC motoneurons present in rostral LS segments, ectopic Hoxd11 again caudalized the motoneuron complement**.**

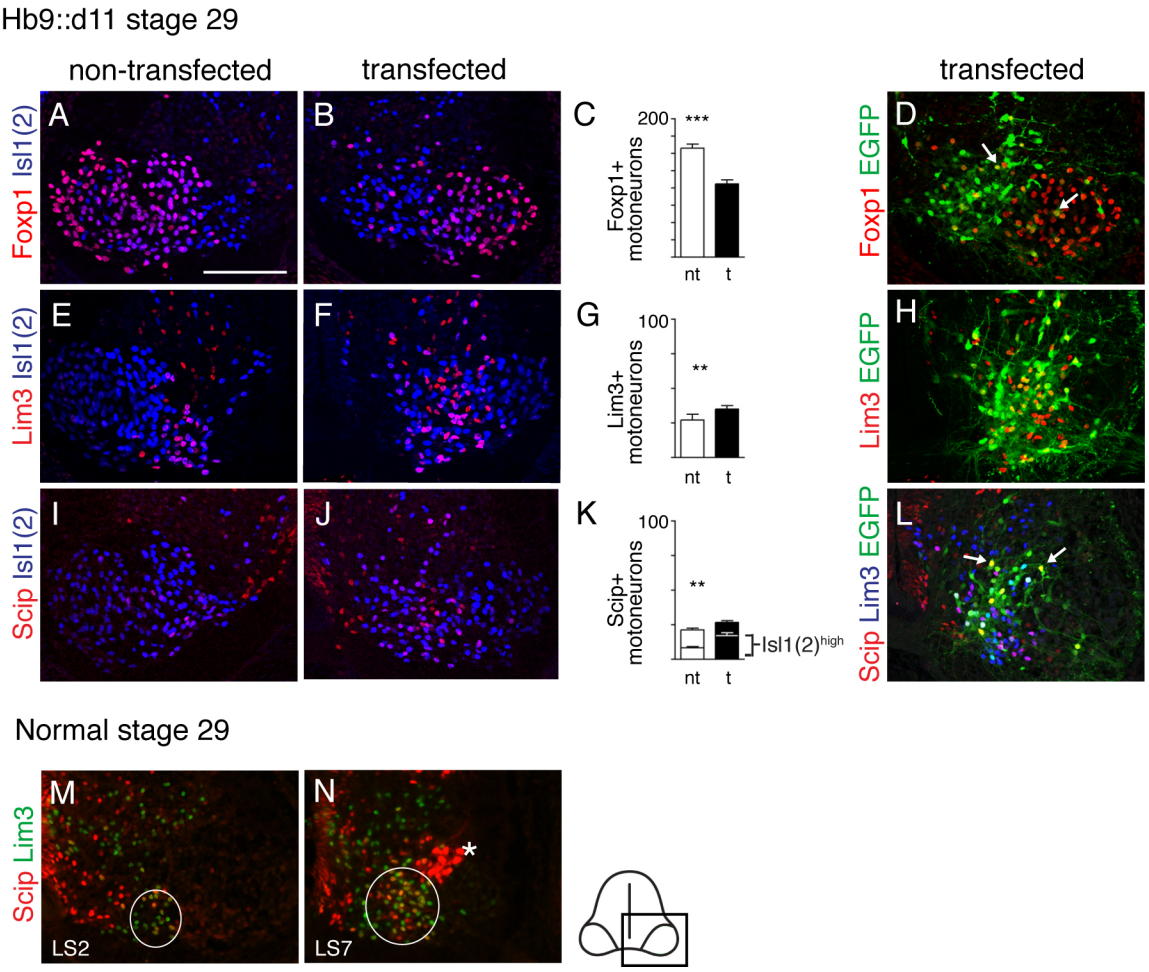

Figure 4.14 Hb9::d11 embryos show decreases in cells with an LMC molecular profile and increases in cells with profiles characteristic of MMC motoneurons.

A-C. Distribution and numbers of Foxp1^{+}, Isl1(2)$^{+}$, LMC MNs on non-transfected and transfected sides of LS2 sections from stage 29 Hb9:d11 embryos. D. Few Hoxd11-transfected cells express Foxp1^{+} (arrows). E-G. Distribution and numbers of Lim3^{+} MMCm MNs. H. Widely distributed transfected cells express Lim3. I-K. Distribution and numbers of Scip^{+} MMC MNs. Lower histogram bars (K) show Scip^{+}, Isl1(2)^{high} cells, a molecular profile characteristic of MMCl MNs. L. Transfected cells express Scip. Not all Scip^{+} cells express Lim3 (arrows). M-N. In a normal stage 29 embryo, Scip^{+} and Lim3^{+} cells are more numerous in caudal LS segments than in rostral LS segments. Circles delineate general outline of the MMC. Also unique to caudal LS sections is a cluster of Scip^{+}, Lim3^{-} cells (asterisk) that are LMC MNs (see Rousso et al., 2008).

4.7 MOTONEURON EXPRESSION OF HOXD11 ALTERS V2A INTERNEURON NUMBERS

As described above, the LIM transcription factor Lim3 is a marker of MMC motoneurons when coexpressed with other general motoneuron markers. When expressed independently of Isl1 or Isl2, however, Lim3 marks the V2 class of ventral interneurons. In embryos stained with antibodies targeting Lim3, transfected sides of stage 29 Hb9::d11 embryos appeared to show an unexpected increase in both $Lim3^+$ motoneurons and Lim3+ interneurons (see Figure 4.14E-F). To quantify this effect, sections from experimental embryos were stained with antibodies against Chx10, which exclusively marks V2 interneurons, and EGFP, to indicate Hoxd11-transfected cells. A few $Chx10^+$ cells were $EGFP^+$, but the vast majority of $Chx10^+$ cells were not transfected, or did not maintain EGFP expression through the time of analysis (Figure 4.15A). Counts of these non-transfected $Chx10^+$ neurons (C.L.-J.) revealed an increase of 30% on transfected sides of the cord (Figure 4.15A-C; mean number =70±5 on transfected side, 54±2 on non-transfected side, n=4, p=0.003). Given that the Hb9 promoter used to drive Hoxd11 expression should be active only in motoneurons, these data raise the possibility of a non-cell autonomous effect of ectopic Hoxd11 on V2a interneurons. Alternatively, these cells may represent a population of motoneurons that, during an early critical period, were driven by ectopic Hoxd11 to activate an interneuron differentiation program. Possible explanations for this unexpected result are discussed at length in the discussion below.

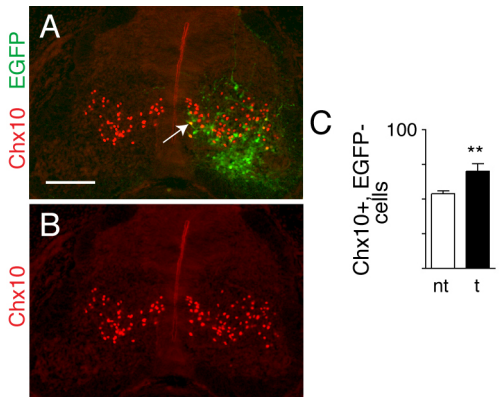

Figure 4.15 Hb9::d11 embryos show an increase in Chx10+ V2 interneuron numbers.

A-B. Transverse section from stage 29 experimental embryo. Transfected sides show more Chx10+ cells, but few among these are transfected (arrow). C. Histogram of non-transfected Chx10+ cell numbers. Scale bar = 100μm.

4.8 HOXD11 DOWNREGULATES EXPRESSION OF RALDH2

As discussed in Chapters 1 and 3, motoneuron production of retinoic acid by the synthetic enzyme RALDH2 is critical for both LMC and LMCl formation (Sockanathan and Jessell., 1998; Sockanathan et al., 2003; Vermot et al., 2005). Given that Hoxd11 appears to prevent LMCl formation and restrict overall LMC size, I examined the effects of Hoxd11 misexpression on RALDH2. The method of analysis was equivalent to that used in Chapter 3 to examine effects of Hoxd10 overexpression on RALDH2. Sections from mid-LS (LS3-4) segments of stage 23-24 Hb9::d11 and β-actin::d11 and stage 29 β-actin::d11 embryos were stained with antibodies against RALDH2 and Isl1(2). The mean pixel intensity of RALDH2 staining within relevant motor regions (i.e., the whole motor column at stage 23-34, and the LMCm at stage 29; Figure

4.16A,D) was determined using NIH ImageJ (see detailed description in Chapter 3). Consistent with the observed LMCl phenotype, embryos transfected with Hoxd11 constructs exhibited a

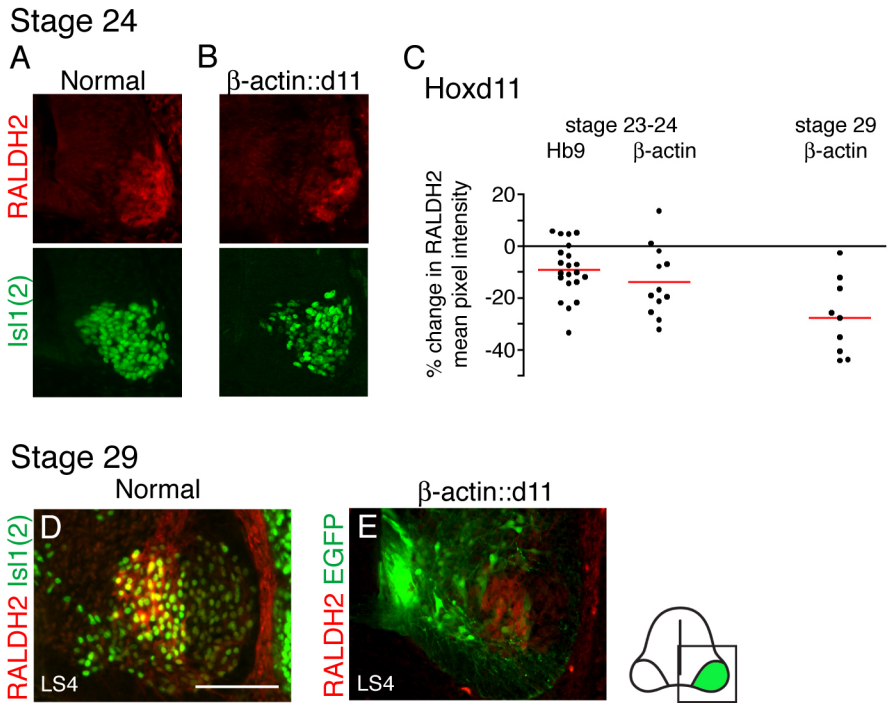

Figure 4.16 Misexpression of Hoxd11 leads to a downregulation of RALDH2.

A-B. Transfected sides of mid-LS sections from normal and β-actin::d11 stage 24 embryos. B. RALDH2 expression is reduced in β-actin::d11 embryos. C. Quantification of mean pixel intensity of RALDH2 staining in the motor regions of stage 24 and stage 29 Hb9::d11 and β-actin::d11 embryos. D. Normal extent of RALDH2 expression in LS4. Staining primarily overlaps with Isl1(2)high region (LMCm). E. Hoxd11-transfected cells rarely express RALDH2. Also, the size of the RALDH2 expressing region is considerably small that in normal embryos. Scale bar = 100μm.

significant decline in mean pixel intensity of RALDH2 staining on the transfected side of the cord (Figure 4.16B-C,E; $p<0.01$; n=11 stage 23-24; n=3 stage 29). Furthermore, few, if any, $EGFP^+$ motoneurons coexpressed RALDH2 in Hoxd11-transfected segments (Figure 4.16E). These data reveal that Hoxd11 is capable of modulating RALDH2 expression. Given that its expression is quite low in caudal segments (see Figure 3.7), where Hoxd11 is highly expressed, it is possible that one of the normal functions of endogenous Hoxd11 is to restrict development of the LMC as a whole and the LMCl in particular via downregulation of RALDH2 expression.

4.9 HOXD11 UNIDIRECTIONALLY REPRESSES HOXD10

Prior studies suggest that cell fate specification can reflect interactions between Hox genes (Manzanares et al., 2001; Dasen et al., 2003 and 2005; Tumpel et al., 2007). By stage 29, Hoxd10 and Hoxd11 exist in complementary but largely exclusive domains within the spinal cord. Their expression, along with their proposed opposing functions in motoneuron subtype specification, suggests that the two may be mutually repressive. To test this possibility, expression of one was examined following electroporation with the other. Electroporation with Hoxd10 did not visibly alter the distribution of endogenous Hoxd11 protein (n=3, stage 24) or *hoxd11* transcript (n=9, stages 27-29) in caudal LS segments. In contrast, ectopic Hoxd11 in anterior LS segments appeared to cell-autonomously repress expression of Hoxd10 protein (Figure 4.17A-B; n=3 stage 24, n=6 stage 29) and *hoxd10* transcript (Figure 4.17C-D; n=2/3 stage 24, n=7/8 stages 27-29). Similar results were obtained from electroporations using either Hb9 or β-actin promoter-driven constructs. These findings suggest that the expression patterns

of Hoxd10 and Hoxd11 in caudal lumbosacral segments by stage 29 may result from a unidirectional repression mechanism by which Hoxd11 downregulates expression of Hoxd10.

4.10 DISCUSSION

4.10.1 Hoxd11 and the development of a caudal LS identity

Prior to this study, little was known of the role of Hoxd11 in neural development. Its contribution to vertebral development, however, had been examined at length. Hoxd11 over-. expressing mice exhibit a reduction in the number of lumbar vertebrae (Boulet and Cappechi, 2002), while loss-of-function mutants show a one-segment gain in lumbar vertebrae at the expense of sacral vertebrae (Davis and Capecchi, 1994; Wellik and Capecchi, 2003). The primary conclusion from these studies was that, in mesoderm-derived structures, Hoxd11 directs the regionalization of the caudal axial skeleton by regulating lumbar size and specifying "sacral" (or caudal lumbosacral) identity. Experiments described in this chapter present a neural parallel to mesodermal gain-of-function studies; they demonstrate that rostral misexpression of Hoxd11 in the spinal cord initiates a phenotypic conversion of rostral LS segments to a more caudal LS identity. Further, the "caudalizing" influence of ectopic Hoxd11 manifested in two ways. First, it extended the rostral boundary of a caudal motor pool. Second, it shifted overall motoneuron proportions in favor of the medial subtypes that dominate the caudal LS.

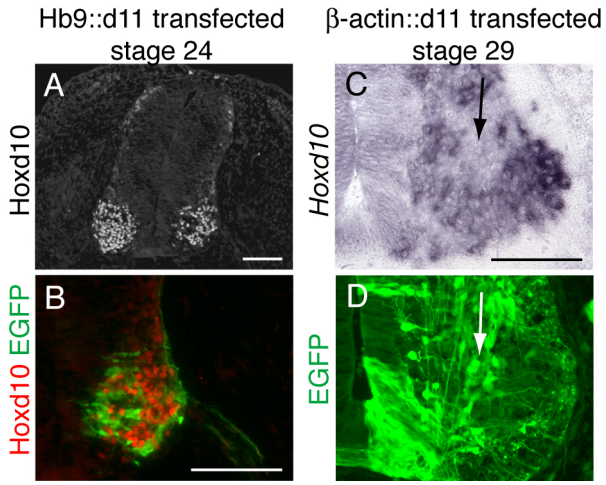

Figure 4.17 Ectopic Hoxd11 represses Hoxd10.

A-B. Transverse section from a stage 24 Hb9::d11 embryo showing absence of Hoxd10 protein in transfected cells. C-D. Transverse views of the rostral LS cord from a stage 29 β-actin::d11 embryo. Adjacent sections show a reduction in *Hoxd10* transcript expression in motor regions rich in EGFP+ cells (arrows). Scale bars = 100μm

Evidence for the first role arose primarily from analyses of the position of motoneurons projecting to the iliofibularis, ventral shank, and caudilioflexorius (Cf) muscles in experimental embryos. The normal Cf motor pool resides entirely within the domain of Hoxd11 expression, while the iliofibularis and ventral shank pools exist both within and rostral to this domain. We have shown that misexpression of Hoxd11 in rostral and middle LS segments is sufficient to induce ectopic axonal projections from these segments to the Cf muscle, but not to the iliofibularis or ventral shank muscles. Thus, the Cf pool appears to be uniquely impacted by the actions of Hoxd11.

Intriguingly, quantification of pool size in experimental embryos showed no significant difference in the absolute number of Cf-innervating motoneurons between transfected and non-

transfected sides of the cord, but rather a spatial expansion of the normal pool into more rostral territory. This finding suggests that the normal role of Hoxd11 may be to constrain the Cf pool along the rostrocaudal axis, rather than to specifically promote a Cf-innervating identity. Such a conclusion is supported by the observation that ectopic Hoxd11-expressing motoneurons only infrequently express Pea3, a specific molecular marker of the Cf pool. Regardless, Hoxd11 appears to be instrumental in the development of Cf-innervating motoneurons. Studies of Hoxc8 at brachial spinal levels have described a similar phenomenon. Expansion of the expression of Hoxc8, which is normally restricted to caudal brachial levels, into rostral segments induced a small number of rostral motoneurons to send novel axonal projections to a caudal target, the pectoralis muscle of the forelimb (Dasen et al., 2005).

Evidence suggesting a second, more general role for Hoxd11 in the regulation of motoneuron subtype development comes from gain-of-function experiments in which the molecular profiles of transfected motoneurons were examined. I first observed that Hoxd11 misexpression in rostral LS segments led to disproportionate decreases in the size of the LMCl, as defined by expression of the marker Lim1. These decreases were accompanied by increases in the expression of several markers of more medial motoneuron subtypes, including Isl1, which designates both LMCm and MMC motoneurons, and Lim3 and Scip, which primarily designate MMC motoneurons. In a normal embryo, Hoxd11-expressing LS segments possess a small population of LMCl motoneurons and an expanded population of LMCm and MMC motoneurons compared to rostral segments. Data presented here strongly suggest that one function of Hoxd11 may be to regulate, via direct or indirect interactions with other factors, the development and maintenance of these subtype proportions.

4.10.2 Hoxd11 and motor column maturation

The medial location of Hoxd11-transfected motoneurons in rostral segments and the molecular profiles of these cells suggest an overall shift in columnar distribution toward medial subtypes, but they may also represent an arrest of motoneuron differentiation and maturation. Isl1, Lim3, and Scip are all factors normally expressed by all motoneurons immediately following birth and subsequently downregulated in specific mature motoneuron subtypes (Ericson et al., 1992; Pfaff et al., 1996; Sharma et al., 1998 and 2000; Holmes et al., 1998). Misexpression of Hoxd11 resulted in increases in the expression of all of these factors and a concomitant decrease in expression of the mature LMC marker Foxp1 (Dasen et al, 2008; Rousso et al., 2008) and the relatively late differentiation marker, Lim1 (Tsuchida et al., 1994; Sockanathan and Jessell, 1998). Therefore, the observed shifts in molecular profile may reflect a failure of transfected motoneurons to mature beyond the initial stages of motoneuron development. Immaturity may also explain the apparent incongruity between a severe loss of $Foxp1^+$ LMC motoneurons and minor gains in $Scip^+$ and/or $Lim3^+$ MMC motoneurons in Hoxd11-transfected embryos, as high levels of Hoxd11 expression may have left an immature population of motoneurons expressing markers of neither LMC nor MMC. Indeed, Wu et al., (2008) noted the existence of such a population in Hoxc10/Hoxd10 loss-of-function mice, and data presented above demonstrate that Hoxd11 can downregulate expression of Hoxd10.

Examinations of the peripheral projections of experimental embryos (C.L.-J.) revealed yet another possible sign of neuronal "immaturity". Many transfected motoneurons possessed aberrant or shortened axons. Furthermore, only a small number of transfected cells contributed to any of the motor pools discussed above. Aberrant axonal trajectories could explain the failure of pool-specific neurons to cluster into defined pools in experimental embryos, as clustering

defects have previously been observed in mouse mutants in which motoneurons do not receive target-derived retrograde signals (Haase et al., 2002; Livet et al., 2002).

4.10.3 Hoxd11 and interneuron development

Analyses of Lim3 expression in Hb9:d11 embryos revealed an unexpected effect on V2a interneurons, a population of excitatory glutamatergic interneurons that provide input to both motoneurons (Al-Mosawie et al., 2007) and contralaterally projecting inhibitory interneurons (Crone et al., 2008). In stage 29 experimental embryos, $Chx10^{+}$ V2a interneuron numbers in LS segments were increased by approximately 30% on transfected sides when compared to non-transfected sides. This finding was puzzling, given that the Hb9 promoter driving Hoxd11 expression should be active only in motoneurons (Tanabe et al., 1998; Arber et al., 1999; Thaler et al., 1999) and in a small group of ventral interneurons distinct from the V2a population (Wilson et al., 2005). Furthermore, most $Chx10^{+}$ cells were EGFP-, suggesting that they had not been transfected, or had not maintained expression of Hoxd11 and EGFP through the stage of analysis. Thus, the effect if Hoxd11 on V2a interneuron number might be caused by non-cell-autonomous factors under the control of the transfected motoneuron population. I have shown above that Hoxd11 downregulates motoneuron expression of the retinoic acid synthetic enzyme RALDH2, thereby presumably reducing local concentrations of RA. Future studies might examine the influence of RA levels the development of $Chx10^{+}$ cells, given evidence from RA reporter studies suggesting retinoic acid signaling in ventral spinal regions including interneurons (see Shiga et al., 1995; Solomin et al., 1998; Pierani et al., 1999; Niederreither et al., 2002; Wilson et al., 2004).

V2 interneurons and motoneurons arise from molecularly similar progenitor populations (see Ericson et al., 1997; Briscoe et al., 2000), differing initially by the absence or presence of pro-motoneuron factors MNR2 and Hb9. Hb9 loss-of-function mutants also exhibit increases in Chx10-expressing cells (Arber et al., 1999; Thaler et al., 1999). In many cases, these ectopic Chx10 cells coexpressed markers of motoneuron identity, and were classified as hybrids or partially converted motoneurons. Therefore, the increase in $Chx10^{+}$ cells in Hb9::d11 embryos may also be the result of cell-autonomous effects of Hoxd11, if those effects facilitated the early downregulation of pro-motoneuron transcription factors in postmitotic transfected motoneurons. Hb9 mutants share several other characteristics with the Hoxd11 overexpression model used here, including a loss of both LMCl motoneurons and RALDH2 expression, suggesting a possible negative interaction between the two. Interestingly, V2 interneurons express Hox10 paralogues (Crone et al., 2008), which I have shown above to be repressed by ectopic Hoxd11. The role of these transcription factors in interneurons and their possible interactions warrant further investigation.

4.10.4 Hoxd10-Hoxd11 interactions

Repressive interactions among Hox genes have long been described as a driving force in segmental diversification (see Duboule and Morata, 1994, Dasen et al., 2005). I have shown here that ectopic Hoxd11 is sufficient to cell-autonomously repress endogenous Hoxd10 transcript and protein expression in rostral lumbar segments. These findings again present parallels to the work of Dasen and colleagues (2005) in the brachial spinal cord, which revealed that unidirectional repression of a rostral brachial Hox gene Hoxc5 by the caudal brachial Hox gene Hoxc8 was required to define subdomains within the brachial cord. Such a mechanism may

be responsible for the decline in Hoxd10 expression seen in caudal LS segments during normal motor column formation. When coupled with the finding that Hoxd10 is necessary for development of the LMC as a whole (Carpenter et al., 1997; Shah et al., 2004) and capable of inducing the expression of $Lim1^+$, a critical determinant of LMCl identity (see Chapter 3), repression of Hoxd10 by Hoxd11 suggests a cell-autonomous mechanism by which endogenous Hoxd11 might regulate subtype complement in caudal LS segments.

Foxp1 and RALDH2 are defining markers of the LS region of the spinal cord, and both are critical to the establishment of the LMC within this region (Sockanathan et al., 2003; Dasen et al., 2008; Rousso et al., 2008). The phenotype observed following Hoxd11 overexpression closely parallels both Foxp1 and RALDH2 loss-of-function mouse mutants (Vermot et al., 2005; Dasen et al., 2008; Rousso et al., 2008). Foxp1 mutants exhibit an overall decrease in the size of the LMC, and an increase in the size of the $Lim3^+$ and $Scip^+$ MMC populations. Furthermore, they show a specific loss of $Lim1^+$ motoneurons and aberrant axonal projections to limb targets. Mice lacking functional motoneuron-derived RALDH2 (Vermot et al., 2005) also demonstrate a disproportionate loss of $Lim1^+$ motoneurons, as well as a premature halt of distal axon growth in the periphery comparable to that observed in Hoxd11-transfected neurons. Recent studies have suggested that expression of both of these factors is closely linked to the presence of Hoxd10 (Shah et al., 2004; Wu et al., 2008; Dasen et al., 2008; Rousso et al., 2008). Ectopic expression of Hoxd10 induces both RALDH2 and Foxp1 expression in thoracic somatic motoneurons (Shah et al., 2004; Dasen et al., 2008), whereas Hox10 mutants show reduced levels of both (Rousso et al., 2008). This apparent linkage suggests that the observed downregulation of Foxp1 and RALDH2 in experimental embryos and in normal caudal LS segments may follow directly from the unidirectional repression of Hoxd10 by Hoxd11.

4.10.5 Summary

Figure 4.18 presents a model of LS spinal cord patterning based on data discussed in Chapters 3 and 4. In this model, the early uniform expression of Hoxd10 and RALDH2 in LS segments is proposed to initially define features unique to the LS cord, such as the presence of an LMC and a $Lim1^+$ LMCl population. It is during these early stages that the first $Lim1^+$ motoneurons normally appear (see Figures 3.1 and 4.1; Table 1.1) in response to ambient retinoic acid levels (Sockanathan and Jessell, 1998). Between stages 24 and 29, however, the function of Hoxd10 shifts from that of a general promoter of LS identity to that of a specific promoter of rostral LS identity. In our model, the mechanisms responsible for this transition stem from direct or indirect interactions between Hoxd10 are Hoxd11. Hoxd11 is expressed exclusively by caudal LS segments throughout this period. These segments ultimately differ from more rostral segments in several ways. First, they possess a larger complement of LMCm motoneurons due to the prevalence of ventral muscle motor pools at these levels (Figure 4.3; Landmesser, 1978). Second, their motoneurons send projections to more caudal muscle groups (such as the caudilioflexorius). Finally, they express lower levels of the LMC markers RALDH2 (Figure 3.7) and Foxp1, and high levels of the MMC markers Lim3 and Scip (Figure 4.14). We have proposed that these three differentiating features arise by a combination of the specific effects of Hoxd10 and Hoxd11 on motoneuron subtype specification and the repressive effects of Hoxd11 on Hoxd10. Thus, the opposing actions of Hoxd10 and Hoxd11 dictate the subregionalization of the LS cord.

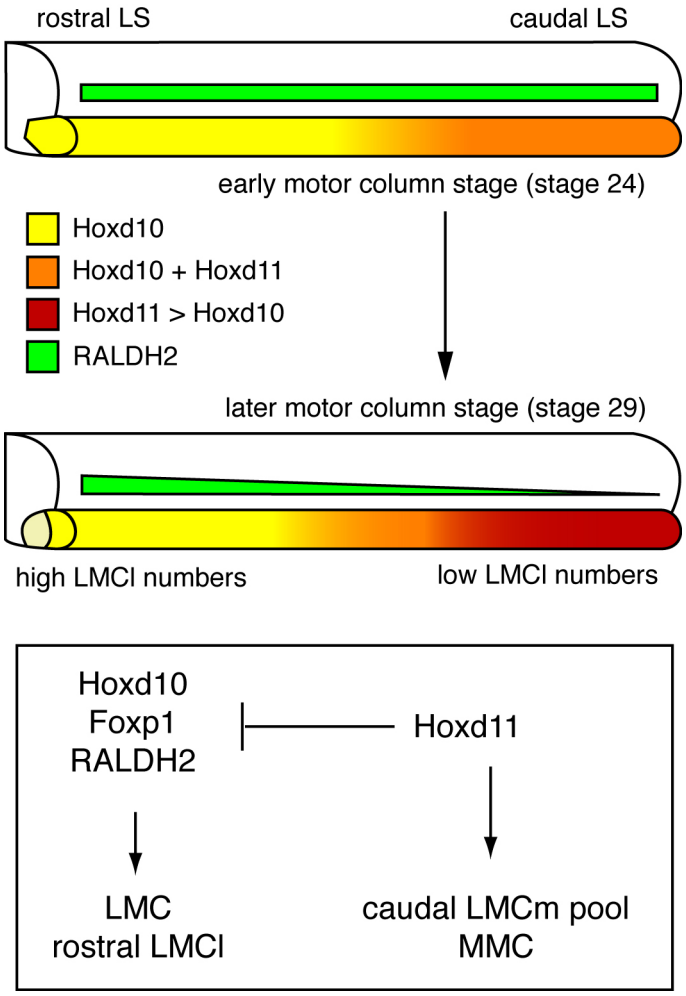

Figure 4.18 A model of LS motoneuron patterning.

5.0 FUNCTIONAL SPECIFICITY OF THE HOXD11 HOMEODOMAIN

5.1 INTRODUCTION

Data presented in Chapters 3 and 4 and in prior studies by other investigators have demonstrated that members of the Hox family of transcription factors contribute to the specification of spinal motoneuron subtypes and segmental identity (Tiret et al., 1998; Shah et al., 2004; Dasen et al., 2003 and 2005; Vermot et al., 2005; Wu et al., 2008). A lingering question is that of how members of this family are able to deliver specialized instructions regarding motoneuron fate, given that most possess highly homologous homeodomains that bind to similar or identical DNA recognition sites (Gehring, 1994; Desplan et al., 1988; Chang et al., 1996; Shen et al., 1997a). For example, Hoxd10 and Hoxd11 are members of the same ancestral family of Hox genes, sharing homology with Drosophila AbdB (Izpisua-Belmonte et al., 1991). Their DNA binding homeodomains share 68% amino acid sequence identity, and 88% similarity. Despite these structural similarities, the two proteins act in opposition to pattern the distribution of motoneuron subtypes within the rostral and caudal lumbosacral spinal cord, respectively.

Can subtle variations among homeodomains account for the unique effects of individual Hox proteins? In vitro data has historically shown that the binding selectivity of the homeodomain does not differ significantly among different Hox family members (Hoey and Levine, 1988; Desplan et al., 1988), and that the transcriptional activities of homeodomain-

containing proteins are likely guided by interactions with cofactors such as Pbx and Meis (Chang et al., 1995 and 1996; Shen et al., 1997b; reviewed in Moens and Selleri, 2006). Some in vivo data, however, have contradicted this assertion. One such study (Zhao and Potter, 2001) described the effects of replacing the Hoxa11 homeodomain with that of Hoxa13 in a transgenic mouse line. These mice developed normal kidneys, male reproductive organs, and axial skeletons, demonstrating a level of functional redundancy between the Hoxa11 and Hoxa13 homeodomains; however, their limbs and female reproductive tracts exhibited obvious mutant phenotypes suggestive of segmental posteriorization, as might be observed in a Hoxa13 overexpression model. This experiment and subsequent domain swapping studies by the same investigators (Zhao and Potter, 2002) raised the possibility that the homeodomain may play a greater role in the specification of segmental identity than previously thought.

The importance, or lack thereof, of the homeodomain in Hox-guided specification of spinal motoneuron fate has not yet been characterized, but is worthy of consideration given that Hox proteins have proven to be instrumental at nearly every level of spinal motoneuron diversification, from the gross regionalization of the spinal cord (Carpenter et al., 1997; Dasen et al., 2003; Shah et al., 2004) to the assignation of individual motor pool identities (Dasen et al., 2005). To begin to address the role of the homeodomain in these processes, I have utilized an experimental strategy similar to that of Zhao and Potter (2001, 2002) described above. I have constructed a hybrid form of *hoxd10* in which the sequence encoding its homeodomain has been replaced with the homeodomain-encoding sequence of *hoxd11* (denoted Hoxd10^{d11HD}; for methods, see Chapter 2), and expressed this construct in thoracic (T) and lumbosacral (LS) motoneurons of the developing chick using *in ovo* electroporation. Preliminary results suggest

that Hoxd10^{d11HD} in some ways mimics the effects of Hoxd10 misexpression on motoneuron subtype specification, and in other ways, adopts characteristics of Hoxd11.

5.2 HOXD10^{D11HD} DOES NOT ALTER THE ROSTROCAUDAL EXTENT OF THE LUMBOSACRAL LMC

Hoxd10 and Hoxd11 have profoundly different effects on the development of the lumbosacral LMC. Hoxd10 has been implicated in the establishment of the lumbosacral region as a whole, and manipulations of its expression result in shifts of the thoraco-lumbosacral border. Hoxd10 loss-of-function mice exhibit a caudal half-segment shift in this boundary (Carpenter et al., 1997; recent quantification by C.L.-J.), whereas ectopic expression of Hoxd10 in thoracic segments causes a rostral shift by inducing the expression of molecular markers and axon projections characteristic of rostral LS motoneurons (Shah et al., 2004; Dasen et al., 2008). Conversely, I have suggested that Hoxd11 represses LMC development (see Chapter 4). These pronounced differences presented a straightforward phenotypic assay by which to gauge the role of the non-homeodomain region of Hoxd10 and/or the homeodomain of Hoxd11 in the development of the LMC.

Embryos were electroporated as described in previous chapters with a construct encoding Hoxd10^{d11HD} under the control of the Hb9 promoter. The inclusion of an *ires-egfp* sequence facilitated the identification of transfected motoneurons. To examine expression levels of the mutant protein in experimental embryos, thoracic sections from a few embryos were stained with a Hoxd10 antibody that recognizes an epitope located N-terminal to the homeodomain, and therefore identifies both wild type Hoxd10 and the mutated form described here (Figure 5.1A).

Initial analyses revealed that, as with Hb9::d10, Hb9 promoter-driven expression of Hoxd10^{d11HD} was not sustained in transfected motoneurons; at stage 24, only the most recently born transfected cells expressed the mutant protein (Figure 5.1B). Given that the effects of Hb9::d10 misexpression were found to be transient, present at stage 24 but not stage 29, I confined my analysis of motoneuron development in Hb9:: Hoxd10^{d11HD} embryos to stage 24.

As stated above, ectopic expression of Hoxd10 at thoracic levels induces the appearance of markers characteristic of rostral LS segments, including the LMCl marker Lim1 (Shah et al., 2004). I therefore began my examination of Hoxd10^{d11HD} by expressing it in the thoracic cord and comparing the effects to those resulting from thoracic misexpression of Hoxd10 and Hoxd11. Sections from thoracic segment 6 (T6) of Hb9::Hoxd10^{d11HD}, Hb9::d10, and Hb9::d11 embryos were stained with antibodies against Lim1 and the pan-motoneuron marker Isl1(2). Hb9::d10 embryos were included in this analysis because prior studies (Shah et al., 2004) had focused on effects at later developmental stages and utilized a different promoter. As expected, ectopic expression of Hb9::d10 caused a clear induction of Lim1 in T6 (n=3; Figure 5.1C-D). However, neither, Hb9::d11 nor Hb9::Hoxd10^{d11HD} appeared to share this effect (n=3 each; Figure 5.1E-H). No ectopic Lim1 expression was detected in thoracic segments transfected with these constructs, suggesting that the homeodomains of Hoxd10 and Hoxd11 are not functionally redundant in this respect, and that the non-homeodomain region of Hoxd10 is insufficient to respecify thoracic motoneurons to adopt an LS-like fate.

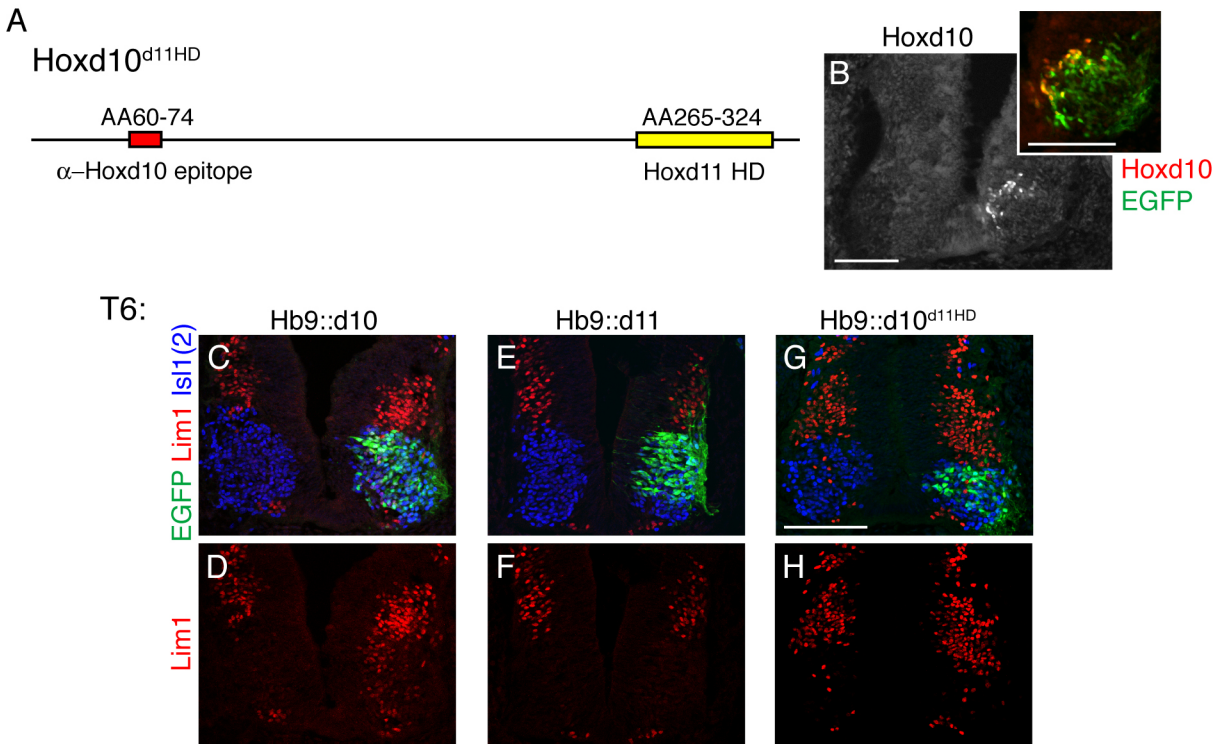

Figure 5.1 Hb9::d10^{d11HD} does not induce expression of the LMCl marker Lim1 in thoracic motoneurons.

A. Schematic representation of Hoxd10^{d11HD}. Due to the relative distance of the Hoxd10 antibody epitope from the homeodomain, the Hoxd10 antibody may be used to detect ectopic protein expression. B. Transverse section through T6 of a stage 24 embryo. Expression of Hoxd10^{d11HD} is limited to the most recently born motoneurons. Inset shows extent of EGFP/Hox colocalization. C-H. Transverse sections through T6 of experimental embryos demonstrating the presence of absence of Lim1^{+} motoneurons. Isl1(2) is used a pan-motoneuron marker. C-D. Ectopic expression of Hoxd10 in T6 induces Lim1. E-H. Expression of Hoxd11 or Hoxd10d11HD does not induce Lim1. Red cells in the ventral regions of G-H do not coexpress Isl1(2), and therefore are not motoneurons. Scale bars = 100μm.

5.3 HOXD10^{D11HD} REPRESSES THE EXPRESSION OF THE LATERAL LMC MARKER LIM1

Misexpression of Hoxd10 and Hoxd11 also affected the development of the LS spinal cord within its normal segmental boundaries. In particular, Hoxd10 promoted the differentiation of the lumbosacral lateral LMC (LMCl), while Hoxd11 repressed it. In order to determine to what extent these effects were guided by the homeodomains or non-homeodomain regions of these transcription factors, I next analyzed the distribution of Lim1 at LS levels following expression of Hoxd10^{d11HD}. Sections from stage 24 experimental embryos were stained with antibodies against Lim1 and Isl1(2) to reveal changes in LMCl proportions. Initial counts of Isl1(2)$^{+}$ cells in LS2 revealed a slight decrease in total motoneuron numbers on transfected sides, echoing changes seen in Hb9::d11 embryos, but not in Hb9::d10 embryos (n=5; mean motoneurons on the non-transfected (nt) side = 198±9, transfected (t) side = 183±9; p=0.044; Figure 5.2E,G). Subsequent counts of Lim1^{+} cells revealed a significant decrease in the number and percentage of motoneurons expressing this marker on the transfected side of the cord (n=5; mean Lim1^{+} motoneurons nt = 75±8, t = 41±5; p<0.0001; Figure 5.2E-F,H), again paralleling Hb9::d11 effects on subtype development (Figure 5.2C-D), and in contrast to Hb9::d10 effects (Figure 5.2A-B). Thus, with respect to LMCl development, Hoxd10^{d11HD} appears to have adopted the properties of Hoxd11, suggesting that the homeodomain of Hoxd11 is sufficient to restrict the development of the LMCl.

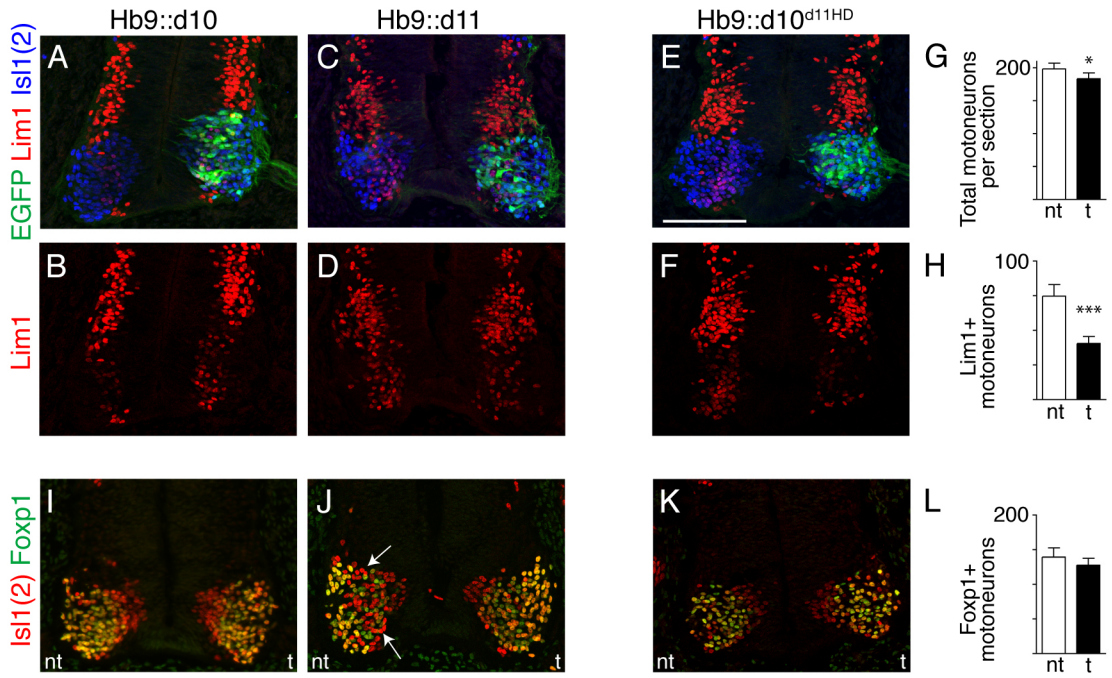

Figure 5.2 Hb9::d10^{d11HD} represses expression of Lim1 in rostral LS motoneurons.

A-F. Transverse sections through LS2-3 of stage 24 experimental embryos showing expression of Lim1 and the pan-motoneuron marker Isl1(2). A-B. Overexpression of Hoxd10 increases the number of motoneurons expressing Lim1. C-D. Ectopic expression of Hoxd11 decreases the number of motoneurons expressing Lim1. E-F. Hoxd10^{d11HD} also represses Lim1 expression. G-H. Quantification of total motoneuron numbers and Lim1^{+} motoneuron numbers on non-transfected (nt) and transfected (t) sides of Hb9::d10^{d11HD} embryos. I-K. Expression of the LMC marker Foxp1 in experimental embryos. I. Hoxd10 does not affect Foxp1 expression. J. Hoxd11 downregulates Foxp1 expression. Arrows indicates non-Foxp1 expressing motoneurons among the Foxp1 population. K-L. Hoxd10^{d11HD} does not effect Foxp1 expression. Scale bar = 100μm.

I next examined the effects of Hoxd10^{d11HD} expression on LMC development within the LS cord. I have shown that overexpression of Hoxd10 has no effect on LMC size in LS segments, as indicated by expression of the LMC marker Foxp1 (Figure 5.2I). In contrast, Hoxd11 reduces the number of motoneurons expressing Foxp1 and upregulates the expression of markers of MMC identity (Figure 5.2J). Counts of sections from Hb9::Hoxd10^{d11HD} embryos stained with antibodies against Foxp1 and Isl1(2) revealed that Hoxd10^{d11HD} has no effect on the expression Foxp1 (n=4; mean Foxp1^{+} motoneurons nt = 140±13, t = 128±10; Figure 5.2K-L). This result implies that the observed effect of Hoxd11 on Foxp1 expression in LS segments requires the non-homeodomain region of the protein. It also suggest that the "lost" Lim1^{+} motoneurons in Hb9:: Hoxd10^{d11HD} embryos were likely converted to a Lim1^{-} LMCm identity, rather than MMC.

5.4 THE EFFECTS OF HOXD10^{D11HD} MAY OCCUR INDEPENDENTLY OF RALDH2

In Chapter 4, I hypothesized that Hoxd11 restricts LMCl development by downregulating expression of RALDH2, the synthetic enzyme responsible for motoneuron production of retinoic acid. Prior studies have determined that retinoic acid secreted by early-born presumptive LMCm motoneurons likely induces the expression of the LMCl marker Lim1 in late-born motoneurons as they migrate laterally (Sockanathan and Jessell, 1998). Ectopic expression of Hoxd11 in mid-LS segments led to decreases in RALDH2 expression levels. Given that, like Hoxd11, Hoxd10^{d11HD} misexpression also affects Lim1^{+} motoneuron numbers, I next assessed possible

changes in RALDH2 expression in these experimental embryos. Expression levels were measured as described previously, by determining the mean pixel intensity of RALDH2 staining within the limits of the motor column. Preliminary results suggest no alteration in RALDH2 expression (n=3; p=0.12; Figure 5.3). This finding, if true of a larger sample size, implies that, while the Hoxd11 homeodomain may be sufficient to restrict LMCl development, it does so through a RALDH2-independent mechanism. Furthermore, the repression of RALDH2 observed in Hb9::d11 embryos requires the presence of the non-homeodomain region of Hoxd11.

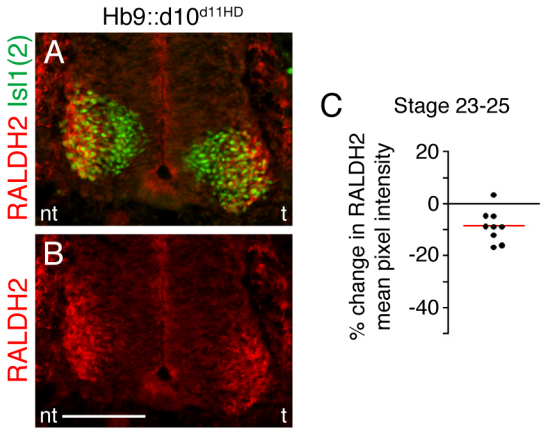

Figure 5.3 Hb9::d10^{d11HD} may not significantly affect RALDH2.

A-B. Transverse sections through mid-LS segments of experimental embryos showing total motoneurons (Isl1(2)+) and RALDH3 expression. C. Percent change in mean pixel intensity of RALDH2 staining between transfected and non-transfected sides. The decrease is not significant. Scale bar = 100μm.

5.5 DISCUSSION

5.5.1 Functional specificity of the homeodomain

In Chapters 2 and 3, I discussed the opposing effects of Hoxd10 and Hoxd11 on the patterning of the LS spinal cord. Hoxd10 appears to impart characteristics of the rostral LS motoneurons, while Hoxd11 shapes motoneuron subtype distribution in caudal segments. In the current chapter, I have presented preliminary evidence that the homeodomains of these transcription factors, though highly homologous, are responsible in part for the differences in their actions (Table 5.1). This hypothesis is supported by two observations. First, Hoxd10^{d11HD}, a modified version of Hoxd10 in which the homeodomain was replaced with that of Hoxd11, was unable to mimic the effects of Hoxd10 on thoracic motoneurons. Ectopic Hoxd10 has previously been shown to induce and LS-like molecular profile in thoracic segments (Shah et al., 2004; Dasen et al, 2008). Hoxd10^{d11HD} had no such effect, implying that the Hoxd10 homeodomain was necessary for the LS-specifying properties of Hoxd10, and that the presence of the Hoxd11 homeodomain was inadequate to compensate for this loss. Second, Hoxd10^{d11HD} behaved in a manner similar to Hoxd11 when misexpressed in rostral LS segments. Like Hoxd11, it suppressed the differentiation of presumptive LMCl motoneurons, as assessed by expression of the LMCl marker Lim1. In contrast, I have shown that Hoxd10 actually increases the proportion of motoneurons expressing Lim1 (see Chapter 3). Thus, the addition of the Hoxd11 homeodomain effectively reversed the effects of Hoxd10 on rostral LS motoneurons, suggesting that the Hoxd11 homeodomain is both functionally specific and sufficient to repress LMCl development.

Table 5.1 Comparison of the effects of Hoxd10, Hoxd11, and Hoxd10^{d11HD} on motoneuron subtype development.

	Hoxd10	Hoxd11	Hoxd10^{d11HD}
Lim1 expression in T6	Increase	None	None
Lim1 expression in LS2	Increase	Decrease	Decrease
Foxp1 expression in LS2	None	Decrease	None
RALDH2 expression in LS3-4	None	Decrease	None

Despite parallels with respect to LMCl suppression, Hoxd10^{d11HD} failed to mimic the effects of Hoxd11 misexpression in other aspects of motoneuron patterning (e.g., repression of the LMC), implying that those effects may be dependent on non-homeodomain regions of Hoxd11. Zhao and Potter (2001, 2002) reported such a phenomenon in transgenic mice expressing a mutant form of Hoxa11 in which the homeodomain had been replaced with that of Hoxa13: some aspects of embryonic development were unperturbed, while others (development of the appendicular skeleton and the female reproductive tract) adopted characteristics of Hoxa13 overexpression models (see also Williams et al., 2006). Thus, the importance (or lack thereof) of the homeodomain to Hox function appears to be context-dependent; in some cases, non-homeodomain-binding regions of Hox genes may be functionally critical. A few recent investigations have uncovered evidence of protein:protein interactions between Hox factors and known morphogenetic effectors, suggesting a novel, non-homeodomain-dependent mechanism by which Hox genes might control regional patterning. For example, as discussed in Chapter 1, interactions between Hoxd12 and the Shh effector Gli3 influence digit formation in the limb (Chen et al., 2004). Further, Hox13 proteins have been shown to interact with Smad5, a mediator of BMP signaling, independently of the homeodomain (Williams et al., 2005), though

the precise role of this interaction in patterning is not yet understood. A few recent studies have demonstrated a surprising degree of functional equivalence between Hoxd13 and a mutated, non-DNA binding form thereof the patterning of the appendicular skeleton (Caronia et al., 2003, Williams et al., 2006), asserting that DNA binding is irrelevant altogether for at least some aspects of Hox-directed regionalization.

5.5.2 Repressive versus activating functions of Hox proteins

Dasen and colleagues (2003, 2005) have proposed that the mechanisms of Hox action in spinal motoneuron patterning rely on both the repression and activation of downstream targets. By fusing the constitutive repressor domain from the Drosophila engrailed protein to a number of different mammalian HoxC family members, these investigators determined that the normal repressor activities of Hox proteins result in the exclusion of other Hox genes from a common region, while their activating functions induce the expression of regional and subtype-specific markers. A recent analysis of the downstream factors affected by misexpression of Hoxd13 and a non-DNA-binding form thereof determined that the binding mutant could upregulate expression of several of the same genes as Hoxd13, but was unable to repress those that were downregulated by Hoxd13 (Williams et al., 2004). This intriguing finding implies that Hox homeodomain:DNA binding may be required primarily for gene repression, rather than activation. Thus, the repressive activities of Hox proteins (for example, the repression of LMCl development by Hoxd11) would be intimately linked to their homeodomain. This hypothesis seems to fit with data described above – expression of Hoxd10^{d11HD} mimics Hoxd11 in its repression of the LMCl marker Lim1. In light of the combined implications of these findings, a further examination of the repressive versus activating functions of Hoxd10, Hoxd11, and

Hoxd10^{d11HD} would be particularly useful in interpreting the role of the homeodomain in Hox-directed motoneuron specification.

5.5.3 Future directions

The data described in this chapter represent the preliminary findings in an ongoing study of the mechanisms of Hox action as relates to the acquisition of regional spinal identity. To further investigate the contributions of the homeodomain to Hox functional specificity, I plan to create a form of Hoxd11 in which this domain has been replaced with that of Hoxd10 (Hoxd11^{d10HD}), and to assay the effects of misexpression in both thoracic and LS spinal cord segments. I believe that a manipulation of this sort will clarify the results described above and aid in the definitive determination of which aspects of motoneuron specification in the LS cord are dependent on the Hox homeodomain and which are not. As a supplement to these investigations, I also plan to examine the effects of misexpressing non-DNA binding forms of Hoxd10 and Hoxd11. I have used site directed mutagenesis to create constructs in which residues 47, 50, and 51 of the homeodomain, which are essential for DNA binding (Gehring, 1994), have been mutated from isoleucine (I), glutamine (Q), and asparagine (N), respectively, to alanine residues. This study will determine which motoneuron effects of Hoxd10 and Hoxd11 are due to transcriptional activities, and which are due to protein:protein interactions.

6.0 GENERAL DISCUSSION

The formation of functional neural circuitry relies on the establishment of precise connections among groups of neurons, and between central neurons and their peripheral targets. These connections are patterned very early in development by intrinsic molecular factors and later refined by activity-dependent mechanisms. The spinal cord is an ideal system in which to study early molecular events in neuron specification, because in it, investigators have identified clear parallels between neuronal molecular profile, position, and function.

The diversification of motoneurons into the numerous subtypes required for accurate circuit formation begins even before they are born, with the gross regionalization of the neural tube. Once this structure has been divided into limb-innervating and non-limb-innervating regions by its responses to competing morphogenetic gradients, newly born motoneurons acquire specific molecular profiles, settle in specific locations within the cord, and send projections to appropriate targets.

The induction and maintenance of the expression of members of the Hox family of transcription factors in motoneuron populations has proven to be critical to the process of motoneuron diversification (Dasen et al., 2003, 2005; Shah et al., 2004; Wu et al., 2008). In the preceding chapters, I have discussed the roles of two members of this family, Hoxd10 and Hoxd11, in the patterning of the lumbosacral spinal cord of the chick. I utilized in ovo electroporation to overexpress Hoxd10 and ectopically express Hoxd11 in rostral LS segments,

then assessed changes in the expression of members of the LIM HD family of transcription factors, markers of motoneuron columnar identity.

6.1 HOXD10, HOXD11, AND MOTONEURON IDENTITY

One of the most pronounced effects of Hox misexpression in the LS cord was the resultant shift in motoneuron subtype proportions. Hoxd10 increased the proportion of motoneurons expressing the LMCl marker Lim1 (Tsuchida et al., 1994), while Hoxd11 shifted proportions in favor of motoneurons expressing the LMCm and MMC marker Isl1. An examination of subtype identity within the transfected populations alone revealed that Hoxd10-transfected motoneurons were likely to express Lim1, and that Hoxd11-transfected motoneurons preferentially expressed Isl1. Based on these results, I concluded that both Hoxd10 and Hoxd11 were capable of directing motoneurons to adopt specific molecular characteristics indicative of motor column divisional identity.

Dasen and colleagues (2005) have described a similar effect in the brachial spinal cord. They observed that Hox misexpression altered the complement of motoneuron subtypes at a given rostrocaudal level. In addition, these investigators were able to correlate spatially restricted Hox expression with the specification of individual motor pools. Whether Hoxd10 and Hoxd11 also specify the identities of motor pools within columnar subdivisions remains to be seen. The expression patterns of Hoxd10 at stage 29 (see Figure 3.1) certainly imply a subtype-specific role. Hoxd11, in contrast, remains diffusely expressed within the ventral spinal cord at this stage. Er81 and Pea3, two members of the ETS family of transcription factors, have been shown to demarcate several motor pools in LS segments, and therefore might be utilized to

examine the induction of pool subtypes following Hox misexpression. However, the expression of these factors appears to be dependent on peripheral signals. Therefore, using them to identify motor pools in experimental embryos presupposes that the axons of Hox-misexpressing cells penetrate the limb and form meaningful connections therein. Our own data suggests that this may not be the case (see Figure 4.13). Thus, an analysis of Hox effects on pool formation would require the identification of additional molecular markers specific to individual LS motor pools. Possible candidates include Scip and Runx, which are expressed by unique pools in brachial segments (Dasen et al., 2005).

6.2 ESTABLISHING SEGMENTAL IDENTITY WITHIN THE LS CORD

A major aim of this thesis was to place the processes governing motoneuron development into the larger context of rostrocaudal (or anteroposterior) embryonic patterning. Previous studies of Hox function had elaborated on the mechanisms by which gross morphological regions of the spinal cord were established (see Liu et al., 2001; Lance-Jones et al., 2001; Dasen et al., 2003; Shah et al., 2004), but few had explicitly examined "subregionalization", or segmental diversity within the rostrocaudal boundaries of a greater region (see Carpenter et al., 1997; Dasen et al., 2005). We therefore chose to examine the development of segmental diversity in the lumbosacral spinal cord. In doing so, we noted a striking feature of the motor columns therein. In rostral segments, dorsal-projecting LMCl motoneurons were abundant. However, in caudal segments, their numbers dwindled, and the LMC appeared to be dominated by ventral-projecting motoneurons (see Figure 4.3; Landmesser, 1978). The diminution of the LMCl in caudal segments also corresponded spatially with the region of high Hoxd11 expression (see Figure

4.1). This observation allowed us to interpret the suppression of LMCl development by ectopic Hoxd11 as a partial phenotypic conversion of rostral segments to caudal. Such transformations have been observed in a number of other developmental systems, including the axial skeleton (see Boulet and Capecchi, 2002), and reproductive tracts of vertebrates (Zhao and Potter, 2000), and, most famously, in the homeotic transformations of Drosophila (Lewis, 1978). Our analysis of motoneuron projections to the caudilioflexorius further confirmed of the ability of ectopic Hoxd11 to "caudalize" rostral segments; its expression induce middle and rostral LS motoneurons to send novel projections to a far caudal muscle target normally innervated by LS6-8.

The caudal LS of the chick spinal cord is roughly homologous to the sacral region of the mouse spinal cord. The "caudalizing" properties of Hoxd11 can therefore be equated in some respects with a "sacralization". A similar phenomenon has been noted in the axial skeleton of Hoxd11 over-expressing mice, which exhibit an increase in sacral vertebrae at the expense of lumbar vertebrae (Boulet and Capecchi, 2002). It would be of interest, therefore, to examine the ability of Hoxd11 to induce other characteristic features of caudal LS/sacral segments of the spinal cord. For example, caudal LS and sacral segments contain two unique populations of non-limb innervating motoneurons: the visceral preganglionic motoneurons that project to the pelvic ganglia, and the somatic motoneurons that project to the pelvic floor musculature. Induction of these cell types following rostral misexpression of Hoxd11 would be further evidence that Hoxd11 is instrumental in the specification of sacral-like segmental characteristics.

6.3 DOWNSTREAM TARGETS OF HOXD10 AND HOXD11

I have shown here that misexpression of Hoxd10 or Hoxd11 altered both the organization of motoneurons within the spinal cord and the trajectories of their axons. Overexpression of Hoxd10 in rostral LS segments caused motoneurons to adopt a lateral position within the cord and a dorsal axonal trajectory at the base of the limb. Ectopic expression of Hoxd11 in these segments directed motoneurons to adopt a medial position regardless of the time of their birth, and to send aberrant projections to a caudal muscle, the caudilioflexorius. Furthermore, Hoxd11 appeared to disrupt the clustering of the caudilioflexorius motor pool within the spinal cord. These effects strongly suggest that the agents downstream of Hox signaling must include various factors linked to axon guidance and to cell adhesion. As discussed in Chapter 1, surprisingly few direct transcriptional targets of Hox genes have been definitively identified (reviewed in Akin and Nazarali, 2005). Among them, however, are a number of cell adhesion and axon guidance molecules, including N-CAM (Jones et al., 1993; reviewed in Edelman and Jones, 1998), osteopontin (Shi et al., 1999 and 2001), Eph/ephrins (Bruhl et al., 2004; Salsi and Zappavigna, 2006), Slit/Robos (Geisen et al., 2008) and basic FGF (Caré et al., 1996).

Based on current models of motor axon outgrowth, members of the Eph/ephrin family of repulsive guidance molecules are likely candidates for regulation by Hoxd10 and Hoxd11. LMCl motoneurons express EphA4, while the ventral half of the nearby limb mesenchyme expresses its ligands, ephrinAs (Helmbacher et al., 2000; Eberhart et al., 2002; Kania and Jessell, 2003). Because of the repulsive interactions between EphAs and ephrinAs, LMCl motoneurons preferentially adopt a dorsal trajectory. Interestingly, the expression of EphA4 by motoneurons appears to be under the direct control of the LIM homeodomain protein Lim1 (Kania and Jessell, 2003), which I have shown to be upregulated by Hoxd10 in LS segments. Based on these

connections, one would expect an increase in motoneuron expression of EphA4 in Hoxd10-electroporated embryos. Conversely, EphB receptors and ephrinB ligands have been implicated in routing LMCm motor axons into the ventral limb, and their expression is directly linked to that of the medial motoneuron marker Isl1 (Luria et al., 2008), which I have shown to be upregulated by misexpression of Hoxd11. However, we found no evidence of an increased preference for ventral trajectories in Hoxd11-transfected motoneurons, suggesting that the presence of Hoxd11 may have uncoupled LIM HD identity from axonal trajectory. Given specific links between Hox and LIM transcription factors (also see Dasen et al., 2003; 2005), and between LIM transcription factors and Eph/ephrin expression, an examination of the impact of it Hoxd10 and/or Hoxd11 manipulations on the expression of EphA and EphB receptors by LS motoneurons would be of particular interest.

The disruption of caudilioflexorius motor pool clustering in Hoxd11-transfected embryos points to cell adhesion molecules as possible downstream targets of Hox transcriptional activity. Though no definitive link has been established between the two, members of the cadherin family have often been identified in microarray screens as likely targets for Hox transcription factors (Inoue et al., 1997; Shen et al., 2000). Homotypic interactions between motoneurons expressing the same type II cadherins appear to be necessary for the clustering of individual motor pools (Price et al., 2001). It would therefore be of interest to examine changes in cadherin expression in Hox-transfected spinal cords.

6.4 THE ROLE OF HOX GENES IN CIRCUIT FORMATION

The spinal cord at the level of the limbs is organized such that the cell bodies of all motoneurons innervating a specific limb muscle are clustered into motor pools occupying a stereotyped position within the LMC (Landmesser, 1978). In the simplest of motor circuitry, the monosynaptic stretch reflex, type Ia sensory afferents from the dorsal root ganglia relay information regarding a muscle's length and elongation directly to its corresponding motoneuron pool in the spinal cord (reviewed in Chen et al., 2003). Despite the relative simplicity of this circuit, the mechanisms governing its formation have only recently become clearer. The establishment of precise connections between the axons of afferent sensory neurons and the dendrites of motoneurons is currently thought to depend upon the coordinated expression of repulsive axon guidance factors and their receptors (Pecho-Vrieseling et al., 2009). The motor circuitry responsible for locomotion adds an additional layer of complexity on to the monosynaptic stretch reflex by incorporating the inputs of ipsilateral and contralateral ventral interneurons (reviewed in Goulding and Pfaff, 2005). The consolidated input of these diverse interneurons to motoneuron activity within the spinal cord allows the accurate control of both flexor-extensor coordination and left-right alternation in simple locomotor behaviors. The factors responsible for directing connections among interneurons and between interneurons and motoneurons are almost entirely unknown, though members of the Eph/ephrin family have been implicated (Kullander et al., 2003). Furthermore, the diversity of interneuron subtypes at a given spinal level has not yet been thoroughly characterized.

Given their proposed role in motoneuron development (Dasen et al., 2003, 2005; see Chapters 3-4), the expression of Hox genes in dorsal root ganglia and in non-motoneuron populations in the spinal cord (Ensini et al., 1998, Dasen et al., 2005; Hostege et al., 2008; Crone

et al., 2008) suggests the intriguing possibility that they may contribute to the patterning of the sensory and interneurons involved in the formation of the monosynaptic stretch and basic locomotor circuitry. Evidence of such a role, however, is scarce. In the hindbrain, recent studies have suggested that loss of Hoxb1 or Hox3 paralogue function shifts the development of first order sensory interneurons in r4 and r5 to a more r3-like profile, as determined by expression of molecular markers. No comparable finding applies to the spinal cord, but in a Hoxc8 loss-of-function mutant, investigators did note a marked disorganization of dorsal laminae of the lumbar spinal cord. Further, Crone et al. (2008) have reported that different classes of V2 interneurons may have different Hox10 expression profiles, and I have shown that Hoxd11 misexpression can alter the number of Chx10+V2 interneurons. These findings begin to lay the groundwork for a serious inquiry into the role of Hox genes in circuit formation. Such an inquiry would begin with both electrophysiological and histological examinations of the sensory-motor connectivity of Hox transfected motoneurons to address the question of whether sensory inputs are altered in response to changes in motor pools size/motoneuron subtype numbers. Alternatively, one might examine the effects of Hox misexpression in sensory motoneurons themselves. The neurons of the dorsal root ganglia (including Ia proprioceptive neurons) arise from a multipotent population of cells, termed the neural crest, that occupy the dorsal neural tube (Weston, 1963). Some investigators have successfully labeled the cells of the dorsal root ganglia by using standard neural tube in ovo electroporation methods to transfect their neural crest precursors (see George et al., 2007). Similar means could be utilized to transfect DRG motoneurons with a Hox gene of interest.

BIBLIOGRAPHY

Agalliu, D., Takada, S., Agalliu, I., McMahon, A. P., Jessell, T. M., 2009. Motor neurons with axial muscle projections specified by Wnt4/5 signaling. Neuron. 61**,** 708-20.

Akin, Z. N., Nazarali, A. J., 2005. Hox genes and their candidate downstream targets in the developing central nervous system. Cell Mol Neurobiol. 25**,** 697-741.

Al-Mosawie, A., Wilson, J. M., Brownstone, R. M., 2007. Heterogeneity of V2-derived interneurons in the adult mouse spinal cord. Eur J Neurosci. 26**,** 3003-15.

Appel, B., Korzh, V., Glasgow, E., Thor, S., Edlund, T., Dawid, I. B., Eisen, J. S., 1995. Motoneuron fate specification revealed by patterned LIM homeobox gene expression in embryonic zebrafish. Development. 121**,** 4117-25.

Arber, S., Han, B., Mendelsohn, M., Smith, M., Jessell, T. M., Sockanathan, S., 1999. Requirement for the homeobox gene Hb9 in the consolidation of motor neuron identity Neuron. 23**,** 659-74.

Barik, S., 2002. Megaprimer PCR. Methods Mol Biol. 192**,** 189-96.

Bel-Vialar, S., Itasaki, N., Krumlauf, R., 2002. Initiating Hox gene expression: in the early chick neural tube differential sensitivity to FGF and RA signaling subdivides the HoxB genes in two distinct groups. Development. 129**,** 5103-15.

Bell, E., Wingate, R. J., Lumsden, A., 1999. Homeotic transformation of rhombomere identity after localized Hoxb1 misexpression. Science. 284**,** 2168-71.

Berggren, K., McCaffery, P., Drager, U., Forehand, C. J., 1999. Differential distribution of retinoic acid synthesis in the chicken embryo as determined by immunolocalization of the retinoic acid synthetic enzyme, RALDH-2. Dev Biol. 210**,** 288-304.

Boulet, A. M., Capecchi, M. R., 2002. Duplication of the Hoxd11 gene causes alterations in the axial and appendicular skeleton of the mouse. Dev Biol. 249**,** 96-107.

Boulet, A. M., Capecchi, M. R., 2004. Multiple roles of Hoxa11 and Hoxd11 in the formation of the mammalian forelimb zeugopod. Development. 131**,** 299-309.

Briscoe, J., Pierani, A., Jessell, T. M., Ericson, J., 2000. A homeodomain protein code specifies progenitor cell identity and neuronal fate in the ventral neural tube. Cell. 101**,** 435-45.

Briscoe, J., Sussel, L., Serup, P., Hartigan-O'Connor, D., Jessell, T. M., Rubenstein, J. L., Ericson, J., 1999. Homeobox gene Nkx2.2 and specification of neuronal identity by graded Sonic hedgehog signalling. Nature. 398**,** 622-7.

Bruhl, T., Urbich, C., Aicher, D., Acker-Palmer, A., Zeiher, A. M., Dimmeler, S., 2004. Homeobox A9 transcriptionally regulates the EphB4 receptor to modulate endothelial cell migration and tube formation. Circ Res. 94**,** 743-51.

Burke, A. C., Nelson, C. E., Morgan, B. A., Tabin, C., 1995. Hox genes and the evolution of vertebrate axial morphology. Development. 121**,** 333-46.

Care, A., Silvani, A., Meccia, E., Mattia, G., Stoppacciaro, A., Parmiani, G., Peschle, C., Colombo, M. P., 1996. HOXB7 constitutively activates basic fibroblast growth factor in melanomas. Mol Cell Biol. 16**,** 4842-51.

Caronia, G., Goodman, F. R., McKeown, C. M., Scambler, P. J., Zappavigna, V., 2003. An I47L substitution in the HOXD13 homeodomain causes a novel human limb malformation by producing a selective loss of function. Development. 130**,** 1701-12.

Carpenter, E. M., Goddard, J. M., Davis, A. P., Nguyen, T. P., Capecchi, M. R., 1997. Targeted disruption of Hoxd-10 affects mouse hindlimb development. Development. 124**,** 4505-14.

Chang, C. P., Brocchieri, L., Shen, W. F., Largman, C., Cleary, M. L., 1996. Pbx modulation of Hox homeodomain amino-terminal arms establishes different DNA-binding specificities across the Hox locus. Mol Cell Biol. 16**,** 1734-45.

Chang, C. P., Shen, W. F., Rozenfeld, S., Lawrence, H. J., Largman, C., Cleary, M. L., 1995. Pbx proteins display hexapeptide-dependent cooperative DNA binding with a subset of Hox proteins. Genes Dev. 9**,** 663-74.

Chen, H. H., Hippenmeyer, S., Arber, S., Frank, E., 2003. Development of the monosynaptic stretch reflex circuit. Curr Opin Neurobiol. 13**,** 96-102.

Chen, Y., Knezevic, V., Ervin, V., Hutson, R., Ward, Y., Mackem, S., 2004. Direct interaction with Hoxd proteins reverses Gli3-repressor function to promote digit formation downstream of Shh. Development. 131**,** 2339-47.

Chizhikov, V. V., Millen, K. J., 2005. Roof plate-dependent patterning of the vertebrate dorsal central nervous system. Dev Biol. 277**,** 287-95.

Cohen, S., Funkelstein, L., Livet, J., Rougon, G., Henderson, C. E., Castellani, V., Mann, F., 2005. A semaphorin code defines subpopulations of spinal motor neurons during mouse development. Eur J Neurosci. 21**,** 1767-76.

Crone, S. A., Quinlan, K. A., Zagoraiou, L., Droho, S., Restrepo, C. E., Lundfald, L., Endo, T., Setlak, J., Jessell, T. M., Kiehn, O., Sharma, K., 2008. Genetic ablation of V2a ipsilateral interneurons disrupts left-right locomotor coordination in mammalian spinal cord. Neuron. 60**,** 70-83.

Dasen, J. S., De Camilli, A., Wang, B., Tucker, P. W., Jessell, T. M., 2008. Hox repertoires for motor neuron diversity and connectivity gated by a single accessory factor, FoxP1. Cell. 134**,** 304-16.

Dasen, J. S., Liu, J. P., Jessell, T. M., 2003. Motor neuron columnar fate imposed by sequential phases of Hox-c activity. Nature. 425**,** 926-33.

Dasen, J. S., Tice, B. C., Brenner-Morton, S., Jessell, T. M., 2005. A Hox regulatory network establishes motor neuron pool identity and target-muscle connectivity. Cell. 123**,** 477-91.

Davis, A. P., Capecchi, M. R., 1994. Axial homeosis and appendicular skeleton defects in mice with a targeted disruption of hoxd-11. Development. 120**,** 2187-98.

Davis, A. P., Witte, D. P., Hsieh-Li, H. M., Potter, S. S., Capecchi, M. R., 1995. Absence of radius and ulna in mice lacking hoxa-11 and hoxd-11. Nature. 375**,** 791-5.

De Marco Garcia, N. V., Jessell, T. M., 2008. Early motor neuron pool identity and muscle nerve trajectory defined by postmitotic restrictions in Nkx6.1 activity. Neuron. 57**,** 217-31.

Desplan, C., Theis, J., O'Farrell, P. H., 1988. The sequence specificity of homeodomain-DNA interaction. Cell. 54**,** 1081-90.

Diez del Corral, R., Olivera-Martinez, I., Goriely, A., Gale, E., Maden, M., Storey, K., 2003. Opposing FGF and retinoid pathways control ventral neural pattern, neuronal differentiation, and segmentation during body axis extension. Neuron. 40**,** 65-79.

Duboule, D., 2000. Developmental genetics. A Hox by any other name. Nature. 403**,** 607, 609-10.

Duboule, D., Morata, G., 1994. Colinearity and functional hierarchy among genes of the homeotic complexes. Trends Genet. 10**,** 358-64.

Eberhart, J., Swartz, M. E., Koblar, S. A., Pasquale, E. B., Krull, C. E., 2002. EphA4 constitutes a population-specific guidance cue for motor neurons. Dev Biol. 247**,** 89-101.

Echelard, Y., Epstein, D. J., St-Jacques, B., Shen, L., Mohler, J., McMahon, J. A., McMahon, A. P., 1993. Sonic hedgehog, a member of a family of putative signaling molecules, is implicated in the regulation of CNS polarity. Cell. 75**,** 1417-30.

Edelman, G. M., Jones, F. S., 1998. Gene regulation of cell adhesion: a key step in neural morphogenesis. Brain Res Brain Res Rev. 26**,** 337-52.

Ensini, M., Tsuchida, T. N., Belting, H. G., Jessell, T. M., 1998. The control of rostrocaudal pattern in the developing spinal cord: specification of motor neuron subtype identity is initiated by signals from paraxial mesoderm. Development. 125**,** 969-82.

Ericson, J., Morton, S., Kawakami, A., Roelink, H., Jessell, T. M., 1996. Two critical periods of Sonic Hedgehog signaling required for the specification of motor neuron identity. Cell. 87**,** 661-73.

Ericson, J., Rashbass, P., Schedl, A., Brenner-Morton, S., Kawakami, A., van Heyningen, V., Jessell, T. M., Briscoe, J., 1997. Pax6 controls progenitor cell identity and neuronal fate in response to graded Shh signaling. Cell. 90**,** 169-80.

Ericson, J., Thor, S., Edlund, T., Jessell, T. M., Yamada, T., 1992. Early stages of motor neuron differentiation revealed by expression of homeobox gene Islet-1. Science. 256**,** 1555-60.

Gehring, W. J., Qian, Y. Q., Billeter, M., Furukubo-Tokunaga, K., Schier, A. F., Resendez-Perez, D., Affolter, M., Otting, G., Wuthrich, K., 1994. Homeodomain-DNA recognition. Cell. 78**,** 211-23.

Geisen, M. J., Di Meglio, T., Pasqualetti, M., Ducret, S., Brunet, J. F., Chedotal, A., Rijli, F. M., 2008. Hox paralog group 2 genes control the migration of mouse pontine neurons through slit-robo signaling. PLoS Biol. 6**,** e142.

George, L., Chaverra, M., Todd, V., Lansford, R., Lefcort, F., 2007. Nociceptive sensory neurons derive from contralaterally migrating, fate-restricted neural crest cells. Nat Neurosci. 10**,** 1287-93.

Goff, D. J., Tabin, C. J., 1997. Analysis of Hoxd-13 and Hoxd-11 misexpression in chick limb buds reveals that Hox genes affect both bone condensation and growth. Development. 124**,** 627-36.

Gould, A., Itasaki, N., Krumlauf, R., 1998. Initiation of rhombomeric Hoxb4 expression requires induction by somites and a retinoid pathway. Neuron. 21**,** 39-51.

Goulding, M., Pfaff, S. L., 2005. Development of circuits that generate simple rhythmic behaviors in vertebrates. Curr Opin Neurobiol. 15**,** 14-20.

Grapin-Botton, A., Bonnin, M. A., Le Douarin, N. M., 1997. Hox gene induction in the neural tube depends on three parameters: competence, signal supply and paralogue group. Development. 124**,** 849-59.

Greer, J. M., Puetz, J., Thomas, K. R., Capecchi, M. R., 2000. Maintenance of functional equivalence during paralogous Hox gene evolution. Nature. 403**,** 661-5.

Guidato, S., Prin, F., Guthrie, S., 2003. Somatic motoneurone specification in the hindbrain: the influence of somite-derived signals, retinoic acid and Hoxa3. Development. 130**,** 2981-96.

Gutman, C. R., Ajmera, M. K., Hollyday, M., 1993. Organization of motor pools supplying axial muscles in the chicken. Brain Res. 609**,** 129-36.

Haase, G., Dessaud, E., Garces, A., de Bovis, B., Birling, M., Filippi, P., Schmalbruch, H., Arber, S., deLapeyriere, O., 2002. GDNF Acts through PEA3 to Regulate Cell Body Positioning and Muscle Innervation of Specific Motor Neuron Pools. Neuron. 35**,** 893.

Hamburger, V., Hamilton, H. L., 1951. A series of normal stages in the development of the chick embryo. J Morphol. 88**,** 49-92.

Hamburger, V., Levi-Montalcini, R., 1949. Proliferation, differentiation and degeneration in the spinal ganglia of the chick embryo under normal and experimental conditions. J Exp Zool. 111**,** 457-501.

Helmbacher, F., Dessaud, E., Arber, S., deLapeyriere, O., Henderson, C. E., Klein, R., Maina, F., 2003. Met signaling is required for recruitment of motor neurons to PEA3-positive motor pools. Neuron. 39**,** 767-77.

Helmbacher, F., Schneider-Maunoury, S., Topilko, P., Tiret, L., Charnay, P., 2000. Targeting of the EphA4 tyrosine kinase receptor affects dorsal/ventral pathfinding of limb motor axons. Development. 127**,** 3313-3324.

Hobert, O., Westphal, H., 2000. Functions of LIM-homeobox genes. Trends Genet. 16**,** 75-83.

Hoey, T., Levine, M., 1988. Divergent homeo box proteins recognize similar DNA sequences in Drosophila. Nature. 332**,** 858-61.

Hollyday, M., 1980. Organization of motor pools in the chick lumbar lateral motor column. J Comp Neurol. 194**,** 143-70.

Hollyday, M., Hamburger, V., 1977. An autoradiographic study of the formation of the lateral motor column in the chick embryo. Brain Res. 132**,** 197-208.

Holmes, G. P., Negus, K., Burridge, L., Raman, S., Algar, E., Yamada, T., Little, M. H., 1998. Distinct but overlapping expression patterns of two vertebrate slit homologs implies functional roles in CNS development and organogenesis. Mech Dev. 79**,** 57-72.

Holstege, J. C., de Graaff, W., Hossaini, M., Cano, S. C., Jaarsma, D., van den Akker, E., Deschamps, J., 2008. Loss of Hoxb8 alters spinal dorsal laminae and sensory responses in mice. Proc Natl Acad Sci U S A. 105**,** 6338-43.

Huber, A. B., Kania, A., Tran, T. S., Gu, C., De Marco Garcia, N., Lieberam, I., Johnson, D., Jessell, T. M., Ginty, D. D., Kolodkin, A. L., 2005. Distinct roles for secreted semaphorin signaling in spinal motor axon guidance. Neuron. 48**,** 949-64.

Hunt, P., Krumlauf, R., 1991. Deciphering the Hox code: clues to patterning branchial regions of the head. Cell. 66**,** 1075-8.

Inoue, T., Chisaka, O., Matsunami, H., Takeichi, M., 1997. Cadherin-6 expression transiently delineates specific rhombomeres, other neural tube subdivisions, and neural crest subpopulations in mouse embryos. Dev Biol. 183**,** 183-94.

Itasaki, N., Bel-Vialar, S., Krumlauf, R., 1999. 'Shocking' developments in chick embryology: electroporation and in ovo gene expression. Nat Cell Biol. 1**,** E203-7.

Itasaki, N., Sharpe, J., Morrison, A., Krumlauf, R., 1996. Reprogramming Hox expression in the vertebrate hindbrain: influence of paraxial mesoderm and rhombomere transposition. Neuron. 16**,** 487-500.

Izpisua-Belmonte, J. C., Falkenstein, H., Dolle, P., Renucci, A., Duboule, D., 1991. Murine genes related to the Drosophila AbdB homeotic genes are sequentially expressed during development of the posterior part of the body. EMBO J. 10**,** 2279-89.

Jessell, T. M., 2000. Neuronal specification in the spinal cord: inductive signals and transcriptional codes. Nat Rev Genet. 1**,** 20-9.

Ji, S. J., Zhuang, B., Falco, C., Schneider, A., Schuster-Gossler, K., Gossler, A., Sockanathan, S., 2006. Mesodermal and neuronal retinoids regulate the induction and maintenance of limb innervating spinal motor neurons. Dev Biol. 297**,** 249-61.

Jones, F. S., Holst, B. D., Minowa, O., De Robertis, E. M., Edelman, G. M., 1993. Binding and transcriptional activation of the promoter for the neural cell adhesion molecule by HoxC6 (Hox-3.3). Proc Natl Acad Sci U S A. 90**,** 6557-61.

Joshi, R., Passner, J. M., Rohs, R., Jain, R., Sosinsky, A., Crickmore, M. A., Jacob, V., Aggarwal, A. K., Honig, B., Mann, R. S., 2007. Functional specificity of a Hox protein mediated by the recognition of minor groove structure. Cell. 131**,** 530-43.

Jungbluth, S., Bell, E., Lumsden, A., 1999. Specification of distinct motor neuron identities by the singular activities of individual Hox genes. Development. 126**,** 2751-8.

Kania, A., Jessell, T. M., 2003. Topographic motor projections in the limb imposed by LIM homeodomain protein regulation of ephrin-A:EphA interactions. Neuron. 38**,** 581-96.

Kania, A., Johnson, R. L., Jessell, T. M., 2000. Coordinate roles for LIM homeobox genes in directing the dorsoventral trajectory of motor axons in the vertebrate limb. Cell. 102**,** 161-73.

Kmita, M., Duboule, D., 2003. Organizing axes in time and space; 25 years of colinear tinkering. Science. 301**,** 331-3.

Knoepfler, P. S., Kamps, M. P., 1995. The pentapeptide motif of Hox proteins is required for cooperative DNA binding with Pbx1, physically contacts Pbx1, and enhances DNA binding by Pbx1. Mol Cell Biol. 15**,** 5811-9.

Kramer, E. R., Knott, L., Su, F., Dessaud, E., Krull, C. E., Helmbacher, F., Klein, R., 2006. Cooperation between GDNF/Ret and ephrinA/EphA4 signals for motor-axon pathway selection in the limb. Neuron. 50**,** 35-47.

Krull, C. E., 2004. A primer on using in ovo electroporation to analyze gene function. Dev Dyn. 229**,** 433-9.

Krumlauf, R., 1994. Hox genes in vertebrate development. Cell. 78**,** 191-201.

Kullander, K., Butt, S. J., Lebret, J. M., Lundfald, L., Restrepo, C. E., Rydstrom, A., Klein, R., Kiehn, O., 2003. Role of EphA4 and EphrinB3 in local neuronal circuits that control walking. Science. 299**,** 1889-92.

Lance-Jones, C., Landmesser, L., 1980. Motoneurone projection patterns in the chick hind limb following early partial reversals of the spinal cord. J Physiol. 302**,** 581-602.

Lance-Jones, C., Landmesser, L., 1981. Pathway selection by chick lumbosacral motoneurons during normal development. Proc R Soc Lond B Biol Sci. 214**,** 1-18.

Lance-Jones, C., Omelchenko, N., Bailis, A., Lynch, S., Sharma, K., 2001. *Hoxd10* induction and regionalization in the developing lumbosacral spinal cord. Development. 128**,** 2255-2268.

Landmesser, L., 1978. The distribution of motoneurones supplying chick hind limb muscles. J Physiol. 284**,** 371-89.

LaRonde-LeBlanc, N. A., Wolberger, C., 2003. Structure of HoxA9 and Pbx1 bound to DNA: Hox hexapeptide and DNA recognition anterior to posterior. Genes Dev. 17**,** 2060-72.

Leber, S. M., Breedlove, S. M., Sanes, J. R., 1990. Lineage, arrangement, and death of clonally related motoneurons in chick spinal cord. J Neurosci. 10**,** 2451-62.

Lee, S. K., Pfaff, S. L., 2003. Synchronization of neurogenesis and motor neuron specification by direct coupling of bHLH and homeodomain transcription factors. Neuron. 38**,** 731-45.

Lewis, E. B., 1978. A gene complex controlling segmentation in Drosophila. Nature. 276**,** 565-70.

Lin, A. W., Carpenter, E. M., 2003. Hoxa10 and Hoxd10 coordinately regulate lumbar motor neuron patterning. J Neurobiol. 56**,** 328-37.

Lin, J. H., Saito, T., Anderson, D. J., Lance-Jones, C., Jessell, T. M., Arber, S., 1998. Functionally related motor neuron pool and muscle sensory afferent subtypes defined by coordinate ETS gene expression. Cell. 95**,** 393-407.

Liu, J. P., Laufer, E., Jessell, T. M., 2001. Assigning the Positional Identity of Spinal Motor Neurons. Rostrocaudal Patterning of Hox-c Expression by FGFs, Gdf11, and Retinoids. Neuron. 32**,** 997-1012.

Livet, J., Sigrist, M., Stroebel, S., De Paola, V., Price, S. R., Henderson, C. E., Jessell, T. M., Arber, S., 2002. ETS gene Pea3 controls the central position and terminal arborization of specific motor neuron pools. Neuron. 35**,** 877-92.

Luria, V., Krawchuk, D., Jessell, T. M., Laufer, E., Kania, A., 2008. Specification of motor axon trajectory by ephrin-B:EphB signaling: symmetrical control of axonal patterning in the developing limb. Neuron. 60**,** 1039-53.

Luria, V., Laufer, E., 2007. Lateral motor column axons execute a ternary trajectory choice between limb and body tissues. Neural Develop. 2**,** 13.

Manley, N. R., Selleri, L., Brendolan, A., Gordon, J., Cleary, M. L., 2004. Abnormalities of caudal pharyngeal pouch development in Pbx1 knockout mice mimic loss of Hox3 paralogs. Dev Biol. 276**,** 301-12.

Mann, R. S., Affolter, M., 1998. Hox proteins meet more partners. Curr Opin Genet Dev. 8**,** 423-9.

Manzanares, M., Bel-Vialar, S., Ariza-McNaughton, L., Ferretti, E., Marshall, H., Maconochie, M. M., Blasi, F., Krumlauf, R., 2001. Independent regulation of initiation and maintenance phases of Hoxa3 expression in the vertebrate hindbrain involve auto- and cross-regulatory mechanisms. Development. 128**,** 3595-607.

Matise, M. P., Lance-Jones, C., 1996. A critical period for the specification of motor pools in the chick lumbosacral spinal cord. Development. 122**,** 659-69.

McGinnis, W., Krumlauf, R., 1992. Homeobox genes and axial patterning. Cell. 68**,** 283-302.

Moens, C. B., Selleri, L., 2006. Hox cofactors in vertebrate development. Dev Biol. 291**,** 193-206.

Moustakas, A., Souchelnytskyi, S., Heldin, C. H., 2001. Smad regulation in TGF-beta signal transduction. J Cell Sci. 114**,** 4359-69.

Muramatsu, T., Mizutani, Y., Ohmori, Y., Okumura, J., 1997. Comparison of three nonviral transfection methods for foreign gene expression in early chicken embryos in ovo. Biochem Biophys Res Commun. 230**,** 376-80.

Neuteboom, S. T., Murre, C., 1997. Pbx raises the DNA binding specificity but not the selectivity of antennapedia Hox proteins. Mol Cell Biol. 17**,** 4696-706.

Niederreither, K., Vermot, J., Fraulob, V., Chambon, P., Dolle, P., 2002. Retinaldehyde dehydrogenase 2 (RALDH2)- independent patterns of retinoic acid synthesis in the mouse embryo. Proc Natl Acad Sci U S A. 99**,** 16111-6.

Niederreither, K., Vermot, J., Schuhbaur, B., Chambon, P., Dolle, P., 2000. Retinoic acid synthesis and hindbrain patterning in the mouse embryo. Development. 127**,** 75-85.

Nieto, M. A., Patel, K., Wilkinson, D. G., 1996. In situ hybridization analysis of chick embryos in whole mount and tissue sections. Methods Cell Biol. 51**,** 219-35.

Novitch, B. G., Chen, A. I., Jessell, T. M., 2001. Coordinate regulation of motor neuron subtype identity and pan-neuronal properties by the bHLH repressor Olig2. Neuron. 31**,** 773-89.

Novitch, B. G., Wichterle, H., Jessell, T. M., Sockanathan, S., 2003. A requirement for retinoic acid-mediated transcriptional activation in ventral neural patterning and motor neuron specification. Neuron. 40**,** 81-95.

Omelchenko, N., Lance-Jones, C., 2003. Programming neural Hoxd10: in vivo evidence that early node-associated signals predominate over paraxial mesoderm signals at posterior spinal levels. Dev Biol. 261**,** 99-115.

Pearson, J. C., Lemons, D., McGinnis, W., 2005. Modulating Hox gene functions during animal body patterning. Nat Rev Genet. 6**,** 893-904.

Pecho-Vrieseling, E., Sigrist, M., Yoshida, Y., Jessell, T. M., Arber, S., 2009. Specificity of sensory-motor connections encoded by Sema3e-Plxnd1 recognition. Nature. 459**,** 842-6.

Pfaff, S. L., Mendelsohn, M., Stewart, C. L., Edlund, T., Jessell, T. M., 1996. Requirement for LIM homeobox gene Isl1 in motor neuron generation reveals a motor neuron-dependent step in interneuron differentiation. Cell. 84**,** 309-20.

Pierani, A., Brenner-Morton, S., Chiang, C., Jessell, T. M., 1999. A sonic hedgehog-independent, retinoid-activated pathway of neurogenesis in the ventral spinal cord. Cell. 97**,** 903-15.

Prasad, A., Hollyday, M., 1991. Development and migration of avian sympathetic preganglionic neurons. J Comp Neurol. 307**,** 237-58.

Price, S. R., De Marco Garcia, N. V., Ranscht, B., Jessell, T. M., 2002. Regulation of motor neuron pool sorting by differential expression of type II cadherins. Cell. 109**,** 205-16.

Pruitt, S. C., 1994. Primitive streak mesoderm-like cell lines expressing Pax-3 and Hox gene autoinducing activities. Development. 120**,** 37-47.

Remacle, S., Abbas, L., De Backer, O., Pacico, N., Gavalas, A., Gofflot, F., Picard, J. J., Rezsohazy, R., 2004. Loss of function but no gain of function caused by amino acid substitutions in the hexapeptide of Hoxa1 in vivo. Mol Cell Biol. 24**,** 8567-75.

Roelink, H., Porter, J. A., Chiang, C., Tanabe, Y., Chang, D. T., Beachy, P. A., Jessell, T. M., 1995. Floor plate and motor neuron induction by different concentrations of the amino-terminal cleavage product of sonic hedgehog autoproteolysis. Cell. 81**,** 445-55.

Rousso, D. L., Gaber, Z. B., Wellik, D., Morrisey, E. E., Novitch, B. G., 2008. Coordinated actions of the forkhead protein Foxp1 and Hox proteins in the columnar organization of spinal motor neurons. Neuron. 59**,** 226-40.

Salsi, V., Zappavigna, V., 2006. Hoxd13 and Hoxa13 directly control the expression of the EphA7 Ephrin tyrosine kinase receptor in developing limbs. J Biol Chem. 281**,** 1992-9.

Sander, M., Paydar, S., Ericson, J., Briscoe, J., Berber, E., German, M., Jessell, T. M., Rubenstein, J. L., 2000. Ventral neural patterning by Nkx homeobox genes: Nkx6.1 controls somatic motor neuron and ventral interneuron fates. Genes Dev. 14**,** 2134-9.

Schaeren-Wiemers, N., Gerfin-Moser, A., 1993. A single protocol to detect transcripts of various types and expression levels in neural tissue and cultured cells: in situ hybridization using digoxigenin-labelled cRNA probes. Histochemistry. 100**,** 431-40.

Selleri, L., Depew, M. J., Jacobs, Y., Chanda, S. K., Tsang, K. Y., Cheah, K. S., Rubenstein, J. L., O'Gorman, S., Cleary, M. L., 2001. Requirement for Pbx1 in skeletal patterning and programming chondrocyte proliferation and differentiation. Development. 128**,** 3543-57.

Shah, V., The Role of Hoxd10 in the Development of Motoneurons in the Posterior Spinal Cord. Department of Neurobiology, Vol. PhD. University of PIttsburgh, Pittsburgh, 2006, pp. 148.

Shah, V., Drill, E., Lance-Jones, C., 2004. Ectopic expression of Hoxd10 in thoracic spinal segments induces motoneurons with a lumbosacral molecular profile and axon projections to the limb. Dev Dyn. 231**,** 43-56.

Sharma, K., Leonard, A. E., Lettieri, K., Pfaff, S. L., 2000. Genetic and epigenetic mechanisms contribute to motor neuron pathfinding. Nature. 406**,** 515-9.

Sharma, K., Sheng, H. Z., Lettieri, K., Li, H., Karavanov, A., Potter, S., Westphal, H., Pfaff, S. L., 1998. LIM homeodomain factors Lhx3 and Lhx4 assign subtype identities for motor neurons. Cell. 95**,** 817-28.

Shen, J., Wu, H., Gudas, L. J., 2000. Molecular cloning and analysis of a group of genes differentially expressed in cells which overexpress the Hoxa-1 homeobox gene. Exp Cell Res. 259**,** 274-83.

Shen, W. F., Montgomery, J. C., Rozenfeld, S., Moskow, J. J., Lawrence, H. J., Buchberg, A. M., Largman, C., 1997a. AbdB-like Hox proteins stabilize DNA binding by the Meis1 homeodomain proteins. Mol Cell Biol. 17**,** 6448-58.

Shen, W. F., Rozenfeld, S., Lawrence, H. J., Largman, C., 1997b. The Abd-B-like Hox homeodomain proteins can be subdivided by the ability to form complexes with Pbx1a on a novel DNA target. J Biol Chem. 272**,** 8198-206.

Shi, X., Bai, S., Li, L., Cao, X., 2001. Hoxa-9 represses transforming growth factor-beta-induced osteopontin gene transcription. J Biol Chem. 276**,** 850-5.

Shi, X., Yang, X., Chen, D., Chang, Z., Cao, X., 1999. Smad1 interacts with homeobox DNA-binding proteins in bone morphogenetic protein signaling. J Biol Chem. 274**,** 13711-7.

Shiga, T., Gaur, V. P., Yamaguchi, K., Oppenheim, R. W., 1995. The development of interneurons in the chick embryo spinal cord following in vivo treatment with retinoic acid. J Comp Neurol. 360**,** 463-74.

Shirasaki, R., Lewcock, J. W., Lettieri, K., Pfaff, S. L., 2006. FGF as a target-derived chemoattractant for developing motor axons genetically programmed by the LIM code. Neuron. 50**,** 841-53.

Shirasaki, R., Pfaff, S. L., 2002. Transcriptional codes and the control of neuronal identity. Annu Rev Neurosci. 25**,** 251-81.

Simeone, A., Acampora, D., Arcioni, L., Andrews, P. W., Boncinelli, E., Mavilio, F., 1990. Sequential activation of HOX2 homeobox genes by retinoic acid in human embryonal carcinoma cells. Nature. 346**,** 763-6.

Sockanathan, S., Jessell, T. M., 1998. Motor neuron-derived retinoid signaling specifies the subtype identity of spinal motor neurons. Cell. 94**,** 503-14.

Sockanathan, S., Perlmann, T., Jessell, T. M., 2003. Retinoid receptor signaling in postmitotic motor neurons regulates rostrocaudal positional identity and axonal projection pattern. Neuron. 40**,** 97-111.

Solomin, L., Johansson, C. B., Zetterstrom, R. H., Bissonnette, R. P., Heyman, R. A., Olson, L., Lendahl, U., Frisen, J., Perlmann, T., 1998. Retinoid-X receptor signalling in the developing spinal cord. Nature. 395**,** 398-402.

Sreenath, T. L., Pollock, R. A., Bieberich, C. J., 1996. Functional specificity of Hoxa-4 in vertebral patterning lies outside of the homeodomain. Proc Natl Acad Sci U S A. 93**,** 9636-40.

Studer, M., Lumsden, A., Ariza-McNaughton, L., Bradley, A., Krumlauf, R., 1996. Altered segmental identity and abnormal migration of motor neurons in mice lacking Hoxb-1. Nature. 384**,** 630-4.

Studer, M., Popperl, H., Marshall, H., Kuroiwa, A., Krumlauf, R., 1994. Role of a conserved retinoic acid response element in rhombomere restriction of Hoxb-1. Science. 265**,** 1728-32.

Suzuki, A., Chang, C., Yingling, J. M., Wang, X. F., Hemmati-Brivanlou, A., 1997. Smad5 induces ventral fates in Xenopus embryo. Dev Biol. 184**,** 402-5.

Svingen, T., Tonissen, K. F., 2006. Hox transcription factors and their elusive mammalian gene targets. Heredity. 97**,** 88-96.

Tanabe, Y., Roelink, H., Jessell, T. M., 1995. Induction of motor neurons by Sonic hedgehog is independent of floor plate differentiation. Curr Biol. 5**,** 651-8.

Tanabe, Y., William, C., Jessell, T. M., 1998. Specification of motor neuron identity by the MNR2 homeodomain protein. Cell. 95**,** 67-80.

Tang, J., Rutishauser, U., Landmesser, L., 1994. Polysialic acid regulates growth cone behavior during sorting of motor axons in the plexus region. Neuron. 13**,** 405-14.

Taniguchi, M., Yuasa, S., Fujisawa, H., Naruse, I., Saga, S., Mishina, M., Yagi, T., 1997. Disruption of semaphorin III/D gene causes severe abnormality in peripheral nerve projection. Neuron. 19**,** 519-30.

Thaler, J., Harrison, K., Sharma, K., Lettieri, K., Kehrl, J., Pfaff, S. L., 1999. Active suppression of interneuron programs within developing motor neurons revealed by analysis of homeodomain factor HB9. Neuron. 23**,** 675-87.

Thaler, J. P., Lee, S. K., Jurata, L. W., Gill, G. N., Pfaff, S. L., 2002. LIM factor Lhx3 contributes to the specification of motor neuron and interneuron identity through cell-type-specific protein-protein interactions. Cell. 110**,** 237-49.

Theokli, C., Morsi El-Kadi, A. S., Morgan, R., 2003. TALE class homeodomain gene Irx5 is an immediate downstream target for Hoxb4 transcriptional regulation. Dev Dyn. 227**,** 48-55.

Thor, S., Andersson, S. G., Tomlinson, A., Thomas, J. B., 1999. A LIM-homeodomain combinatorial code for motor-neuron pathway selection. Nature. 397**,** 76-80.

Tiret, L., Le Mouellic, H., Maury, M., Brulet, P., 1998. Increased apoptosis of motoneurons and altered somatotopic maps in the brachial spinal cord of Hoxc-8-deficient mice. Development. 125**,** 279-91.

Tosney, K. W., Landmesser, L. T., 1985a. Development of the major pathways for neurite outgrowth in the chick hindlimb. Dev Biol. 109**,** 193-214.

Tosney, K. W., Landmesser, L. T., 1985b. Specificity of early motoneuron growth cone outgrowth in the chick embryo. J Neurosci. 5**,** 2336-44.

Tsuchida, T., Ensini, M., Morton, S. B., Baldassare, M., Edlund, T., Jessell, T. M., Pfaff, S. L., 1994. Topographic organization of embryonic motor neurons defined by expression of LIM homeobox genes. Cell. 79**,** 957-70.

Tumpel, S., Cambronero, F., Ferretti, E., Blasi, F., Wiedemann, L. M., Krumlauf, R., 2007. Expression of Hoxa2 in rhombomere 4 is regulated by a conserved cross-regulatory mechanism dependent upon Hoxb1. Dev Biol. 302**,** 646-60.

Vallstedt, A., Muhr, J., Pattyn, A., Pierani, A., Mendelsohn, M., Sander, M., Jessell, T. M., Ericson, J., 2001. Different levels of repressor activity assign redundant and specific roles to Nkx6 genes in motor neuron and interneuron specification. Neuron. 31**,** 743-55.

Vermot, J., Schuhbaur, B., Le Mouellic, H., McCaffery, P., Garnier, J. M., Hentsch, D., Brulet, P., Niederreither, K., Chambon, P., Dolle, P., Le Roux, I., 2005. Retinaldehyde dehydrogenase 2 and Hoxc8 are required in the murine brachial spinal cord for the specification of Lim1+ motoneurons and the correct distribution of Islet1+ motoneurons. Development. 132**,** 1611-21.

Wang, G., Scott, S. A., 2000. The "waiting period" of sensory and motor axons in early chick hindlimb: its role in axon pathfinding and neuronal maturation. J Neurosci. 20**,** 5358-66.

Wellik, D. M., Capecchi, M. R., 2003. Hox10 and Hox11 genes are required to globally pattern the mammalian skeleton. Science. 301**,** 363-7.

Weston, J. A., 1963. A radioautographic analysis of the migration and localization of trunk neural crest cells in the chick. Dev Biol. 6**,** 279-310.

William, C. M., Tanabe, Y., Jessell, T. M., 2003. Regulation of motor neuron subtype identity by repressor activity of Mnx class homeodomain proteins. Development. 130**,** 1523-36.

Williams, M. E., Lehoczky, J. A., Innis, J. W., 2006. A group 13 homeodomain is neither necessary nor sufficient for posterior prevalence in the mouse limb. Dev Biol. 297**,** 493-507.

Williams, T. M., Williams, M. E., Heaton, J. H., Gelehrter, T. D., Innis, J. W., 2005a. Group 13 HOX proteins interact with the MH2 domain of R-Smads and modulate Smad transcriptional activation functions independent of HOX DNA-binding capability. Nucleic Acids Res. 33**,** 4475-84.

Williams, T. M., Williams, M. E., Kuick, R., Misek, D., McDonagh, K., Hanash, S., Innis, J. W., 2005b. Candidate downstream regulated genes of HOX group 13 transcription factors with and without monomeric DNA binding capability. Dev Biol. 279**,** 462-80.

Wilson, J. M., Hartley, R., Maxwell, D. J., Todd, A. J., Lieberam, I., Kaltschmidt, J. A., Yoshida, Y., Jessell, T. M., Brownstone, R. M., 2005. Conditional rhythmicity of ventral spinal interneurons defined by expression of the Hb9 homeodomain protein. J Neurosci. 25**,** 5710-9.

Wilson, L., Gale, E., Chambers, D., Maden, M., 2004. Retinoic acid and the control of dorsoventral patterning in the avian spinal cord. Dev Biol. 269**,** 433-46.

Wu, Y., Wang, G., Scott, S. A., Capecchi, M. R., 2008. Hoxc10 and Hoxd10 regulate mouse columnar, divisional and motor pool identity of lumbar motoneurons. Development. 135**,** 171-82.

Yip, J. W., Yip, Y. P., Capriotti, C., 1998. Specific projections of sympathetic preganglionic neurons are not intrinsically determined by segmental origins of their cell bodies. J Neurobiol. 35**,** 371-8.

Zakany, J., Duboule, D., 1999. Hox genes in digit development and evolution. Cell Tissue Res. 296**,** 19-25.

Zakany, J., Gerard, M., Favier, B., Potter, S. S., Duboule, D., 1996. Functional equivalence and rescue among group 11 Hox gene products in vertebral patterning. Dev Biol. 176**,** 325-8.

Zhao, Y., Potter, S. S., 2001. Functional specificity of the Hoxa13 homeobox. Development. 128**,** 3197-207.

Zhao, Y., Potter, S. S., 2002. Functional comparison of the Hoxa 4, Hoxa 10, and Hoxa 11 homeoboxes. Dev Biol. 244**,** 21-36.